THE UNIVERSITY OF CALGARY

MODELLING AND ADAPTIVE TECHNIQUE APPLICATION TO A CELL LEVITATION APPARATUS

by

Zhi-Ming Shu

A THESIS

SUBMITTED TO THE FACULTY OF GRADUATE STUDIES

IN PARTIAL FULFILMENT OF THE REQUIREMENT FOR THE

DEGREE OF MASTER OF SCIENCE

DEPARTMENT OF ELECTRICAL AND COMPUTER ENGINEERING

CALGARY, ALBERTA

September, 1992

ISBN 0-315-83267-3

THE UNIVERSITY OF CALGARY

FACULTY OF GRADUATE STUDIES

The undersigned certify that they have read and recommend to the Faculty of Graduate Studies for acceptance, a thesis entitled "Modelling and Adaptive Technique Application to a Cell Levitation Apparatus", submitted by Zhi-Ming Shu in partial fulfilment of the requirements for the degree of Master of Science.

Supervisor, Dr. G.S. Hope
(Electrical and Computer Engineering)

Dr. K.V.I.S.Kaler
(Electrical and Computer Engineering)

Dr.O.P. Malik
(Electrical and computer Engineering)

Dr.M.C.Singh
(Mechanical Engineering)

17 Nov 92

(Date)

ABSTRACT

In this thesis, adaptive methods are studied and used to develop a cell levitation apparatus control system. Modelling is used to study the apparatus. The most promising adaptive algorithm is implemented for the control of the apparatus.

Eight identification methods are used to determine system model parameters. They are a least squares method, an extended least squares method, a generalized least squares method, an instrumental variable method, a correlation function least squares two step method, a maximum likelihood method, a nonlinear least squares method and FFT method. The model is identified for the first time.

Four adaptive control algorithms were simulated in this study. A PI parameter optimal adaptive controller, a pole-assignment adaptive controller and two new adaptive algorithms are proposed. The newer algorithms are a pole-shifting dual loop adaptive controller and an approximate series compensation adaptive controller. Real time control are used to verify the simulation results.

ACKNOWLEDGEMENTS

The author is deeply indebted to Dr. G.S. Hope for his financial support to this project, his patient review of this draft for many times, his thoughtful, constructive comments and criticism, and also for his prompt coordination of the experiment condition.

The financial support received from the department of Electrical and Computer Engineering is gratefully acknowledged.

Thanks are due to Dr. Kaler and graduate students Jingping Xie, Jack Yang and Yanya Sheng for their friendly assistance in the experimental investigation, and also for Dr. Kaler's detailed explanation and criticism on bio-engineering aspects of this manuscript.

Special thanks are due to Dr. Stein, the graduate student adviser of this department, and international student advisers of the university for their help during last three years.

The author is deeply obligated to his former colleague in China for his academic guidance, advice and suggestion throughout the course of this project, especially for his immediate reply to author's letters. His reply always pointed out the correct research direction and methods whenever there were the technical problems and academic disagreements about this project. His great theoretical learning, extensive industrial experience, keen scientific insight and proficient engineering skills helped the author to finish this project under very difficult circumstances.

Finally, the author thankfully remembers those who gave the author friendly help when the author met difficulties during the last three years in this department, especially when the author was in his most difficult time.

To My Parents

TABLE OF CONTENTS

	Page
APPROVAL	ii
ABSTRACT	iii
ACKNOWLEDGEMENTS	iv
DEDICATION	v
TABLE OF CONTENTS	vi
LIST OF TABLES	x
LIST OF FIGURES	xi
LIST OF SYMBOLS	xiv
LIST OF ABBREVIATIONS	xvii
1. INTRODUCTION	1
1.1 SIGNIFICANCE OF THE CELL LEVITATION APPARATUS	1
1.2 PREVIOUS DIELECTRIC STUDIES	1
1.3 SIGNIFICANCE OF ADAPTIVE CONTROL	2
1.4 PREVIOUS WORK ON ADAPTIVE CONTROLLER	2
1.5 THESIS OUTLINE	4
2. CELL LEVITATION APPARATUS CONTROL SYSTEM	5
2.1 INTRODUCTION TO CELL LEVITATION	5
2.2 INTRODUCTION TO CELL LEVITATION APPARATUS	5
2.3 INTRODUCTION TO CONVENTIONAL CONTROL SYSTEM	9
3. MODELLING OF CELL LEVITATION APPARATUS	11

TABLE OF CONTENTS (CONT'D)

Page

3.1 INTRODUCTION 11

3.2 ANALYTICAL MODEL OF THE CELL LEVITATION APPARATUS 11

3.3 IDENTIFICATION OF CELL LEVITATION APPARATUS 14

3.3.1 INTRODUCTION TO IDENTIFICATION ALGORITHMS 14

3.3.2 FFT METHOD 14

3.3.3 RECURSIVE LEAST SQUARES METHOD 15

3.3.4 RECURSIVE EXTENDED LEAST SQUARES METHOD 17

3.3.5 RECURSIVE GENERALIZED LEAST SQUARES METHOD .. 18

3.3.6 RECURSIVE INSTRUMENTAL VARIABLE METHOD 20

3.3.7 CORRELATION FUNCTION LEAST SQUARES TWO STEPS METHOD 21

3.3.8 RECURSIVE MAXIMUM LIKELIHOOD METHOD 23

3.3.9 NONLINEAR LEAST SQUARES METHOD 24

3.4 MODEL ORDER JUDGEMENT 25

3.5 IDENTIFICATION EXPERIMENT DESIGN 27

3.6 IDENTIFICATION OF CELL-LEVITATION APPARATUS 29

3.6.1 RESULTS AT IMPORTANT POINTS 29

3.6.2 RESULTS FOR THE SINGLE FREQUENCY CONDITION 36

TABLE OF CONTENTS (CONT'D)

Page

3.6.3 RESULTS FOR THE DUAL FREQUENCY CONDITION... 37

4. ADAPTIVE CONTROL SYSTEM DESIGN..... 44

4.1 INTRODUCTION..... 44

4.2 POLE ASSIGNMENT ADAPTIVE CONTROLLER..... 44

4.2.1 INTRODUCTION TO ALGORITHM..... 44

4.2.2 SIMULATION RESULTS..... 50

4.3 PI ADAPTIVE CONTROLLER..... 58

4.3.1 INTRODUCTION TO ALGORITHM..... 58

4.3.2 SIMULATION RESULTS..... 61

4.4 POLE-SHIFTING DUAL LOOP ADAPTIVE CONTROLLER..... 68

4.4.1 INTRODUCTION TO ALGORITHM..... 68

4.4.2 SIMULATION RESULT..... 73

4.5 APPROXIMATE SERIES COMPENSATION

ADAPTIVE CONTROLLER..... 79

4.5.1 INTRODUCTION TO ALGORITHM..... 79

4.5.2 SIMULATION RESULT..... 82

5 EXPERIMENTAL RESULTS..... 87

5.1 INTRODUCTION..... 87

5.2 POLE ASSIGNMENT ADAPTIVE CONTROLLER..... 89

5.2.1 THE SYSTEM CHARACTERISTICS

TABLE OF CONTENTS (CONT'D)

Page

FOR THE STARTING PHASE..... 89

5.2.2 THE SYSTEM CHARACTERISTICS IN LOW

FREQUENCY BAND..... 89

5.3 PI ADAPTIVE CONTROLLER..... 91

5.3.1 THE SYSTEM CHARACTERISTICS IN STARTING PHASE.. 91

5.3.2 THE SYSTEM CHARACTERISTICS

IN LOW FREQUENCY BAND..... 91

6 CONCLUSIONS..... 112

6.1 MODEL OF THE CELL LEVITATION APPARATUS..... 112

6.2 ADAPTIVE CONTROL SYSTEM..... 113

6.3 REAL-TIME IMPLEMENTATION..... 113

6.4 FURTHER RESEARCH..... 113

REFERENCES..... 114

LIST OF TABLES

TABLE	Title	Page
3.1	IDENTIFICATION RESULTS OF DATA GROUP 1	31
3.2	IDENTIFICATION RESULTS OF DATA GROUP 2	34
5.1	RELATION BETWEEN IDENTIFICATION RESULTS AND STEP LENGTH	88

LIST OF FIGURES

Figure	Title	Page
2.1	Cell-levitation apparatus electric field structure	6
2.2	Sectional view of the levitation chamber together with the block diagram of the whole system	7
2.3	Control system block diagram	9
3.1	Physical analysis of the cell model	11
3.2	Block diagram of the model	13
3.3	Nonlinear least squares method - Hammerstein model	25
3.4	Parameter a1 of single frequency	38
3.5	Parameter b0 of single frequency	39
3.6	Parameter b1 of single frequency	40
3.7	Parameter a1 of dual frequency	41
3.8	Parameter b0 of dual frequency	42
3.9	Parameter b1 of dual frequency	43
4.1	Block diagram of a pole assignment adaptive control system	45
4.2	Pole assignment adaptive controller-parameter a1	53
4.3	Pole assignment adaptive controller-parameter b0	54
4.4	Pole assignment adaptive controller-parameter b1	55
4.5	Pole assignment adaptive controller-input/output	56
4.6	Pole assignment adaptive controller-control effort	57
4.7	Block diagram of a PI adaptive controller	59

LIST OF FIGURES(CONT'D)

Figure	Title	Page
4.8	PI adaptive controller-parameter a1	63
4.9	PI adaptive controller-parameter b0	64
4.10	PI adaptive controller-parameter b1	65
4.11	PI adaptive controller-input/output	66
4.12	PI adaptive controller-control effort	67
4.13	Dual loop adaptive controller	69
4.14	Pole-shifting dual loop adaptive controller-parameter a1	74
4.15	Pole-shifting dual loop adaptive controller-parameter b0	75
4.16	Pole-shifting dual loop adaptive controller-parameter b1	76
4.17	Pole-shifting dual loop adaptive controller-input/output	77
4.18	Pole-shifting dual loop adaptive controller-control effort	78
4.19	Approximate series compensation adaptive controller-parameter a1	83
4.20	Approximate series compensation adaptive controller-parameter b0	84
4.21	Approximate series compensation adaptive controller-input/output	85
4.22	Approximate series compensation adaptive controller-control effort	86
5.1	Pole assignment adaptive controller-parameter a1(5MHz)	92
5.2	Pole assignment adaptive controller-parameter b0(5MHz)	93
5.3	Pole assignment adaptive controller-system output(5MHz)	94
5.4	Pole assignment adaptive controller-control effort(5MHz)	95
5.5	Pole assignment adaptive controller-parameter a1(80kHz)	96

LIST OF FIGURES(CONT'D)

Figure	Title	Page
5.6	Pole assignment adaptive controller-parameter b0(80kHz).....	97
5.7	Pole assignment adaptive controller-system output(80kHz).....	98
5.8	Pole assignment adaptive controller-control effort(80kHz).....	99
5.9	pole assignment adaptive controller-parameter a1(50kHz).....	100
5.10	Pole assignment adaptive controller-parameter b0(50kHz).....	101
5.11	Pole assignment adaptive controller-system output(50kHz).....	102
5.12	Pole assignment adaptive controller-control effort(50kHz).....	103
5.13	PI adaptive controller - parameter a1(1MHz).....	104
5.14	PI adaptive controller - parameter b0(1MHz).....	105
5.15	PI adaptive controller - system output(1MHz).....	106
5.16	PI adaptive controller - control effort(1MHz).....	107
5.17	PI adaptive controller - parameter a1(1600Hz).....	108
5.18	PI adaptive controller - parameter b0(1600Hz).....	109
5.19	PI adaptive controller - system output(1600Hz).....	110
5.20	PI adaptive controller - control effort(1600Hz).....	111

LIST OF SYMBOLS

(i) MODELLING AND IDENTIFICATION

m	- cell quality
g	- gravity acceleration
F	- force
a	- acceleration
v	- speed
u	- friction factor
p	- position
y	- system output
$u(k)$	- system input
$ref(k)$	- system reference
$e(k)$	- system error
J	- loss function
θ	- parameter vector
φ	- input output vector
ψ	- input output matrix
P	- covariance matrix
ξ	- new information or white noise
$A(z^{-1})$, $B(z^{-1})$, $C(z^{-1})$	- polynomials to describe the system.
$x(k)$	- instrumental variable
n, N_a, N_b, N_c	- polynomial orders

LIST OF SYMBOLS(CONT'D)

R_{uu}	- auto-correlation function
R_{uy}	- cross-correlation function
μ	- correlation function time shift factor
f_s	- break frequency
T_0	- sample interval
T_{min}	- system minimum time constant
$W(k,\theta)$	- non-linear function in recursive maximum likelihood method
K	- gain in recursive algorithm
Ω	- system input output and new information vector
$y_f(k)$, $u_f(k)$ and $\xi(k)$	- filtered system output, input and new information
x^i	- nonlinear items in Hammanstein model
r_i	- nonlinear parameter in Hammanstein model
t	- F distribution test
σ^2	- noise error square estimation
T_a	- system main time constant
λ	- forgetting factor in the exponentially weighted least squares algorithm
V_ξ	- noise vector

(ii) ADAPTIVE CONTROLLER

$F(z^{-1})$, $G(z^{-1})$ and $H(z^{-1})$	- controller polynomials

LIST OF SYMBOLS(CONT'D)

$W_m(z^{-1})$, $B_m(z^{-1})$ and $A_m(z^{-1})$	- closed loop polynomial
$W_m(z^{-1})$, $B_m(z^{-1})$ and $A_m(z^{-1})$	- close loop transfer function polynomials
$F(z^{-1})$, $G(z^{-1})$ and $H(z^{-1})$	- controller polynomials
degF, degG	- order of polynomials
α	- pole shifting factor
β	- the width of -1 slope in approximate series compensation adaptive controller
K_e	- proportional factor in PI adaptive controller
$S(z^{-1})$, $I(z^{-1})$	- outside loop adaptive controller polynomials
PM	- phase margin
td	- half time of system response time to step given signal
w_c	- crossover frequency
$e^{\tau s}$	- system time delay
cb_i, ca_i	- discrete controller parameter

LIST OF SYMBOLS(CONT'D)

LIST OF ABBREVIATIONS

RLS	- Recursive least squares method
RELS	- Recursive extended least squares method
RGLS	- Recursive generalized least squares method
RIV	- Recursive instrumental variable method
RML	- Recursive maximum likelihood method
CORLS	- Correlation function least squares two step method
NRLS	- Nonlinear recursive least squares method
FFT	- Fast Fourier transformation
PID	- Proportional, integral and differential
PI	- Proportional and integral
DEP	- Dielectrophoresis
PRBS	- Pseudo random binary series

CHAPTER 1

INTRODUCTION

1.1 SIGNIFICANCE OF THE CELL LEVITATION APPARATUS

A cell levitation apparatus is used to characterize the dielectric properties of intact biological cells through their dielectropheretic response. The dielectric properties of the cells are of interest in several areas of physiology, biophysics and bio-engineering. It is important in the understanding of the human body to measure the physiological parameters using impedance techniques and study the biological effects of electromagnetic field[1]. The precise measurements of the electrical (dielectric) properties of biological cells and subsequent determination of cellular parameters can provide a diagnostic tool for detection of various physio-chemical effects on cells and discrimination between normal cells and "diseased" cells (such as cancer cells) in the clinical field. In cell electrofusion dipole-dipole cellular interaction plays an important role in membrane destabilization, though the fundamental mechanisms involved remain to be fully understood. Here the requirement for the optimal applied field parameters (such as field strength, pulse shape and duration, and field frequency) is crucial for obtaining better "yield", which requires thorough understanding of the electrical properties of the intact cells, the cell-medium interface, as well as cell-cell interaction.

1.2 PREVIOUS DIELECTRIC STUDIES

The frequency-dependent dielectric properties of biological particles are measured using the cell suspension method. Here the dielectric parameters, capacitance and conductance of the cell in suspension are measured over a wide frequency range using

a sensitive impedance bridge technique. More recently, the micropipette technique has been devised and used to measure the conductance and capacitance of individual cells[2]. Such inquisition, although sensitive enough to detect single channel activation in biomembranes, is restricted to low-frequency measurement. The dielectric parameters may be alternatively obtained by a motional or force response. Here both linear rotating AC electric field (electrorotation) or non-uniform AC electric field (dielectrophoresis or DEP) may be used for such a purpose. The newer methods of electrorotation and dielectrophorion have been applied in many different ways. The use of a feedback controlled non-uniform electric field has facilitated the levitation of individual intact cells. This method enables investigation of cellular frequency dependent polarization response over a wide frequency range.

1.3 SIGNIFICANCE OF ADAPTIVE CONTROL

The frequency dependence of the dielectric response here is monitored by measuring the time averaged levitation voltage squared (V^2) over the frequency range of interest. Past studies reveal that the polarization response of biological cells exhibits a marked frequency dependence, in the region of dielectric dispersion. In such a case, the feedback control parameters require adjustment in order to obtain stable levitation. Thus, full automation of the DEP levitation operation requires an adaptive technique to automatically adjust the feedback controller parameters.

1.4 PREVIOUS WORK OF ADAPTIVE CONTROLLER

The original adaptive control idea can be retraced to Kalman's paper on the design of a self-optimizing control system[3] in 1958. In 1970, Peterka applied this idea to the

parameter-unknown system[4]. By 1973, Astrom and Wittenmark proposed the self-tuning regulator[5]. Their work ushered in the adaptive control epoch. Disadvantage of their algorithm is that it can not be used in a non-minimum phase system. In 1975, Clarke and Gawthrop proposed a self-tuning controller[6] to overcome the disadvantages of a self-tuning regulator, however this method requires the selection of a weight factor in the aim function. Therefore, in 1976, Edmund[7] proposed the pole-shifting/pole assignment adaptive controller. Important work on this algorithm was done by Wellstead, et al.[8] This method has advantage in every field over the above-mentioned algorithms except for the optimal criterion. Although the pole assignment adaptive controller has been used widely in the last decade, it may experience instability problems in some instances. The pole-shifting adaptive controller is therefore proposed to resolve such a problem. Like pole assignment adaptive controller, pole-shifting adaptive controller was proposed by Edmund, and developed and completed at the University of Calgary by O.P Malik and G.S. Hope.[9] This method overcomes the weakness of a pole-assignment adaptive controller. Furthermore, PID adaptive controller, LQG and generalized predictive controller (GPC) etc. were proposed respectively. Goodwin made a useful contribution on stability and convergence of self-tuning controller[10].

The adaptive control method had been used in biomedical instrumentation. Some successful examples are, arterial gas pressure[11], and blood pressure[12]. The adaptive control strategy is new to DEP based cell levitation, which is the topic of discussion in this thesis.

1.5 THESIS OUTLINE

In this thesis, a cell-levitation apparatus control system model is presented. Eight identification methods are used to obtain model parameters. Four kinds of adaptive control methods are presented to resolve the control problem. Two of them are proposed by the author. One is a dual loop adaptive control algorithm. The other is an approximate series compensation adaptive algorithm. The system simulations of these algorithms are presented. Experiments are conducted to verify the salient controller characteristics of the various control methods.

In chapter 2, the cell-levitation apparatus control is discussed. In chapter 3, modelling methods, procedures and results for various different methods are described. In chapter 4, adaptive control algorithms are used to design the control system. Two new adaptive control algorithms proposed by the author are discussed in detail and computer simulation results are given. In chapter 5, the real time control results are shown. Conclusion and evaluation of the theoretical developments as well as the control results are given in Chapter 6.

CHAPTER 2

CELL-LEVITATION APPARATUS CONTROL SYSTEM

2.1. INTRODUCTION TO CELL LEVITATION

In order to develop an adaptive control methodology for application in DEP levitation, the basic knowledge of the cell-levitation apparatus is required. This chapter describes the operational characteristics of the cell-levitation apparatus. The basic knowledge of the cell-levitation apparatus experiment such as the instrument composition, single and dual frequency levitation methods, are discussed. The details of a conventional digital PI controller are presented.

2.2 INTRODUCTION TO CELL-LEVITATION APPARATUS

To measure the characteristics of the biological cells, the cells are required to be immersed in a suspending medium. The electrical dielectric response of the cells is influenced by the electrical properties of the various cellular compartments and those of the suspending medium. For cells denser than the suspending medium, the DEP force is used to counteract the gravitational force to levitate a cell in the suspension liquid. Figure 2.1 shows a schematic view of the cell levitation chamber with a cell (black dot) located in a non-uniform electric field and a positive DEP force shown to be exerted upon the particle between the chamber electrodes.

A sectional view of the levitation chamber and a block diagram of the feedback controlled levitation apparatus is shown in Figure 2.2. The cone-plate electrode assembly is housed in a plexiglass chamber with glass covered windows to aid in the optical monitoring of the chamber contents. The window on one side is removable in order to

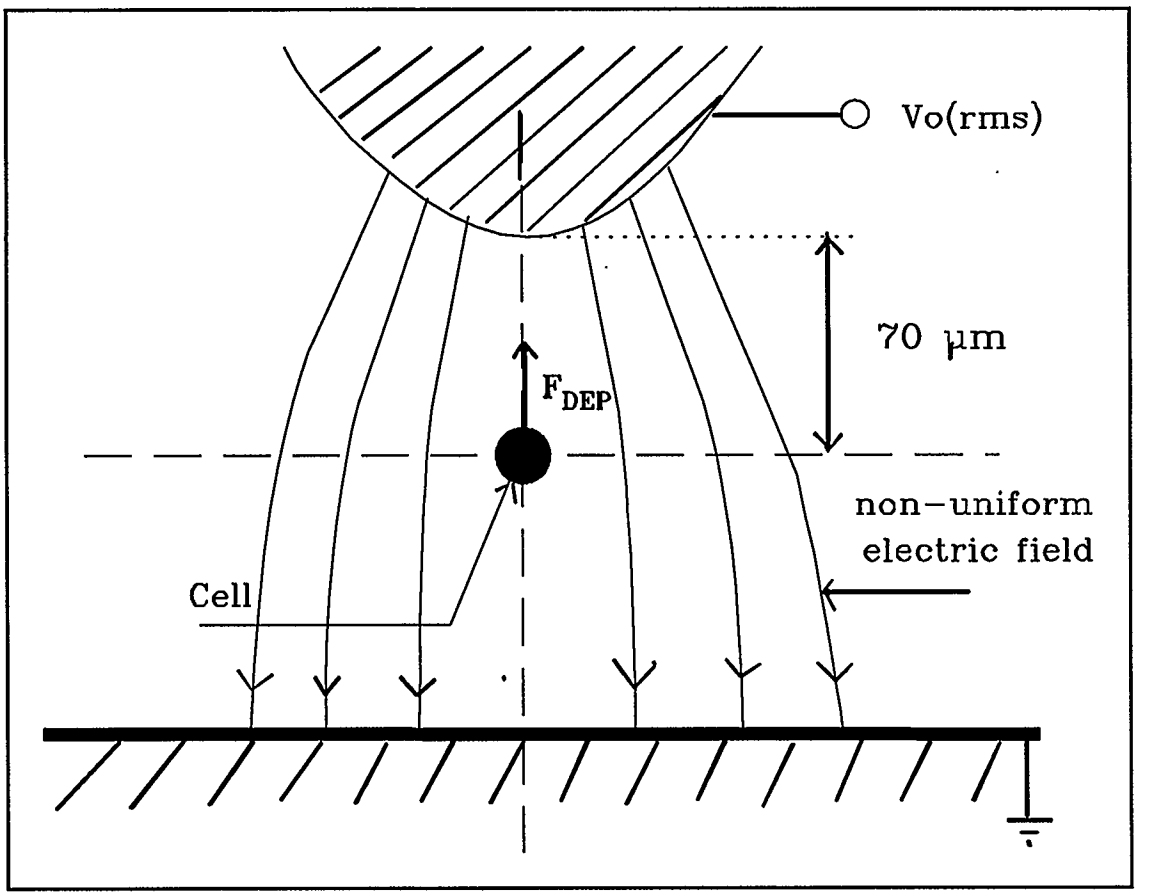

Figure 2.1 Cell-levitation apparatus electric field structure

clean the chamber and introduce a fresh dilute cell suspension each time a new experiment is conducted. In order to eliminate medium evaporation and the influence of the air current, the window is sealed with vacuum grease. The assembled chamber is mounted and held in place with spring-loaded clips on a vertical microscope stage with the chamber electrodes connected to a wide band summing amplifier.

A conventional light source fitted with an infra-red filter is used to illuminate the chamber and the cell image is focused on to a MOS solid state video camera and displayed on a TV monitor. The video signal from the camera is also made available to

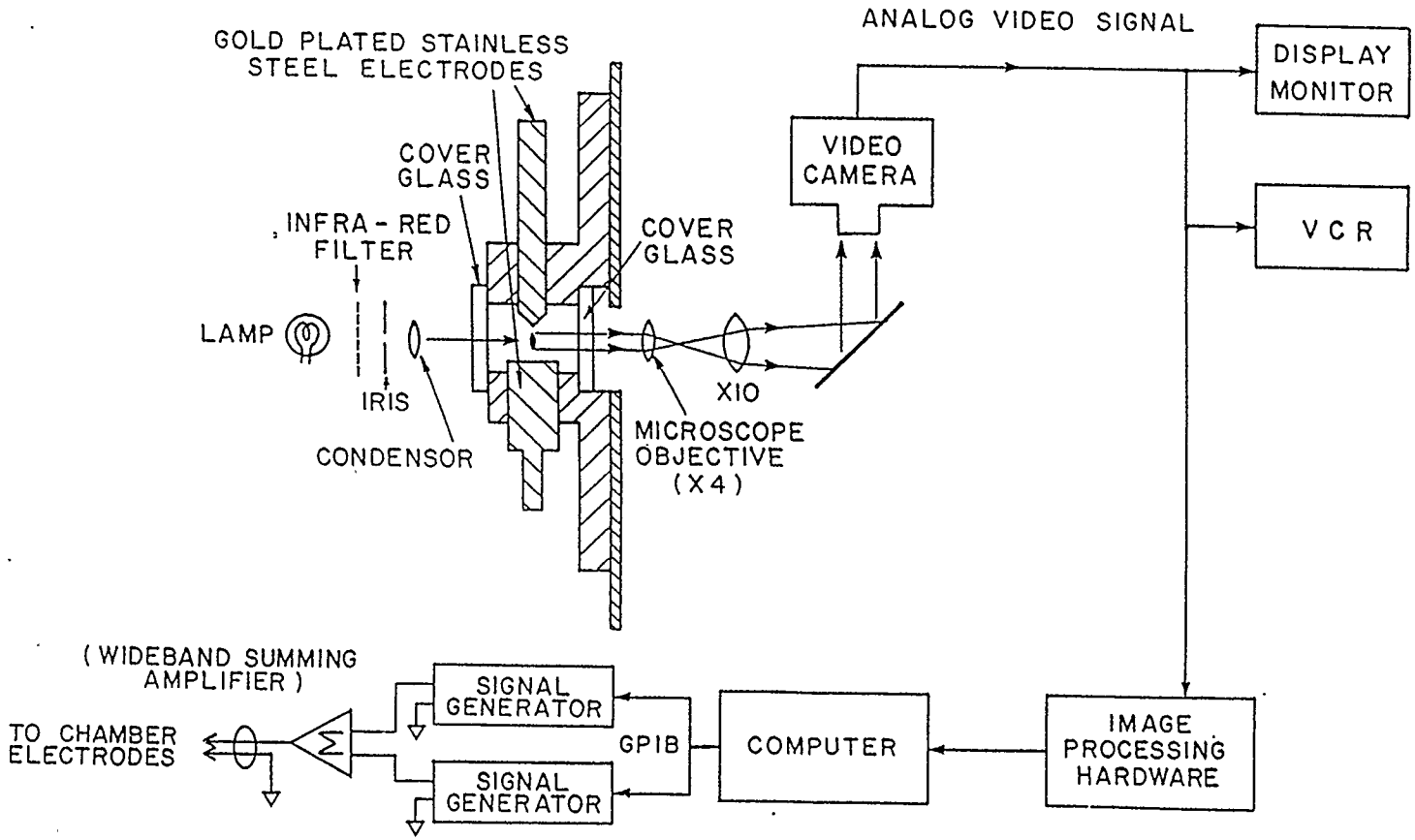

Figure 2.2 Sectional view of the levitation chamber together with the block diagram of the whole system

a real-time image acquisition PC board which is plugged into a 286-based IBM-AT computer. This computer is interfaced to two signal generators via the GPIB-488 bus to facilitate the controls of both the amplitude and frequency of the voltage applied to the chamber electrodes.

To determine the frequency dependent polarized response, the frequency of the applied voltage and the electric field is varied automatically in the range 10 Hz to $5x10^7$ Hz. And then, the instrument records the scanning frequency and root of mean square of control voltage, from which the cell properties may be extracted using a suitable cell model.

At every frequency test point, 25 data samples are taken at the required position of 200 ±1 pixel, (about 70 μm) from the conic electrode as measured on the screen. The error must not exceed ±1 pixel to accurately determine the characteristics of the cell. Sampling continues at the fixed frequency, until 25 consecutive data points are acquired.

Although the above single frequency levitation schematic can give good data samples over its useful range, the frequency band over which the cell can be stably levitated is limited. In the low frequency range, the DEP force becomes negative and hence a single frequency input is inadequate in levitating the cell. In such a case, a dual frequency levitation scheme is used to levitate the cell.

The main principle of dual frequency levitation schematic is to utilize a positive DEP force to compensate the gravitational force when levitating at low frequency, i.e. two ac voltages of different frequencies f_1 and f_2 may be synthesized to achieve this. Analysis shows that the mean-square sum of two sinusoids is approximately equal to the sum of

the mean-squares of each sinusoid, provided the frequencies are well separated.[13] When the frequency is reduced to a point where single frequency DEP force is inadequate, the dual frequency system is invoked. The two sinusoidal voltages are summed and applied to the levitation chamber electrodes, one with fixed frequency, f_H, and controllable amplitude, V_{HC}, and the other a scanning frequency, f, and fixed amplitude, V_f.

2.3 INTRODUCTION TO CONVENTIONAL CONTROL SYSTEM

A conventional digital PID controller has been used to control the levitation voltage.[14] The system is shown in figure 2.3. It consists of a controller, a control executer which converts controller output voltage into DEP force to levitate cell against the gravitational force.

The control aim is to keep the cell levitated at a fixed location between the

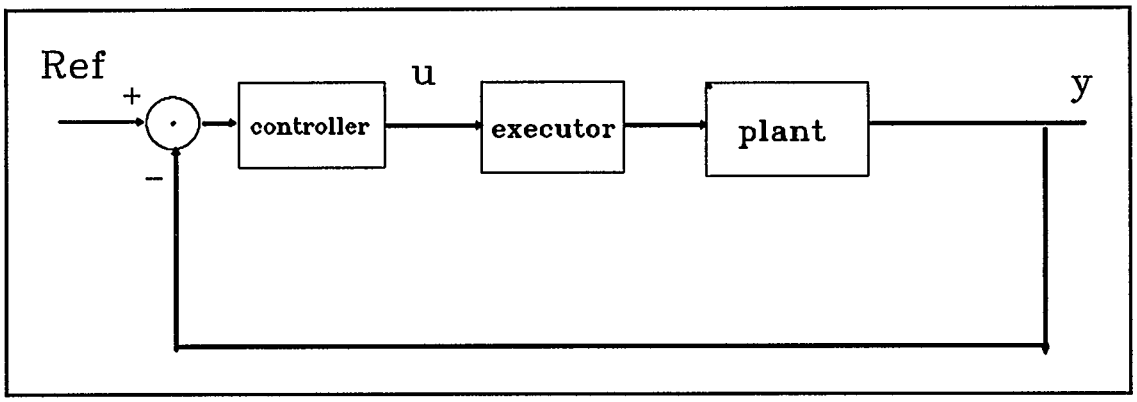

Figure 2.3 Control system block diagram

chamber electrodes (200 pixel - about 70 μm from the upper electrode). When the electric field frequency is varied from 10 Hz to 50 MHz, the PID controller parameters are adjusted manually by an operator. When the system is initialized, the frequency is set to $5x10^6$ Hz, because at this frequency, most cells are readily stabilized by the controller under the action of a positive DEP force. Typical PID parameters are as follows: proportional gain is 0.05, integral gain is 0.005, differential gain is 0.001, controller output range is 0 to 7 r.m.s.(root-mean-square). Since the differential gain is approximately zero (1/50th of the proportional gain), the controller has dominant PI characteristics.

CHAPTER 3

MODELLING OF CELL-LEVITATION APPARATUS

3.1. INTRODUCTION

In order to control the cell position in the cell-levitation apparatus system, it is necessary to determine the plant model so that the control system can be designed and simulated. First, a model from the analysis of the physical characteristics is used to determine knowledge such as structure and disturbance. Second, group system identification methods are used to determine model parameters and time delay.

3.2. ANALYTICAL MODEL OF THE CELL-LEVITATION APPARATUS

The various forces which act on a cell are shown in figure 3.1, assuming a net downward force.

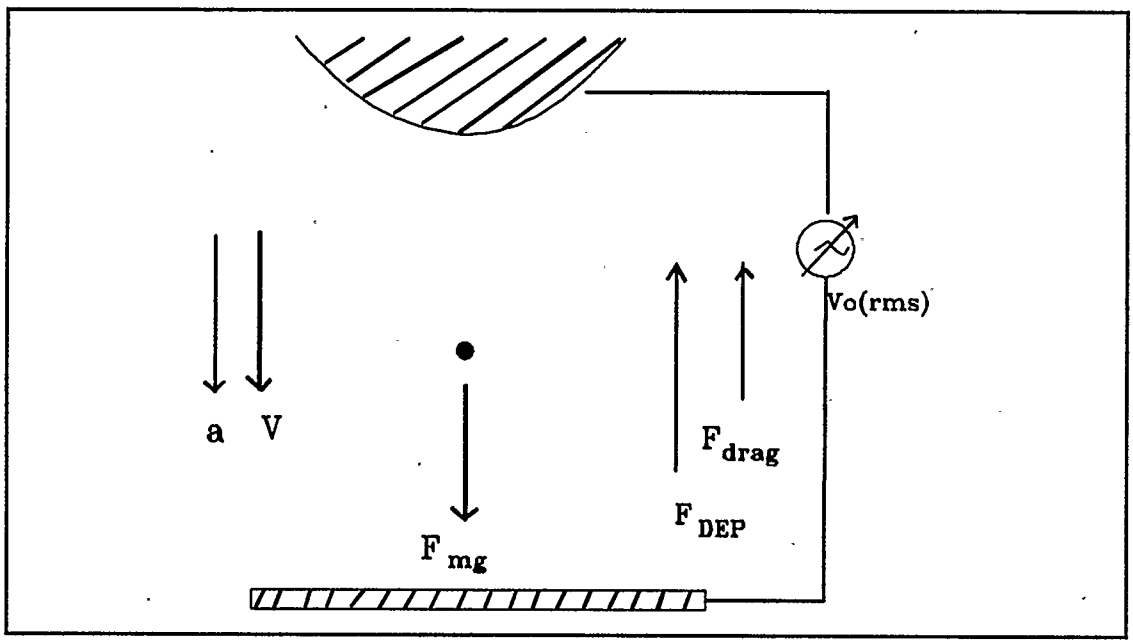

Figure 3.1 Physical analysis of the cell model

In figure 3.1, F_{mg} is the gravitational force, F_{drag} is the viscous drag force, and F_{DEP} is the DEP force required to levitate a cell. V and a are the velocity and acceleration of the cell respectively, m is the mass of the cell. The equation of spherical particles subjected to be above force is given by[16]:

$$F_{mg} - (F_{DEP} + F_{drag}) = m_{eff}a \tag{3.1}$$

where

m_{eff} is effective value of the mass and $m_{eff} = 4\pi r^3(\rho_2-\rho_1)/3$

$m = 4\pi r^3\rho_2/3$, $F_{mg} = mg$

If $F_{drag} = uv$, the equation 3.1 can be written as

$$F_{mg} - F_{DEP} - uv = m_{eff}a \tag{3.2}$$

where

u is the friction factor and $u = 6\pi\eta r$, η is the viscosity of the fluid, r is the radius of the sphere, ρ_1 is a density of the medium and ρ_2 is density of the mass of the cell.

The equation 3.2 can also be written as

$$F_{mg} - F_{DEP} = u\frac{dp}{dt} + m_{eff}\frac{d^2p}{dt^2} \tag{3.3}$$

where

p is the position of the cell.

Rewriting this equation in the Laplace form, the following equations are obtained:

$$P(s) = \frac{1}{s(\, m_{eff}s + u\,)}[\, F_{mg}(s) - F_{DEP}(s)\,] \qquad (3.4a)$$

$$G(s) = \frac{1}{s(\, m_{eff}s + u\,)} \qquad (3.4b)$$

Furthermore, the relation between DEP force and controller output voltage is $F_{DEP} \propto V^2$[17]. The system block diagram is shown in figure 3.2. From the equations 3.4a and 3.4b, some conclusions are apparent:

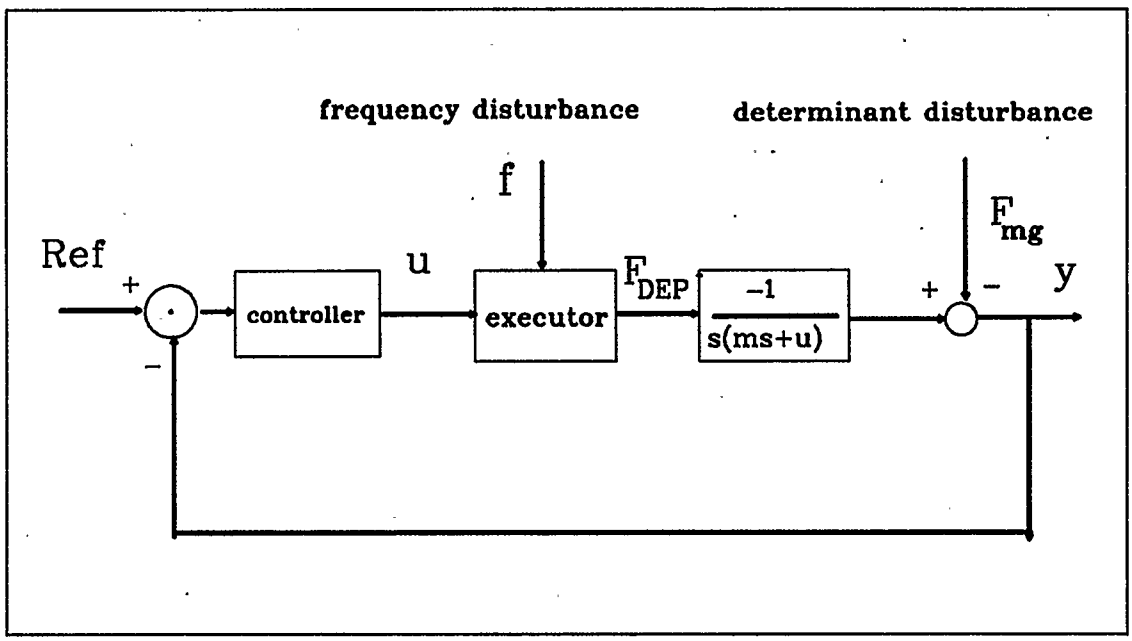

Figure 3.2 Block diagram of the model

1) this system is the second order system with a pure integral part.

2) if the DEP force can be considered as system input, this system has a determinant disturbance which depends upon cell characteristics.

3) the pure integral in the system makes it open loop unstable. Unless the DEP force is exactly equal to mg, the system output changes. Control results in chapter 5 show

that these results are very close to the practical situation.

The system structure, i.e. model order, can be determined. However, the parameters of the model for different cells, different liquid, different frequency, can not be determined by using mechanics analysis. So a system identification method is needed to obtain model parameters.

3.3 IDENTIFICATION OF THE CELL-LEVITATION APPARATUS SYSTEM

3.3.1 INTRODUCTION OF THE IDENTIFICATION ALGORITHMS

The system identification problem includes two points. One is estimating the model order, the other is estimating the model parameters. If the system order is known from the analysis of the physical characteristics, the system identification problem is reduced to a parameter estimation problem. In this stage, the order of the model is known.

There are a number of identification methods which can be used. Generally speaking, each method is suited to a given condition. For other conditions, it may be ill suited. So, based on this view, several methods are used to identify this system.

3.3.2 FFT METHOD

This is a widely used method in the signal processing field[18]. In this project, the FFT method is used as a starting point. The results from this method have some errors because the poles and zeros are obtained using a curve fit on the bode plot of the system transfer function instead of numerical values calculated directly from identification. The system poles and zeros are synthesized to create an equivalent bode plot. In the real application, it is impossible to obtain perfect curve fitting. Thus, the errors of this curve fitting is a minimum based on a least squares fit or some criteria. It is very difficult to

judge which curve gives the best values for poles and zeros. So the results from this method are not very correct and the detailed description is omitted.

3.3.3 RECURSIVE LEAST SQUARES METHOD(RLS)

This is one of the most commonly used identification methods. Theoretical analysis has proven that this method converges to the true value for a white noise disturbance. But this method is inaccurate when the noise is coloured. This method is often used as starting point to determine the basic parameter range. Then for the improved accuracy, a method which will handle coloured noise is needed.

The equation for the system output, y(k), is as follows: [19]

$$y(k)= -\sum_{i=1}^{n} a_i y(k - i) + \sum_{i=1}^{n} b_i u(k-i) + e(k) \tag{3.5}$$

where

u(k) is the system input, e(k) is the system error, a_i, b_i(i = 1, 2, ..., n) are parameters to be identified, n is the order of the model and k is the sample number.

The least squares estimation, θ_{LS}, can be found

$$\min J(\theta) =\left(\frac{1}{N}\right)\sum_{k=n+1}^{n+N} e^2(k) \tag{3.6}$$

Let:

$J(\theta)$ is loss function of the system.

$\varphi^T = [-y(k-1), \ldots , -y(k-n), u(k-1), \ldots ,u(k-n)]$

$\theta^T = [a_1, a_2, \ldots , a_n, b_1, b_2, \ldots , b_n]$

And the PRBS will be used as the input to the system. PRBS is a close approximation

to white noise.

The equation of the least squares method is as follows:

$$\hat{\theta}_{LS} = (\psi^T{}_N \psi_N)^{-1} \psi^T{}_N y_N \tag{3.7}$$

where

$$\psi^T{}_N = [\theta_n, \theta_{n+1}, \ldots, \theta_{N+n-1}]_{2n \times N}$$

This method requires large memory and extensive computation. Therefore a recursive method is needed.

The equation for the recursive least squares method is as follows:[20]

$$\hat{\theta}_{k+1} = \hat{\theta}_k + \frac{P_k \varphi_{k+1}}{1 + \varphi^T{}_{k+1} P_k \varphi_{k+1}} [\, y(k+1) - \varphi^T{}_{k+1} \hat{\theta}_k \,] \tag{3.8a}$$

$$P_{k+1} = [\, P_k - \frac{P_k \varphi_{k+1} \varphi^T{}_{k+1} P_k}{1 + \varphi^T{}_{k+1} P_k \varphi_{k+1}} \,] \tag{3.8b}$$

This recursive methods is not directly applicable when the parameters vary with time since new data are swamped by past data. However, the algorithms can be modified to handle time varying parameters by discounting old data. The exponentially weighted least squares method, which satisfies the following recursive equations, could handle this case.

$$\hat{\theta}_{k+1} = \hat{\theta}_k + \frac{P_k \varphi_{k+1}}{\lambda + \varphi^T{}_{k+1} P_k \varphi_{k+1}} [\, y(k+1) - \varphi^T{}_{k+1} \hat{\theta}_k \,] \tag{3.9a}$$

$$P_{k+1}=\frac{1}{\lambda}\left[P_k - \frac{P_k\varphi_{k+1}\varphi^T_{k+1}P_k}{\lambda + \varphi^T_{k+1}P_k\varphi_{k+1}}\right] \tag{3.9b}$$

where

λ is the forgetting factor.

3.3.4 RECURSIVE EXTENDED LEAST SQUARES METHOD(RELS)

This method is well suited to coloured noise. Although Ljung found that this method does not converge in some cases[21], experience shows that convergence is not a problem in practical applications. Although this method gives more accurate estimation of parameters a_i and b_i than the least squares method in the coloured noise case, its weakness is that it does not give an accurate measurement of the noise parameter c_i. The equation is as follows:

$$A(z^{-1})y(k) = B(z^{-1})u(k) + C(z^{-1})\xi(k) \tag{3.10}$$

where

$$A(z^{-1}) = 1 + a_1z^{-1} + \dots + a_nz^{-n}$$

$$B(z^{-1}) = b_0z^{-1} + \dots + b_{n-1}z^{-n}$$

$$C(z^{-1}) = 1 + c_1z^{-1} + \dots + c_nz^{-n}$$

and $\{\xi(k)\}$ is new information series.

If $\{\xi(k)\}$ is measurable, equation 3.10 can be written as

$$y(k) = \varphi^T_k\theta + \xi(k) \tag{3.11}$$

where

$$\varphi^T_k = [\ -y(k-1), \dots , -y(k-n), u(k-1), \dots , u(k-n),$$
$$\xi(k-1), \dots , \xi(k-n)\ ]$$

$$\theta^T = [\ a_1, \dots , a_n, b_0, \dots , b_{n-1}, c_1, \dots , c_n\ ]$$

but { $\xi(k)$} is unknown. Defining $\hat{\phi}_k$ as:

$$\hat{\phi}^T_k = [\ -y(k-1), \dots , -y(k-n), u(k-1), \dots , u(k-n),$$
$$\hat{\xi}(k-1), \dots , \hat{\xi}(k-n)\ ] \tag{3.12}$$

{$\hat{\xi}(k)$} is given by the following equation,

$$\hat{\xi}\ (k) = y(k) - \hat{\phi}^T_k\hat{\theta}_{k-1} \tag{3.13}$$

$$\hat{\theta}_{k+1} = \hat{\theta}_k + \frac{P_k\hat{\phi}_{k+1}}{1 + \hat{\phi}^T_{k+1}P_k\hat{\phi}_{k+1}}\ [\ y(k+1) - \hat{\phi}^T_{k+1}\hat{\theta}_k\ ] \tag{3.14a}$$

$$P_{k+1} = [\ P_k - \frac{P_k\hat{\phi}_{k+1}\hat{\phi}^T_{k+1}P_k}{1 + \hat{\phi}^T_{k+1}P_k\hat{\phi}_{k+1}}\ ] \tag{3.14b}$$

Because matrix P_k extension corresponds to a least squares method, this method is given an extended least squares designation. The method is widely used.

3.3.5 RECURSIVE GENERALIZED LEAST SQUARES METHOD(RGLS)

This is another method to deal with coloured noise.[22][23] Compared to the extended least squares method, this method gives not only relatively accurate parameters a_i and b_i, but also a relatively accurate noise parameter c_i. But the simulation results show that, at large noise levels, this method may not converge to the proper value. The equations of this method are as follows:

Let a system be described as:

$$A(z^{-1})y(k) = B(z^{-1})u(k) + \frac{1}{C(z^{-1})}\xi(k) \tag{3.15}$$

where

$$A(z^{-1}) = 1 + a_1 z^{-1} + \ldots + a_n z^{-n}$$

$$B(z^{-1}) = b_0 z^{-1} + \ldots + b_{n-1} z^{-n}$$

$$C(z^{-1}) = 1 + c_1 z^{-1} + \ldots c_n z^{-n}$$

Let

$$y_f(k) = C(z^{-1})y(k)$$

$$u_f(k) = C(z^{-1})u(k)$$

defining

$$\varphi_k = [\ -y_f(k-1), \ldots , -y_f(k-n), u_f(k-1), \ldots , u_f(k-n)] \tag{3.16}$$

$$\theta^T = [\ a_1, \ldots , a_n, b_0, \ldots ,b_{n-1}]$$

the system model can be written as

$$y_f(k) = \varphi^T_k \theta + \xi(k) \tag{3.17}$$

Because the noise model is unknown, an iterative method is needed to estimate the $C(z^{-1})$ polynomial. Let

$$e(k) = \frac{1}{C(z^{-1})}\xi(k) \tag{3.18}$$

Using the following slack method, polynomials $A(z^{-1})$, $B(z^{-1})$ and $C(z^{-1})$ can be determined.

a) let $C(z^{-1})$ equal I, by the common RLS method to obtain parameters of polynomial $A(z^{-1})$ and $B(z^{-1})$.

b) use $A(z^{-1})$ and $B(z^{-1})$ to get the error series $\{e(k)\}$.

$$e(k)=A(z^{-1})y(k) - B(z^{-1})u(k) \tag{3.19}$$

c) use $\{e(k)\}$ and equation $C(z^{-1})e(k) = \xi(k)$ to get $C(z^{-1})$

d) use $C(z^{-1})$ as a filter to get $y_f(k)$ and $u_f(k)$.

e) use $y_f(k)$ and $u_f(k)$ to get $A(z^{-1})$ and $B(z^{-1})$ by the common RLS method.

f) substitute new values of $A(z^{-1})$ and $B(z^{-1})$ to get new $C(z^{-1})$ repeatedly until the desired accuracy is met.

3.3.6 RECURSIVE INSTRUMENTAL VARIABLE METHOD(RIV)

This is another method used to deal with coloured noise. The main advantage of an RIV method is that it is not necessary to know the order of the noise. RELS and RGLS require that the order of the noise be known, i.e. the order of the $C(z^{-1})$ is known. In a practical application, the order of the noise is unknown. This method cannot be used to get the noise model. The basic idea of this method is described as follow:[24]

From least squares method equation

$$\theta_{LS}=\theta + [\Psi^T\Psi]^{-1}\Psi^T V_\xi \tag{3.20}$$

where

$$V^T_\xi = [\ \xi_1, \xi_2, \dots , \xi_N\ ]$$

if $[\Psi^T\Psi]^{-1}$ is singular and $\Psi^T V_\xi \rightarrow 0$, the estimation converges to the true value. For coloured noise, $\Psi^T V_\xi$ does not converge to the true value. But this equation give us an inspiration. If a matrix Z with the same dimension as Ψ can be found,

$$Y = \Psi^T\theta + V_\xi \tag{3.21}$$

It can be pre-multiplied by Z^T to obtain

$$Z^TY = Z^T\Psi\theta + Z^TV_\xi \tag{3.22a}$$

From least squares method, it is known that if

$$[\Psi^TZZ^T\Psi]^{-1} \tag{3.22b}$$

exists, we can obtain the following estimation

$$\hat{\theta}_{IV}=[\Psi^TZZ^T\Psi]^{-1}\Psi^TZZ^TY=[Z^T\Psi]^{-1}Z^TY \tag{3.22c}$$

Using equation 3.21, we have

$$\hat{\theta}_{IV}=[Z^T\Psi]^{-1}Z^T[\Psi\theta + V_\xi] = \theta + [Z^T\Psi]^{-1}Z^TV_\xi \tag{3.22d}$$

if the matrix $[Z^T\Psi]^{-1}$ is singular and Z^TV_ξ converges to 0 when data number n $\rightarrow$ infinity. Matrix Z is called an instrumental variable. Here the instrumental variable is chosen as

$$x(k) = u(k - n_b) \tag{3.23}$$

where n_b is the order of polynomial $B(z^{-1})$. It can be proven that this instrumental variable makes the estimation converge to the true value in the presence of coloured noise.[25]

Similar with least squares method, recursive instrumental variable algorithm is

$$\hat{\theta}_{IV\ k+1} = \hat{\theta}_{IV\ k} + \frac{P_k\varphi_{k+1}}{1 + \varphi^T_{k+1}P_k\varphi_{k+1}}[\ y(k+1) - \varphi^T_{k+1}\hat{\theta}_k\ ] \tag{3.24a}$$

$$P_{k+1}= [\ P_k - \frac{P_kZ_{k+1}\varphi^T_{k+1}P_k}{1 + \varphi^T_{k+1}P_kZ_{k+1}}\ ] \tag{3.24b}$$

3.3.7 CORRELATION FUNCTION LEAST SQUARES TWO STEP METHOD(CORLS)

This method is also commonly used to handle coloured noise, especially, when the noise is very large. This method uses correlation function in combination with RELS, RGLS and RIV, and it is more accurate than RELS, RGLS or RIV alone. The

disadvantage is that it can not obtain the noise model parameter.[26]

The basic idea is that the correlation function analysis method is used to determine system pulse response, and then the parameter model is obtained by identifying system pulse response with the least squares method.

Step one:

Let system input $\{u(k)\}$ and output $\{y(k)\}$ follow a stationary stochastic process:

$$A(z^{-1})y(k) = B(z^{-1})u(k) + C(z^{-1})\xi(k) \tag{3.25}$$

where

$$A(z^{-1}) = 1 + a_1z^{-1} + \dots + a_nz^{-n}$$

$$B(z^{-1}) = b_0z^{-1} + \dots + b_{n-1}z^{-n}$$

$$C(z^{-1}) = 1 + c_1z^{-1} + \dots + c_nz^{-n}$$

and $\{\xi(k)\}$ is new information series.

The auto-correlation function of an input signal is

$$R_{uu}(\mu) = \lim_{N\to\infty}\frac{1}{N}\ g(\delta)R_{uu}(k-\delta) \tag{3.26}$$

Where an input signal is white noise, equation 3.26 can be written as

$$g(\mu)=\frac{1}{R_{uu}(0)}R_{uy}(\mu) \tag{3.27}$$

If the system input, $\{u(k)\}$, is not related to the random series $\{\xi(k)\}$, the equation

$$y(k) + a_1y(k-1) + \dots + a_ny(k-n) =$$

$$b_0u(k-1) + \dots + b_nu(k-n) + \xi(k) \tag{3.28}$$

can be written as

$$R_{uy}(\mu) + a_1R_{uy}(\mu-1)+ \dots + a_nR_{uy}(\mu-n)$$

$$=b_1R_{uu}(\mu-1) + \dots + b_nR_{uu}(\mu-n). \tag{3.29}$$

Step two:

Use least squares method to identify parameters $a_1, \dots, a_n, b_0, \dots, b_n$. The system model parameters can be calculated and the result is more accurate than the least squares method.

3.3.8 RECURSIVE MAXIMUM LIKELIHOOD METHOD(RML)

This method has a long history, and is widely used. If the noise test is correct, this method gives very good results. The equation of this method is as follows:[27]

Let a system be described as:

$$A(z^{-1})y(k) = B(z^{-1})u(k) + \frac{1}{C(z^{-1})}\xi(k) \tag{3.30}$$

where y(k), u(k) and $\xi(k)$ are model output, input and new information respectively, and

$$A(z^{-1}) = 1 + a_1z^{-1} + \dots + a_nz^{-n}$$

$$B(z^{-1}) = b_0z^{-1} + \dots + b_{n-1}z^{-n}$$

$$C(z^{-1}) = 1 + c_1z^{-1} + \dots + c_nz^{-n}$$

In this case, maximum likelihood estimation is equivalent to minimizing the following equation

$$J_N(\theta) = \sum_{k=1}^{N} W^2(k,\theta) \tag{3.31}$$

where

$$W(k,\theta)=C(z^{-1})[A(z^{-1})y(k) - B(z^{-1})u(k)] \tag{3.32}$$

$$\theta = [a_1, \dots , a_n, b_0, \dots , b_{n-1}, c_1, \dots , c_n]^T \tag{3.33}$$

Using Taylor series, an approximate maximum likelihood recursive method can be obtained. The equations are as follows:

$$\theta_{k+1}=\theta_k + K_{k+1}\xi(k+1) \tag{3.34}$$

$$K_{k+1}=P_k \frac{\Omega_{k+1}}{1 + \Omega^T_{k+1}P_k\Omega_{k+1}} \tag{3.35}$$

$$P_k=[I-K_k\Omega^T_k]P_{k-1} \tag{3.36}$$

$$\xi(k)=y(k) - \varphi^T(k)\theta(k-1) \tag{3.37}$$

$$\Omega(k) = [- y_f(k-1), \dots , -y_f(k-n), u_f(k-1), \dots , u_f(k-n_b), \xi_f(k-1), \dots , \xi_f(k-n_c)]^T \tag{3.38}$$

$$y_f(k) = C(z^{-1})y(k) \tag{3.39}$$

$$u_f(k) = C(z^{-1})u(k) \tag{3.40}$$

$$\xi_f(k) = C(z^{-1})\xi(k) \tag{3.41}$$

Some authors show that this algorithm has better convergence properties than the extended least squares method and converges to a local minimum value of an estimation criterion according to probability 1[28].

3.3.9 NONLINEAR LEAST SQUARES METHOD(NRLS)

According to theoretical analysis, the relation between voltage and electric force is $F_{DEP} \propto V^2$, so a nonlinear method is used. There are lots of methods to solve nonlinear

system identification problem. The method selected here is the Hammerstein model. The equation of this method is as follows:

Let the system nonlinear part be approximated by the following series:

$$r_0 + r_1x + r_2x^2 + r_3x^3 + r_4x^4 + \ldots \tag{3.42}$$

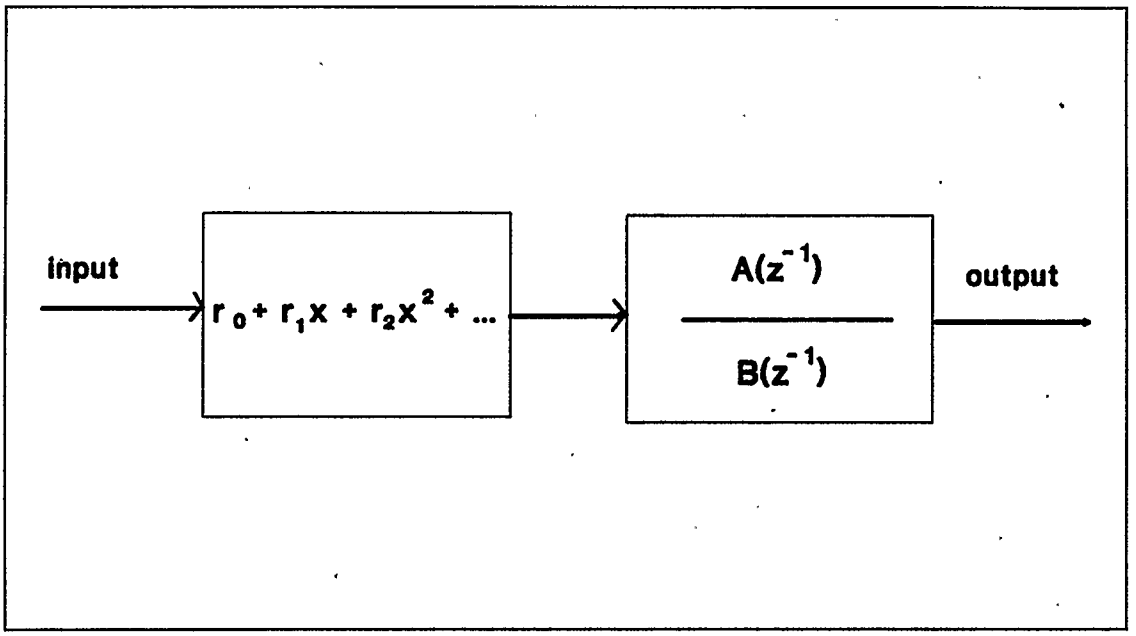

Figure 3.3 Nonlinear least squares method - Hammerstein model

If this part is cascaded with linear system which can be described by an nth order differential equation, this method can describe many kinds of nonlinear systems. If nonlinear part is cascaded before linear part, it is Hammerstein model. For this system, the nonlinear part of the system is only V^2, i.e. it has only the x^2 item. So an identification could use the system input signal squared to identify the system directly.

3.4 MODEL ORDER JUDGEMENT

The above-mentioned methods require that the model order be known. In practical applications, the measured input and output of the system contains other components,

such as video camera and image processing hardware, as shown in figure 2.2. The whole system may be more than second order as shown in equation 3.4b. So the model order is not known. For further verification, several model order estimation criteria are used and the results are compared. If most of results are close, they are considered reasonable. In this project, the following four criteria are used.

1) Loss function (or sum of error squares)

$$J(n) = \frac{1}{2} \sum_{k=1}^{n} e^2(k) \tag{3.43}$$

2) AIC (Akaike information criterion)[29]

$$AIC(K) = -2\log(L)+2K \tag{3.44}$$

where

K is the number of parameters in the polynomials $A(z^{-1})$, $B(z^{-1})$ and $C(z^{-1})$ (if $C(z^{-1})$ is used in the model).

L is the maximum value of the likelihood function[30].

3) Noise error squares estimation

$$\hat{\sigma}^2 = \frac{1}{N} \sum_{k=1}^{N} e^2(k) \tag{3.45}$$

where

N is the length of the sampling data.

4) FPE(final prediction error)[32]

$$FPE(N_a, N_b) = \left(\frac{N + N_a + N_b}{N - N_a + N_b} \right) \hat{\sigma}^2 \tag{3.46}$$

where

N_a and N_b are the orders of the model polynomials $A(z^{-1})$ and $B(z^{-1})$.

N is the length of the sampling data.

$\hat{\sigma}^2$ is the noise error squares estimation.

The model order is usually determined using an open loop identification. In the closed loop identification, the system input and output are correlated with each other, so the methods of model order judgement could be in error. Generally speaking, the model order should be known for closed loop identification. Although there are methods proposed to judge model order in closed loop identification, a complicated calculation is needed. So in practical applications, theoretical analysis and open loop order judgement methods are combined. The results are compared to obtain reasonable values.

3.5 IDENTIFICATION EXPERIMENT DESIGN

In the identification experiment, some problems must be considered.

1) noise length. 2) noise amplitude. 3) sampling period.

1) noise length:

In order to get an accurate identification, the PRBS noise should cover the whole dynamic process. If this process is too long, the system characteristics could change and the identification may be inaccurate. So a method commonly used is to apply a step signal to the system to determine the system dynamic process time.

2) noise amplitude:

In a linear system, larger noise amplitude gives more accurate identification. But for a nonlinear system, which is the normal case in a practical application, large noise

amplitude forces the system beyond the linearized range. The identification will have errors. In this system, the system reference input is equal to 200. 5% of the system reference signal is selected, i.e. noise amplitude is 10.

3) sampling interval

In order to get accurate identification results, a suitable sampling interval must be adopted. As the sampling interval is increased, the identification is more robust. If the system has very close multi-poles, shorter sampling interval must be adopted in order to distinguish these poles. But the shorter sampling interval choice normally makes the system identification very sensitive. Too short a sampling interval, sometimes, interferes with identification convergence if the model order is chosen lower than the practical system order. When sampling interval is too short, the higher poles and zeros cannot be neglected any more.

The sample frequency or break frequency, f_s, is based on Shannon sampling theory.

$$f_s = \frac{1}{2T_0} \tag{3.47}$$

where

T_0 is sampling interval, f_s is break frequency.

Some authors express the sample interval as:[31]

$$T_0=T_{min} \tag{3.48}$$

where T_{min} is system minimum time constant. Practical experience shows that this is the conservative choice. For most systems, a more appropriate choice is $T_0=2T_{min}$. An all

round values often used is [32]

$$T_0=(\ 0.05 \sim\ 0.1\ )T_a \tag{3.49}$$

where T_a is main system time constant.

3.6 IDENTIFICATION OF CELL-LEVITATION APPARATUS

The identification process includes three steps. In the first step, important frequency points are selected and the above-mentioned identification methods are used to determine the parameters. Second step, sample data using the single frequency method to obtain a plot of the identification parameters v.s. frequency from approximately 10^3 Hz to 10^7 Hz. Third step, using the dual frequency method, the parameters in the remaining 10 Hz to 10^3 Hz are obtained.

3.6.1 RESULTS AT IMPORTANT POINTS

The standard frequency band extends from $5x10^5$ Hz to $5x10^6$ Hz. In this frequency band, the model parameters are basically constant, even for different cells. So this frequency band is chosen as a starting point. Two groups of data are obtained at frequencies of $5x10^5$ Hz and $5x10^6$ Hz.

A) Data group 1:

This group data is sampled at frequency $5x10^5$ Hz:

The number of sampling data points is 300 and the sampling interval is 0.317 second. The identification process is as follows:

First step: first, second and third order models are tried respectively;

Second step: the poles and zeros close to origin are cancelled one by one, using theoretical analysis and sum of error squares. Because normally, the poles and zeros close

to origin are very small, if they cancel each other, the sum of error squares does not change significantly.

Third step: the identified parameter from different methods are compared and the most likely values are selected.

The table 3.1 shows the identification results of data group 1. The results from the six different methods are shown for different model orders. After cancelling poles and zeros close to origin, the results from different identification methods are as follows:

algorithm	order	a1	a2	a3	b0	b1	b2	c1	c2	c3
RLS	1	-.9423			-.872					
	2	-1.026	0.7187		-.6754	-3.449				
	3	-.7704	-.2632	0.0067	-.7019	-3.611	-1.031			
RIV	1	-.65			-.01					
	2	-.956	-.1859		-.5503	-3.408				
	3	-.838	0.0414	.09937	-.0574	-3	-.2782			
RELS	1	-.9291			-.8765			.0792		
	2	-1.026	0.007		-.6785	-3.446		.00297	-.0011	
	3	-.7956	-.1928	-.0461	-.7509	-3.519	-1.065	.067	.1487	.2577
RML	1	-.9423			-.872					
	2	-1.026	.0072		-.6754	-3.449				
	3	-.7704	-.2632	.00676	-.7019	-3.611	-1.031			
CORLS	1	-.5503			-1.698			.7632		
	2	-1.048	-.0159		-.8279	-3.529		.1099	.0737	
	3	-.2887	-.8059	-.0216	-.7424	-4.103	-2.661	.2419	.1944	.3219
GRLS	1	-.3943			1.0558			-.812		
	2	-.98	-.0336		-.6515	-3.42		-.0206	-.0779	
	3	-.4629	-.5789	.03342	-.7036	-3.7	-1.892	-.4433	.1746	-.2675

TABLE 3.1 IDENTIFICATION RESULTS OF DATA GROUP 1

1) RLS method:

a1=-1.02	b0=-0.6854	b1=-3.456	
J=103.265	$\hat{\sigma}^2$=.688	AIC=-106	FPE=.702

2) RIV method:

a1=-1.02	b0=-0.6786	b1=-3.4593	
J=103.26	$\hat{\sigma}^2$=.688	AIC=-106	FPE=0.7023

3) RELS method:

a1 = -1.022	b0=-.6877	b1=-3.454	c1=-.042
J=103.26	$\hat{\sigma}^2$=.6884	AIC=-106	FPE=0.702

4) RML method:

a1=-1.019	b0=-0.6766	b1=-3.4584	
J=103.26	$\hat{\sigma}^2$=0.688	AIC=-106	FPE=0.7023

5) CORLS method:

a1=-1.119	b0=-0.952	b1=-3.6153	
J=138.1	$\hat{\sigma}^2$=0.92	AIC=-18.78	FPE=0.939

6) GRLS method:

a1=-1.02	b0=-0.6641	b1=-3.497	c1=0.223
J=103.39	$\hat{\sigma}^2$=.6892	AIC=-105.7	FPE=0.703

From this group of very different identification methods, the following conclusion may be arrived at. The identification results of most of methods are similar. That means this overall identification is reasonable and can be accepted. Correlation function least squares two step method(CORLS) gives an identification which noticeably deviates from the other

techniques. That is because this identification is carried out on a closed loop system and the input signal has an output component which makes correlation function errors. Non-linear least squares method results are as follows

a1=-0.916 b0=0.598 b1=-1.283 J=1532

This method gives results different from the other methods. In this system, the linear factor dominates the square factor and so this method is considered to be inaccurate.

B) Data group 2

The identification results for group 2 are summarized in table 3.2. The identification process is the same as group 1 except that the system frequency is $5x10^6$ Hz. After cancelling pole and zeros close to origin, the model parameters are obtained.

algorithm	order	a1	a2	a3	b0	b1	b2	c1	c2	c3
RLS	1	-.9313			-.0884					
	2	-1.041	.0056		-.6517	-4.15				
	3	-.7747	-.282	.0078	-.6887	-.6527	-4.157			
RIV	1	-.6949			-.019					
	2	-.7517	-.185		-.2462	-4.186				
	3	-.8933	-.518	.4827	-.3253	-4.075	.0825			
RELS	1	-.8959			-.882			-.1785		
	2	-1.064	.021		-.674	-4.17		-.206	-.016	
	3	-.8309	-.223	.0065	-.6864	-4.28	-1.003	-.5518	.0067	.0267
RML	1	-.9313			-.8835					
	2	-1.04	.0056		-.6517	-4.149				
	3	-.7747	-.282	.0078	-.6887	-4.314	-1.237			
CORLS	1	1.02			6.251					
	2	-1.075	.4462		-.677	-4.122				
	3	-1.057	-.02	-.03	-.8839	-4.314	-.261			
GRLS	1	-.191			1.605			-.9047		
	2	-1.004	-.002		-.526	-4.06		-.0931	-.316	
	3	-.647	-.344	-.0171	-.548	-4.25	-1.6	-.399	-.231	-.1077

TABLE 3.2 IDENTIFICATION RESULTS OF DATA GROUP 2

1) RLS method:

a1=-1.0366	b0=-.6527	b1=-4.157	
J=66.25	$\hat{\sigma}^2$=.4417	AIC=-239.2	FPE=.451

2) RIV method:

a1=-.8036	b0=.1302	b1=-3.687	
J=211.1	$\hat{\sigma}^2$=1.407	AIC=108.51	FPE=1.435

3)RELS method:

a1=-1.0494	b0=-.6902	b1=-4.205	
J=66.603	$\hat{\sigma}^2$=.444	AIC=-237.6	FPE=.453

4) RML method:

a1=-1.366	b0=-.6527	b1=-4.1573	
J=66.252	$\hat{\sigma}^2$=.4417	AIC=-239.2	FPE=.4506

5) CORLS method:

a1=-1.12	b0=-.93	b1=-4.324	
J=83.763	$\hat{\sigma}^2$=.5584	AIC=-168.8	FPE=.5697

6) GRLS method:

a1=-1.04	b0=-.678	b1=-4.1895	
J=66.284	$\hat{\sigma}^2$=.4419	AIC=-239	FPE=.4508

From these results, the following observations are made:

1) This system is basically first order system. Although theoretical analysis shows that this system is the second order system, the parameter a2 is small, difficult to be identified and does not affect the results.

2) This system has an approximately one step time delay.

3) This system contains first order coloured noise which has relative small affects on system identification.

3.6.2 RESULTS OF SINGLE FREQUENCY CONDITION

For single frequency method, the frequency changes from $5x10^7$ Hz to $8x10^3$ Hz. The aim of this experiment is to determine how the system parameters vary with frequency. The RELS identification method is used in this identification. If the accuracy of the parameters obtained from this method is suspect, other methods are used to obtain the additional values. The data which is suspected of containing errors is discarded if the identification parameters from these data by different methods are quite different. The experiment conditions are as follows:

cell diameter	40 μm;
distance from electrode to cell	200 pixel (70 μm);

Figure 3.4 shows that the identification value of parameter a_1 is about -1.03±0.02. The parameter bias is about 2% average value, that means that parameter a_1 does not change with frequency change. Figure 3.5 shows the identification result of parameter b_0. The parameter b_0 is about -1.3±0.3, the bias is about 30% of average value. The figure 3.6 shows parameter b_1. From this figure, we can see that parameter b_1 is consistent over much of the frequency range. However at the low end, the DEP force diminishes, which is reflected in the identification value variation at frequency lower than $1x10^5$ Hz. The parameter value changes from -7.5 to -4, the variation is about 50% of the normal value. From these results, some conclusions can be obtained.

1) parameter a_1 is basically constant, does not change with frequency change.

2) $|b_0| << |b_1|$ at normal frequency. That means the parameters b_0 is less important than parameter b_1, and also this system is non-minimum phase system.

3) The parameter $|b_1|$ changes greatly in the lower frequency range($< 1x10^5$ Hz). It becomes smaller.

3.6.3 RESULTS OF DUAL FREQUENCY CONDITION

In order to extend the levitation range to lower frequencies, a dual frequency levitation scheme is introduced into this system. In order to control this system, the dual frequency system is also identified. The results of this system are shown in figures 3.7 to 3.9. From these identification results, the following conclusions are obtained:

1) parameter a_1 is similar to single frequency condition, parameter value is about -1.03±0.02, the bias is about 2% of the average value.

2) The value of the parameter b_0 is small, -0.6±0.2, the bias is 30% of the average value. Compared to single frequency, the value of the b_0 is smaller, that is because the diameter of the cell in figures 3.7 to 3.9 is 30 μm but the diameter of the cell in figures 3.4 to 3.6 is 40 μm. Normally, the larger the diameter of the cell, the heavier the cell.

3) parameter b_1 is quite different from the single frequency parameter value. It does not change as much as the dual frequency. The average value is about -0.95±0.15, the bias is %15 of the average value. The value is also smaller than single frequency because the diameter of the cell for the dual frequency condition is smaller than for the single frequency condition.

4) In dual frequency condition, parameter $|b_0|$ is not << parameter $|b_1|$.

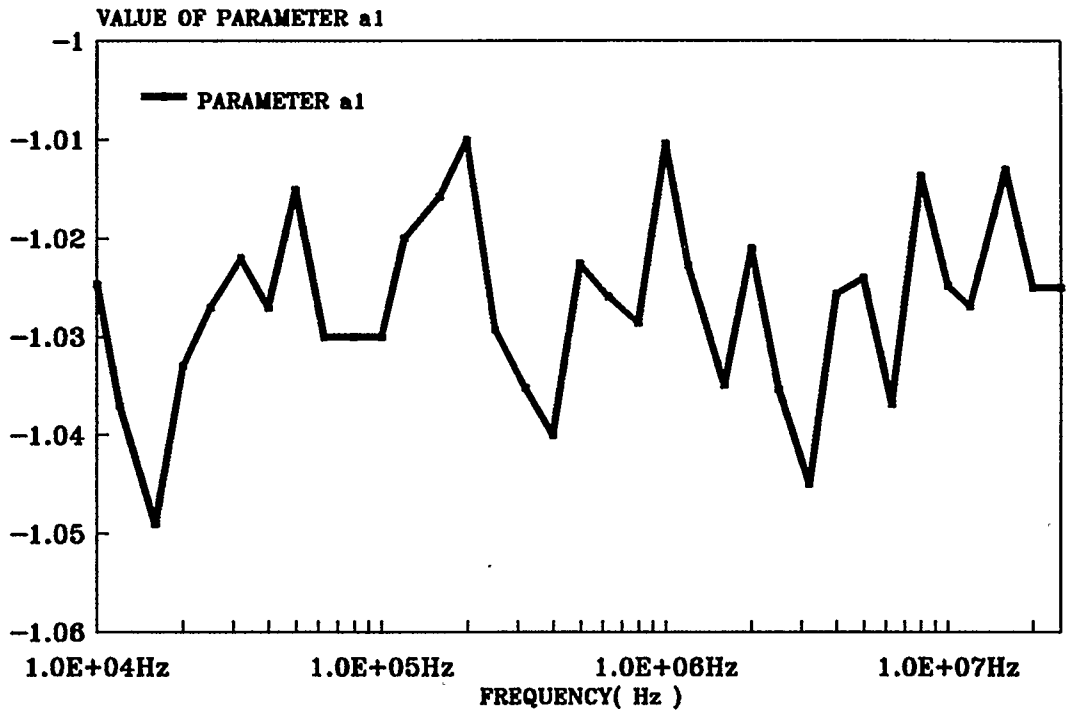

Figure 3.4 parameter a1
diameter=40 um, distance=70 um
– single frequency condition –

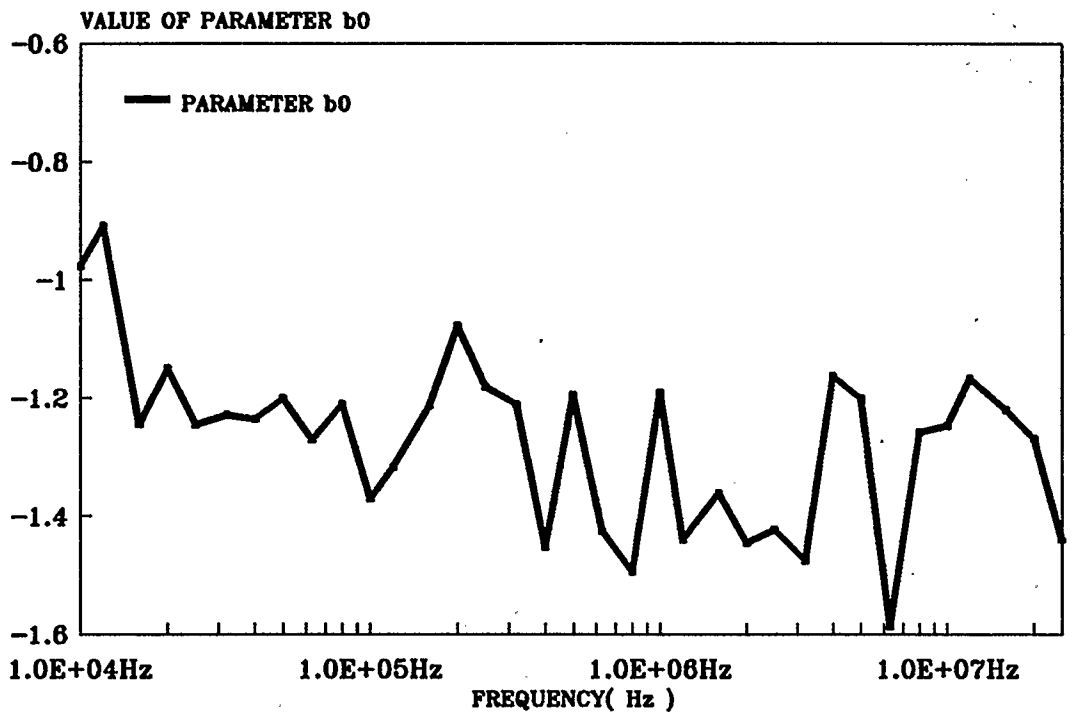

Figure 3.5 Parameter b0
diameter=40 um, distance=70 um
– single frequency condition –

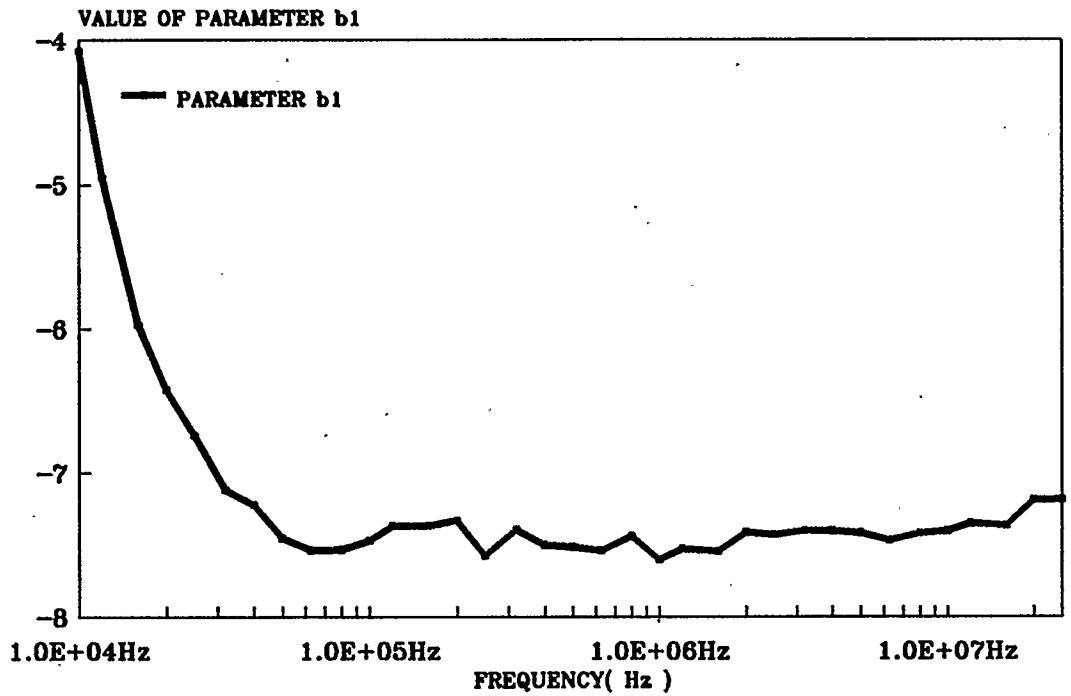

Figure 3.6 Parameter b1
diameter=40 um, distance=70 um
– single frequency condition –

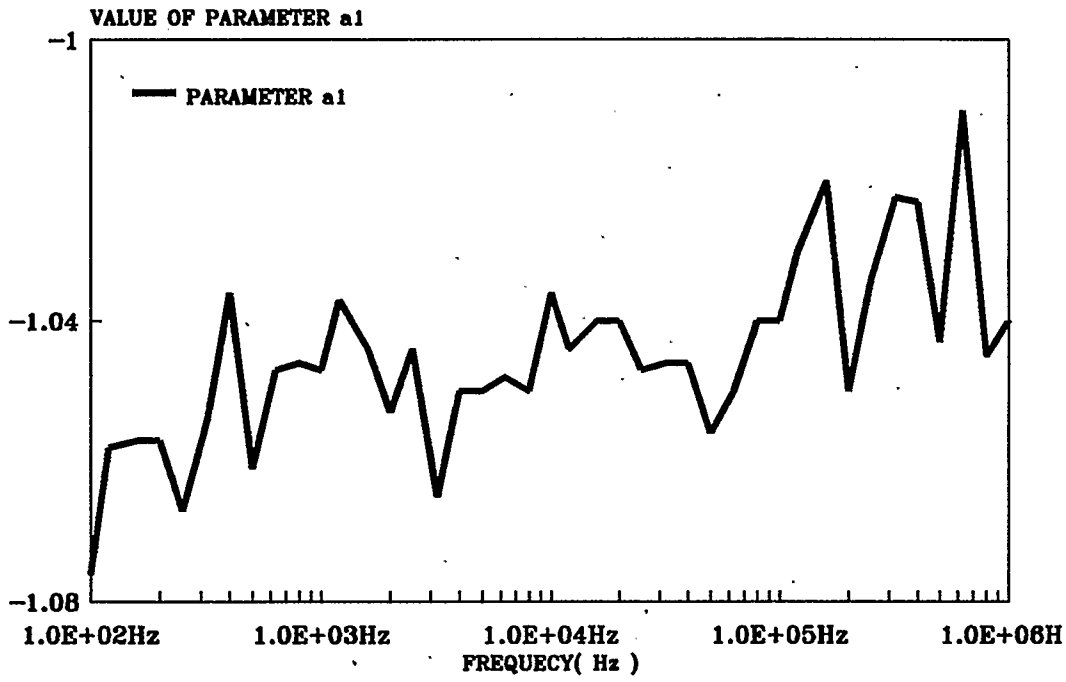

Figure 3.7 Parameter a1
diameter=30 um, distance=70 um
– dual frequency condition –

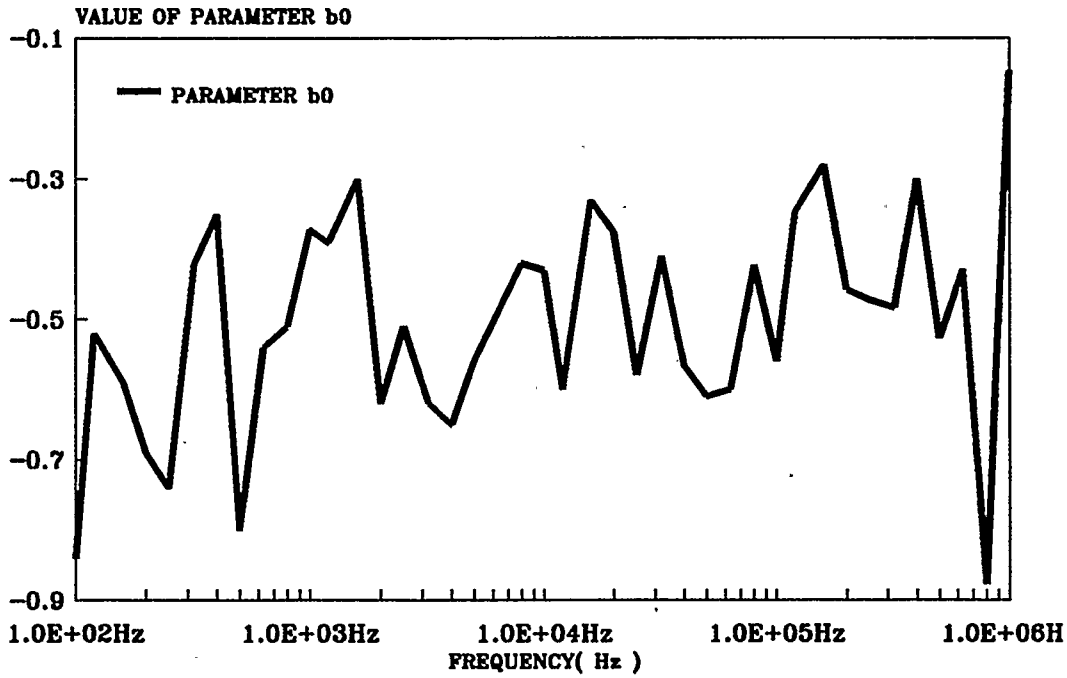

Figure 3.8 Parameter b0
diameter=30 um, distance= 70 um
– dual frequency condition –

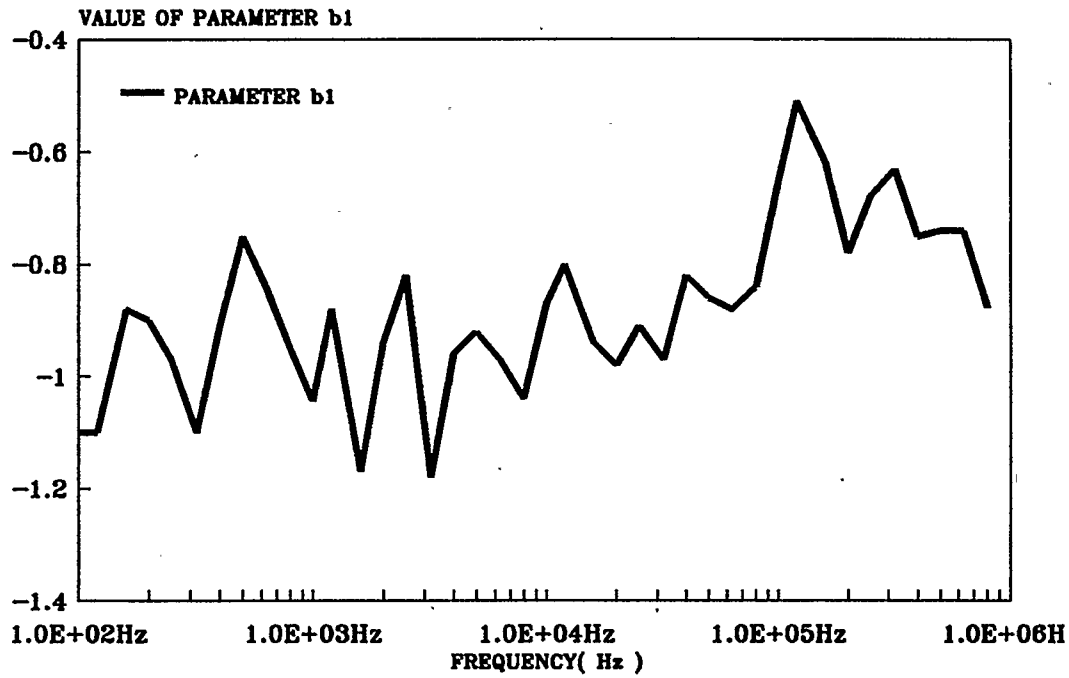

Figure 3.9 parameter b1
diameter=30 um, distance=70 um
– dual frequency condition –

CHAPTER 4

ADAPTIVE CONTROL SYSTEM DESIGN

4.1 INTRODUCTION

Since Astrom's first paper on an adaptive regulator, adaptive techniques have developed very rapidly. They have spread to an adaptive predictor, an adaptive filter, etc, and have been widely used in control system, signal processing, telecommunication and other fields.

In this project, four adaptive algorithms are tested for application in feedback controlled DEP levitation of biological cells. These include a pole assignment adaptive controller, a PI adaptive controller, a pole-shifting dual-loop adaptive controller and an approximate series compensation adaptive controller. The later two adaptive controllers are those that were proposed by the author.

The following sections describe the simulation results. The cell-levitation apparatus model is selected from the identification parameters in section 3.6. The parameters are selected as follows:

$$A(z^{-1}) = 1 - 1.056\ z^{-1}$$

$$B(z^{-1}) = 1.076z^{-1} + 5.226z^{-2}$$

In the simulation, the identification algorithm is recursive least squares algorithm.

4.2 POLE ASSIGNMENT ADAPTIVE CONTROLLER:

4.2.1 INTRODUCTION TO ALGORITHM

Pole assignment adaptive control is a classic design method[9]. This method is adopted in this project as the first step because it has been extensively applied in the past

and proven to be very useful. The block diagram is shown in figure 4.1.

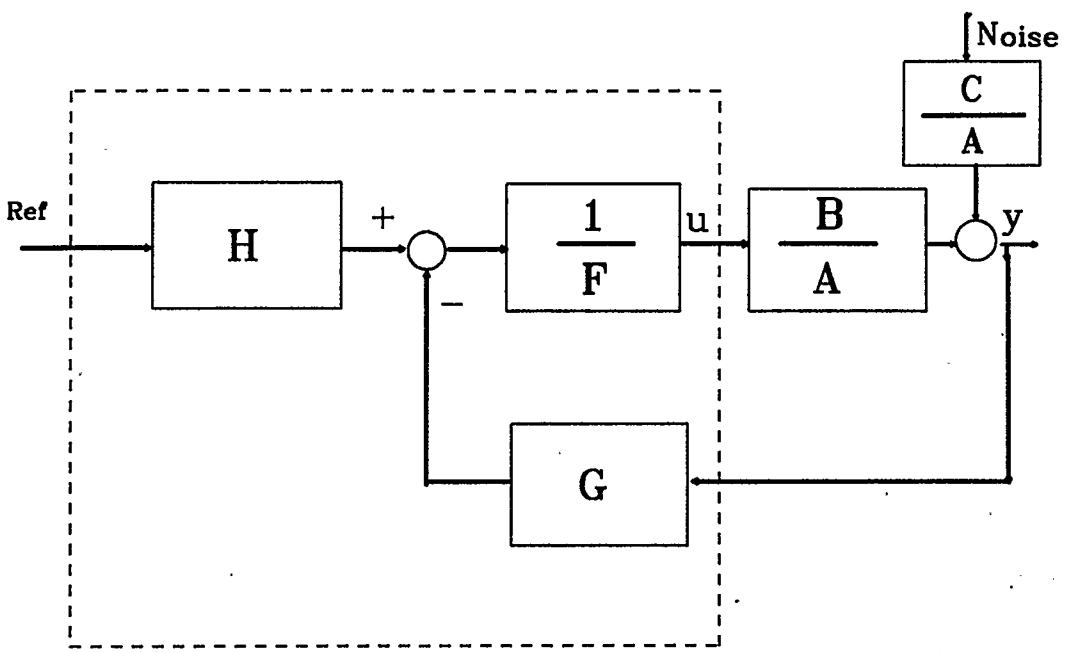

Figure 4.1 Block diagram of a pole assignment adaptive control system

Considering the following system model

$$A(z^{-1})y(k)=B(z^{-1})u(k)+C(z^{-1})\xi(k) \qquad z \geq 1 \tag{4.1}$$

where

$$A(z^{-1})=1+a_1z^{-1}+...+b_nz^{-n}$$

$$B(z^{-1})=b_0z^{-1}+...+b_{n-1}z^{-n}$$

$$C(z^{-1})=1+C_1z^{-1}+...+C_nz^{-n}$$

and $\{u(k)\}$ is the system input, $\{y(k)\}$ is the system output and $\{\xi(k)\}$ is white noise.

The closed loop transfer function is

$$W_m(z^{-1})= B_m(z^{-1})/A_m(z^{-1}) \tag{4.2}$$

The feedback control strategy is as follows,

$$F(z^{-1})u(k) = H(z^{-1})Ref(k) - G(z^{-1})y(k) \tag{4.3}$$

where

$F(z^{-1})$, $G(z^{-1})$ and $H(z^{-1})$ are polynomials and depend on the closed loop poles and zeros. {Ref(k)} is the system reference signal.

The task of control system design is to choose suitable values for F, G and H so that closed loop has stable poles and zeros. i.e.

$$\frac{B(z^{-1})H(z^{-1})}{A(z^{-1})F(z^{-1}) + B(z^{-1})G(z^{-1})} = \frac{B_m(z^{-1})}{A_m(z^{-1})} \tag{4.4}$$

The F and G are determined from a Diophantine equation[33]

$$AF + BG = A_m \tag{4.5}$$

If A and B are coprime, the polynomials F and G of the above equation have minimum resolution for the following conditions:

$$degF = n_f = n_b - 1 \tag{4.6a}$$

$$degG = n_g = n_a - 1 \tag{4.6b}$$

where

degF and degG are the orders of polynomials $F(z^{-1})$ and $G(z^{-1})$, n_f, n_b, n_g and n_a also express the orders of polynomials $F(z^{-1})$, $B(z^{-1})$, $G(z^{-1})$ and $A(z^{-1})$ respectively.

For non-minimum phase system, normally, the control system designers do not cancel the plant zeros. However if $H(z^{-1})$ is chosen as pure gain, it forces the system output to track the input signal.

The closed loop output equation of the system can be written as follows

$$y(k)=\frac{B(z^{-1})H(z^{-1})}{A_m(z^{-1})}Ref(k)+\frac{C(z^{-1})F(z^{-1})}{A_m(z^{-1})}\xi(k) \tag{4.6c}$$

$$u(k)=\frac{A(z^{-1})H(z^{-1})}{A_m(z^{-1})}Ref(k)-\frac{C(z^{-1})G(z^{-1})}{A_m(k)}\xi(k) \tag{4.6d}$$

The system output error equation is

$$e(k) = Ref(k) - y(k)$$

$$=\frac{A_m(z^{-1})-B(z^{-1})H(z^{-1})}{A_m(z^{-1})}Ref(z^{-1})-\frac{C(z^{-1})F(z^{-1})}{A_m(z^{-1})}\xi(k)$$

$$= G_e(z^{-1})Ref(z^{-1}) - G_\xi(z^{-1})\xi(k) \tag{4.6e}$$

where

$$G_e(z^{-1})=\frac{A_m(z^{-1})-B(z^{-1})H(z^{-1})}{A_m(z^{-1})}$$

$$G_\xi(z^{-1})=\frac{C(z^{-1})F(z^{-1})}{A_m(z^{-1})}$$

Using the final value theorem, the steady-state error is given by (if the noise is neglected)

$$e(\infty) = \underset{z^{-1}\to 1}{e(z^{-1})} = \underset{z^{-1}=1}{\lim}(1-z^{-1})G_e(z^{-1})Ref(k) \tag{4.6f}$$

For step input

$$Ref(k)=Rr(k), \qquad Ref(k)=\frac{R}{1-z^{-1}}$$

For ramp input

$$Ref(k)=kRr(k), \qquad Ref(z)=\frac{RT_0z^{-1}}{(1-z^{-1})^2}$$

where

T_0 - sample interval

r(k) - unit step input

In order to eliminate the steady state error, the error transfer function in the z domain should have the following form

$$G_e(z^{-1})=(1-z^{-1})^M F(z^{-1}) \tag{4.6g}$$

where

for step input M=1

for ramp input M=2

From Eqs (4.6f) and (4.6g), for eliminating the steady state error, the feed forward polynomial $H(z^{-1})$ can be calculated as follows:

(1) for step input

$$G_e(z^{-1})=1-B(z^{-1})A_m^{-1}(z^{-1})H(z^{-1}) \underset{z^{-1}\to 1}{=} 1 - z^{-1}$$

$$\therefore \lim_{z^{-1}\to 1} H(z^{-1})=h_0 = A_m(1)B^{-1}(1) \tag{4.6h}$$

(2) for ramp input

the condition of eliminating steady state error becomes

$$\text{(a)}\ G_e(z^{-1}) \underset{z^{-1}\to 1}{=} 1 - B(z^{-1})A_m^{-1}(z^{-1})H(z^{-1}) \tag{4.6i,a}$$

$$\text{(b)}\ \frac{d}{dz^{-1}}[G_e(z^{-1})]\Big|_{z^{-1}} = 0 \tag{4.6i,b}$$

From (4.6i,a)

$$H(z^{-1})=h_0+ h_1z^{-1}= A_m(1)B^{-1}(1)$$

From (4.6i,b)

$$\frac{d}{dz^{-1}} G_e(z^{-1})\Big|_{z^{-1}=1} = \frac{d[1-B(z^{-1})A_m^{-1}(z^{-1})H(z^{-1})]}{dz^{-1}}\Bigg|_{z^{-1}=1}$$

$$= - [B(z^{-1})A_m^{-1}(z^{-1})]h_1-H(z^{-1})[B(z^{-1})A_m(z^{-1})]'\Big|_{z^{-1}=1}$$

$$= - B(z^{-1})A_m^{-1}(z^{-1})h_1 - H(z^{-1})[z^{-1}\bar{B}(z^{-1})A_m^{-1}(z^{-1})]'\Big|_{z^{-1}=1}$$

$$= - B(z^{-1})A_m^{-1}(z^{-1})h_1 - H(z^{-1})\{\bar{B}(z^{-1})A_m^{-1}(z^{-1})+z^{-1}[(B(z^{-1})A_m^{-1}(z^{-1})]'\}\Big|_{z^{-1}=1}$$

$$= -H^{-1}(z^{-1})h_1 - H(z^{-1})\bar{B}(z^{-1})A_m^{-1}(z^{-1})-z^{-1}H(z^{-1})[\bar{B}(z^{-1})A_m^{-1}(z^{-1})]'\Big|_{z^{-1}=1}$$

$$= - H(1)^{-1}h_1 - 1 - H(1)[\bar{B}(z^{-1})A_m^{-1}(z^{-1})]'\Big|_{z^{-1}=1}$$

$$= 0$$

$$\therefore \qquad h_1 = -H(1)\{1+[\bar{B}(z^{-1})A_m^{-1}(z^{-1})]'H(1)\}\Big|_{z^{-1}=1}$$

$$h_0 = H(1) - h_1$$

Moreover, if the Diophantine equation is replaced by

$$A(z^{-1})F(z^{-1}) + B(z^{-1})G(z^{-1}) = C(z^{-1})A_m(z^{-1}) \tag{4.6k}$$

where

$$\deg F = n_b - 1,\ \deg G = n_a - 1,\ \deg A_m \le (n_a + n_b - 1 - n_c)$$

The closed loop equation becomes

$$y(k) = \frac{B(z^{-1})H(z^{-1})}{C(z^{-1})A_m(z^{-1})} Ref(k) + \frac{F(z^{-1})}{A_m(z^{-1})} \xi(k)$$

Comparing Eq. 4.6k with Eq. 4.6c,we can see that the disturbance term

$\frac{F(z^{-1})}{A_m(z^{-1})} \xi(k)$ is rather smaller than $\frac{C(z^{-1})F(z^{-1})}{A_m(z^{-1})} \xi(k)$. Hence,

by introducing polynomial $C(z^{-1})$ into the Diophantine equation (4.6k), the closed loop output disturbance can be suppressed a great deal. So it is reasonable to use Diophantine equation (4.6k) instead of Eq. (4.6c) when the system is contaminated by coloured noise.

4.2.2 SIMULATION RESULTS

According to Diophantine equation, the controller polynomials F and G are:

$$F(z^{-1}) = 1 + f_1 z^{-1}$$

$$G(z^{-1}) = g_0$$

the closed loop pole is selected from the identified plant pole, i.e.

$$A_m(z^{-1}) = 1 + \alpha a_1 z^{-1}$$

where α is a shifting factor. In this system, parameter a_1 is 1.056. The closed loop pole of approximately 0.7 is selected if $\alpha = 0.7$.

The resolution matrix is as follows:

$$\begin{vmatrix} 1 & b_0 \\ a_1 & b_1 \end{vmatrix} \begin{vmatrix} f_1 \\ g_0 \end{vmatrix} = \begin{vmatrix} (\alpha - 1)\, a_1 \\ 0 \end{vmatrix}$$

The simulation results are shown in figures 4.2 to 4.6. From these figures, the following observations can be obtained:

1) The system parameters converge very well.

Figures 4.2, 4.3 and 4.4 show the system parameters a_1, b_0 and b_1 respectively. In less than 20 steps, the parameter a_1 converges to -1.056, and has some ripple. This wave is between -1.05 to -1.06 and the error is less than ±1% of 1.056. This is considered adequately converged. The parameter b_0 converges to 1.1 in 20 steps. The error is equal to (1.1-1.076)/1.076, 3% of 1.076, so it is still considered adequately converged. The parameter b_1 converges to about 5.35, the error is about (5.35-5.23)/5.23, less than 3% of 5.23. So the all of the parameters converge very well in 20 steps.

2) The pole assignment adaptive control system gives good control.

Figure 4.5 shows the system input/output. From this figure, it can be seen that there is no overshoot in the system output during the dynamic process. The value of the closed loop pole is real. The system output is near the reference value 200 pixel but a little larger than reference signal about 1 pixel during steady state. The reason is that the white noise added in the system output is positive and mean square value is 1, which imitates the control requirement that control accuracy should be between 200±1. The control effort becomes stable in 20 steps at value 2, which is equal to 2 volts.

In all of the figures, the dynamic process lasts less than 30 steps. Simulation is

continued beyond 30 steps to demonstrate that the algorithm maintains the output at a continuous stable value. It is felt necessary to verify this point because the open loop unstable system can often be stabilized in the dynamic range by pole cancelling. When the pole is inside the unit circle of the z domain, pole cancelling is an effective method for both dynamic and steady state condition. When the pole is on or outside the unit circle in the z domain, pole cancelling always leads to an increase in the output in the non-dynamic range in the closed loop system.

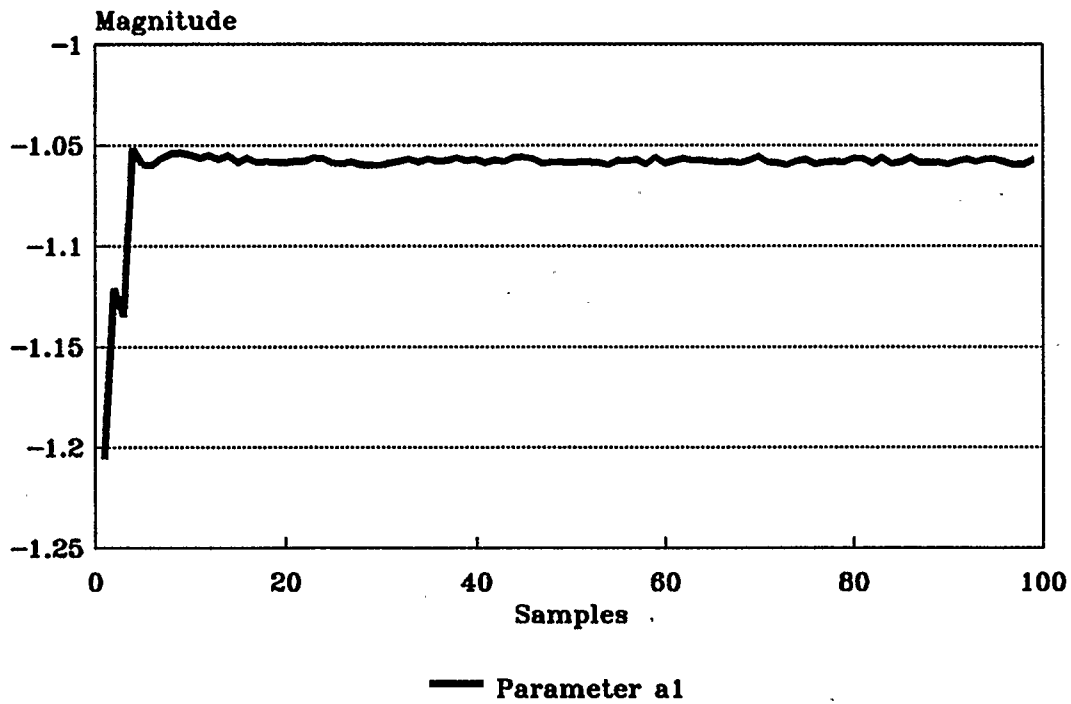

Figure 4.2 Pole assignment adaptive controller – Parameter a1

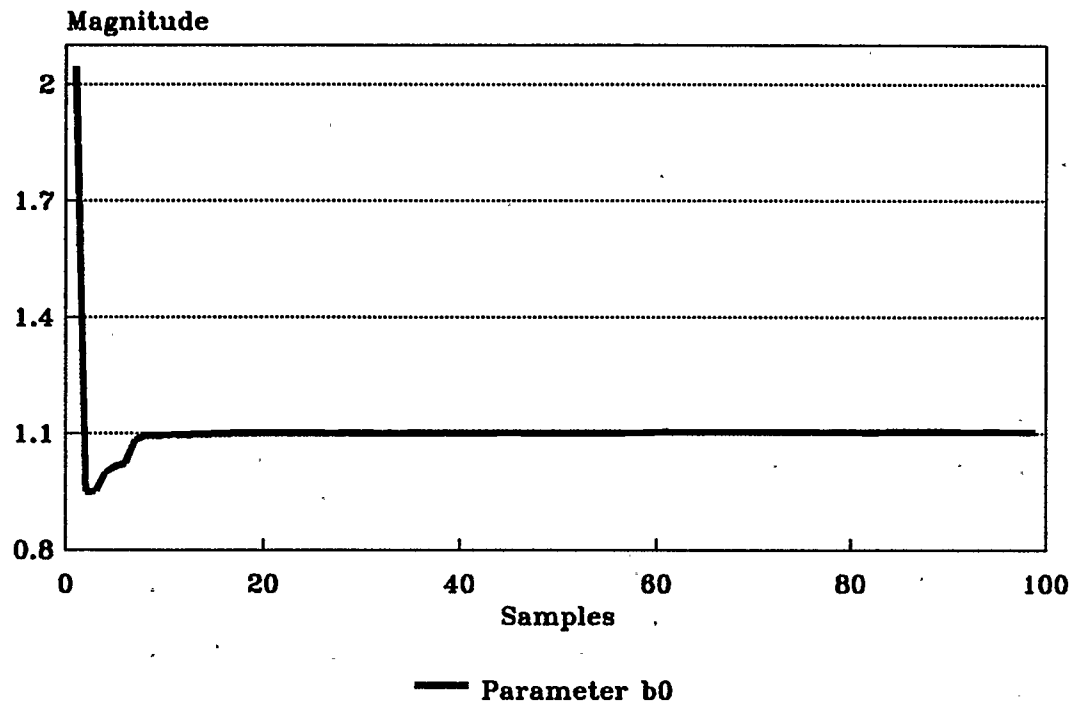

Figure 4.3 Pole assignment adaptive controller – Parameter b0

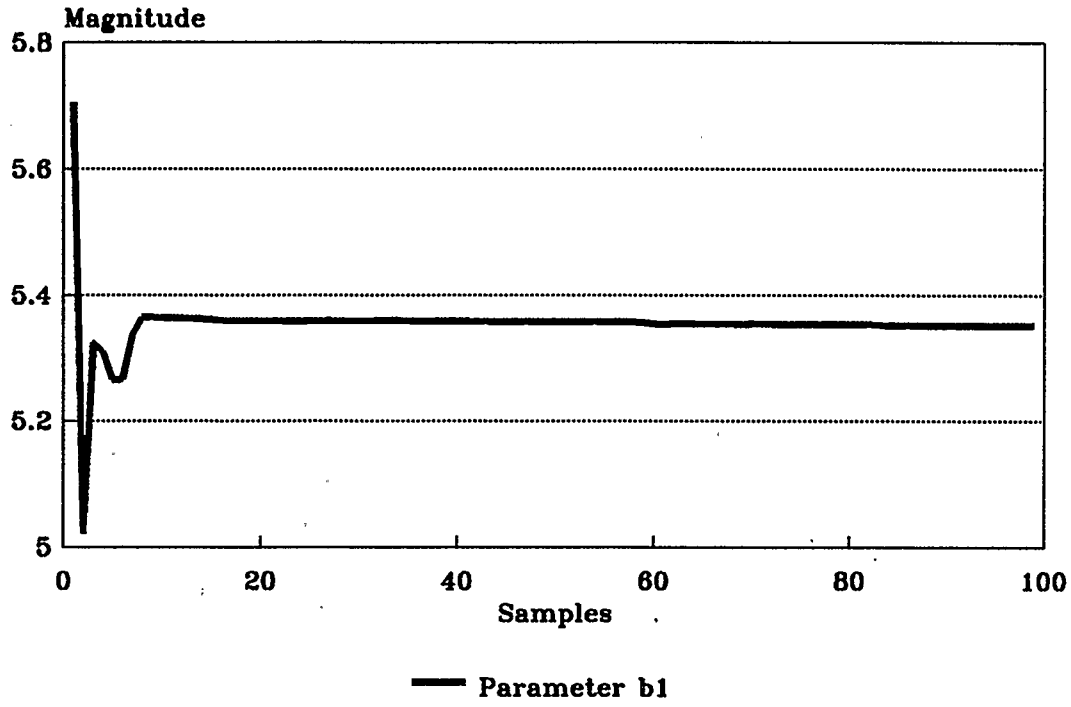

Figure 4.4 Pole assignment adaptive controller – Parameter b1

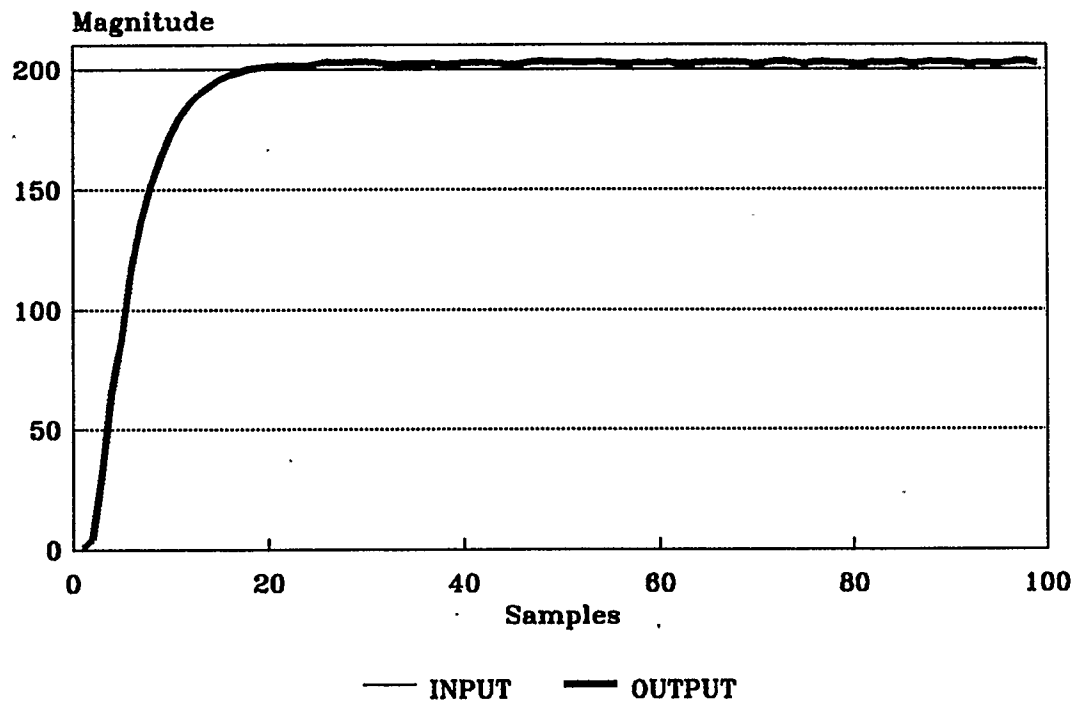

Figure 4.5 Pole assignment adaptive controller – Input / Output

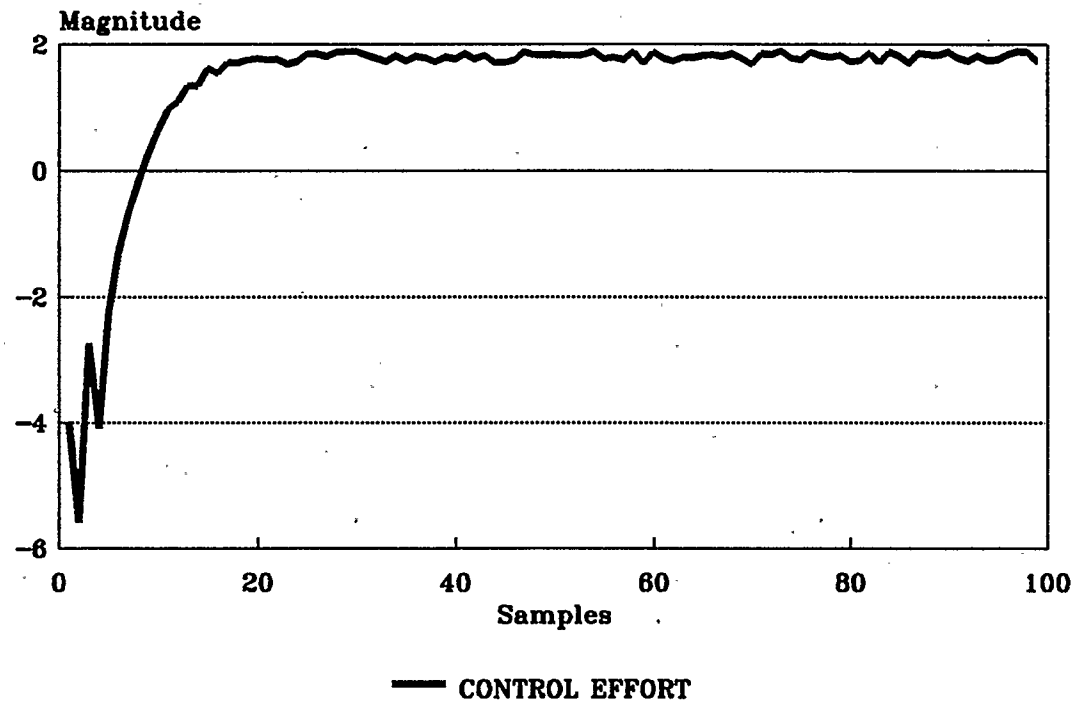

Figure 4.6 Pole assignment adaptive controller – Control effort

4.3 PI ADAPTIVE CONTROLLER

4.3.1 INTRODUCTION TO ALGORITHM

The plant model equation is

$$A(z^{-1})y(k) = B(z^{-1})u(k) + \xi(k) \qquad (C(z^{-1}) = 1) \tag{4.7a}$$

The PI controller equation is

$$u(k)= \frac{G(z^{-1})}{1 - z^{-1}}[Ref(k) - y(k)] \tag{4.7b}$$

where

$$G(z^{-1})=g_0 + g_1z^{-1} = g_0[1 + g'_1z^{-1}]$$

$$g_0 = K_e \frac{T_i + T_o}{T_i}$$

$$g_1 = -K_e$$

$$g'_1 = \frac{g_1}{g_0} = - \frac{T_i}{T_i + T_0}$$

K_e ——— the proportional coefficient of the PI controller

T_i ——— the integral time constant of the PI controller

T_0 ——— the sample interval

Substituting Eq (4.7b) to Eq (4.7a), we have the closed loop output equation

$$y(k)= \frac{B(z^{-1})G(z^{-1})}{(1-z^{-1})A(z^{-1})+B(z^{-1})G(z^{-1})} Ref(k) + \frac{1-z^{-1}}{(1-z^{-1})A(z^{-1})+B(z^{-1})G(z^{-1})} \xi(k)$$

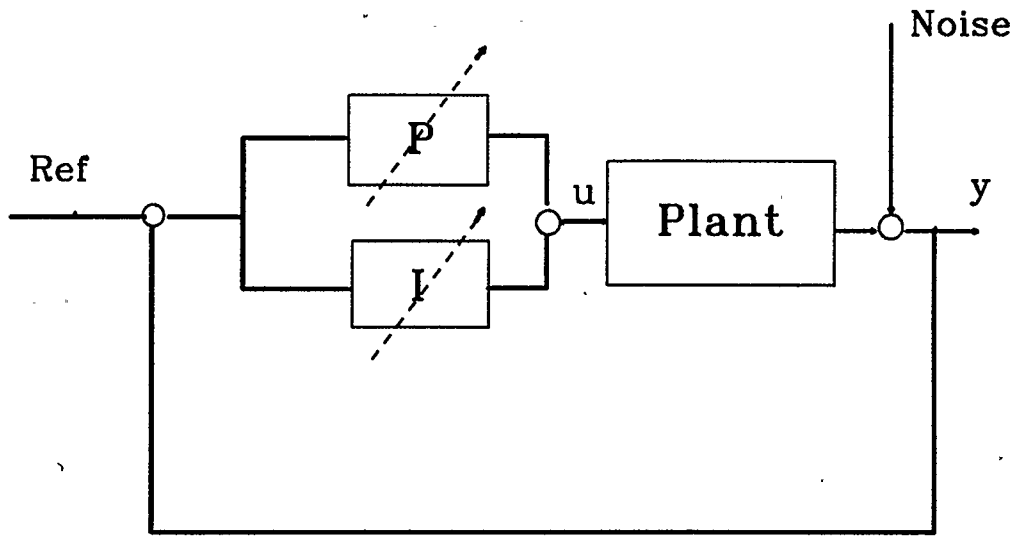

Figure 4.7 Block diagram of a PI adaptive controller

or

$$= \frac{g_0(b_0z^{-1} + b_1z^{-2})(1+g_0z^{-1})}{(1-z^{-1})A(z^{-1})+B(z^{-1})G(z^{-1})} Ref(z^{-1}) + \frac{1-z^{-1}}{(1-z^{-1})A(z^{-1})+B(z^{-1})G(z^{-1})} \xi(k) \qquad (4.7c)$$

From the PI control experience, it is known that good control can be obtained if the steady state gain is kept constant as the frequency changes. So a parameter optimal PI adaptive controller which is based on this idea is adopted. When the identification parameters b_0 and b_1 increase, the controller gain should be automatically reduced so as to maintain the system gain constant, such that

$$g_0(b_0+ b_1) = \text{constant} \qquad (4.7d)$$

$$g'_1 = -\frac{K_e}{g_0} \tag{4.7e}$$

where K_e is predetermined by test.

The error equation of the closed loop system is

$e(k)=Ref(k)-y(k)$

$$= \frac{(1-z^{-1})A}{(1-z^{-1})A+BG} Ref(k) - \frac{1-z^{-1}}{(1-z^{-1})A+BG} \xi(k) \tag{4.7f}$$

It is evidently seen that the steady state error of the stable closed loop system is zero. i.e.

$e(\infty) = 0$

The advantage of this method is that it uses a conventional PID controller structure for all situations. This means that there are no switching dynamics. Sometimes, switching dynamics harm the system. Problems arise when a cell is light in colour which may arise from being out of focus of the camera. In this case, it is very difficult for the image processing part of the system to detect the cell position.

The stability of this system is checked by identifying the closed loop poles at frequency $5x10^5$ Hz and $5x10^6$ Hz respectively, 1 decade apart in the flat band region of the DEP spectrum. The typical values at these frequencies are as follows:

$5x10^5$ Hz: $a_1 = -1.27$ $a_2 = 0.419$

The closed loop poles are calculated approximately

$p_1 = 0.689 + j0.3045$

$p_2 = 0.689 - j0.3045$

$6x10^6$ Hz: $a_1 = -1.32$ $a_2 = 0.52$

The closed loop poles are calculated approximately

$p_1 = 0.6735 + j0.32$

$p_2 = 0.6735 - j0.32$

The closed loop pole position shows that system is very stable and with damping in the system.

4.3.2 SIMULATION RESULTS

The plant model equation from section 3.6 is used here also:

$$A(z^{-1}) = 1 - 1.056z^{-1}$$

$$B(z^{-1}) = 1.076z^{-1} + 5.226z^{-2}$$

The identification uses the exponentially weighted least squares method. The forgetting factor, λ, is chosen as 0.99. The parameters b_0 and b_1, which are used to calculate the system gain, use the average value of the last 50 steps.

Figure 4.7 shows the PI adaptive controller block diagram. Figures 4.8 to 4.12 show simulation results. Figure 4.8 shows the parameter a_1. The parameter converges to -1.056 in 20 steps. After 20 steps, the parameter is around -1.056 with slight wave, oscillating between -1.054 and -1.058. Figure 4.9 shows the parameter b_0. The parameter converges to about 1.1 in 20 steps. After 20 steps, the parameter b_0 holds constant. Figure 4.10 shows parameter b_1. The parameter converges to 5.23 in 20 steps and then hold constant. Figure 4.11 shows control system output. The system output has very large overshoot, which is (390-200)/200, almost 100%. The system dynamic process lasts 40 steps. In control experimentation, the operator puts the cell close to the set point manually

before switching to closed loop system control. This large overshoot does not exist unless the operator switches to the closed loop control when the cell is far away from 200 pixel (70 μm from top electrode), which, normally, is not considered as good experimental practice. Figure 4.12 shows the control effort, which has large overshoot, and after 40 steps, the control effort is stable at 1.5 volt. From these observations, the following conclusions can be obtained:

1) The system is very stable, which can be seen from step 30 to step 100.

2) The system has a large overshoot, but, this dynamics is not troublesome in the application.

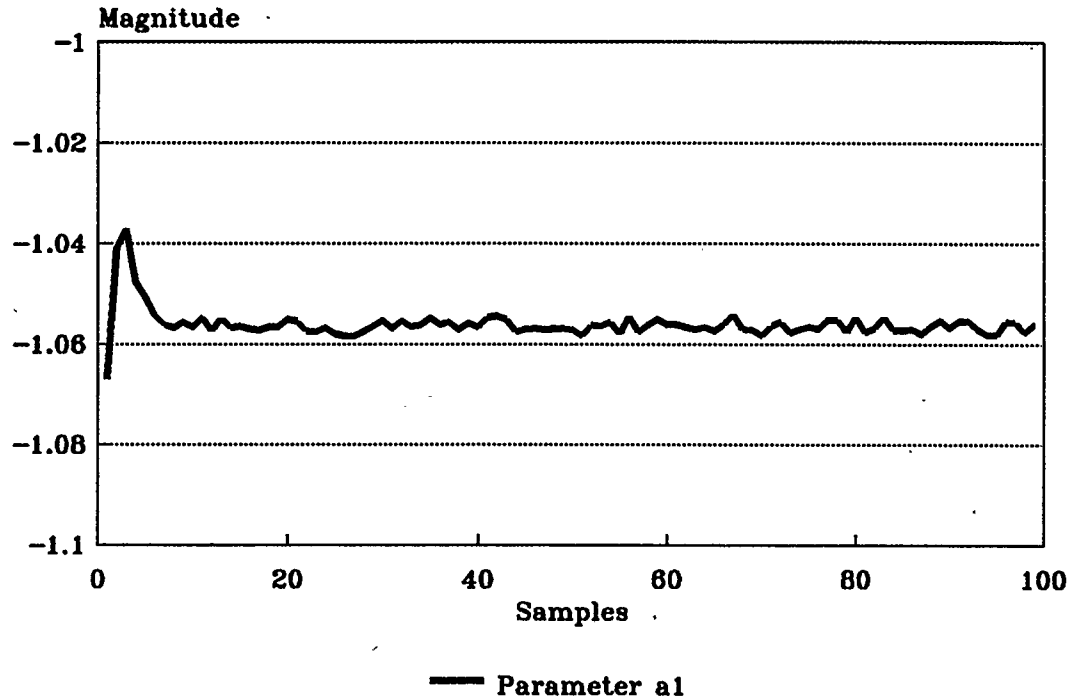

Figure 4.8 PI adaptive controller
– Parameter a1

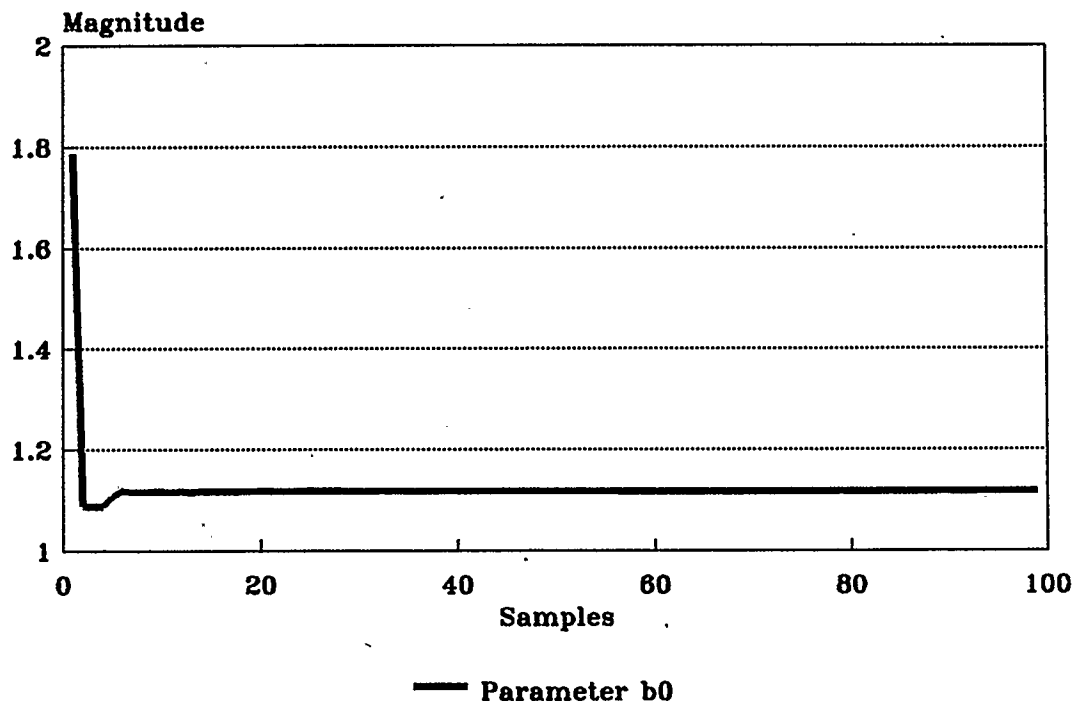

Figure 4.9 PI adaptive controller
– Parameter b0

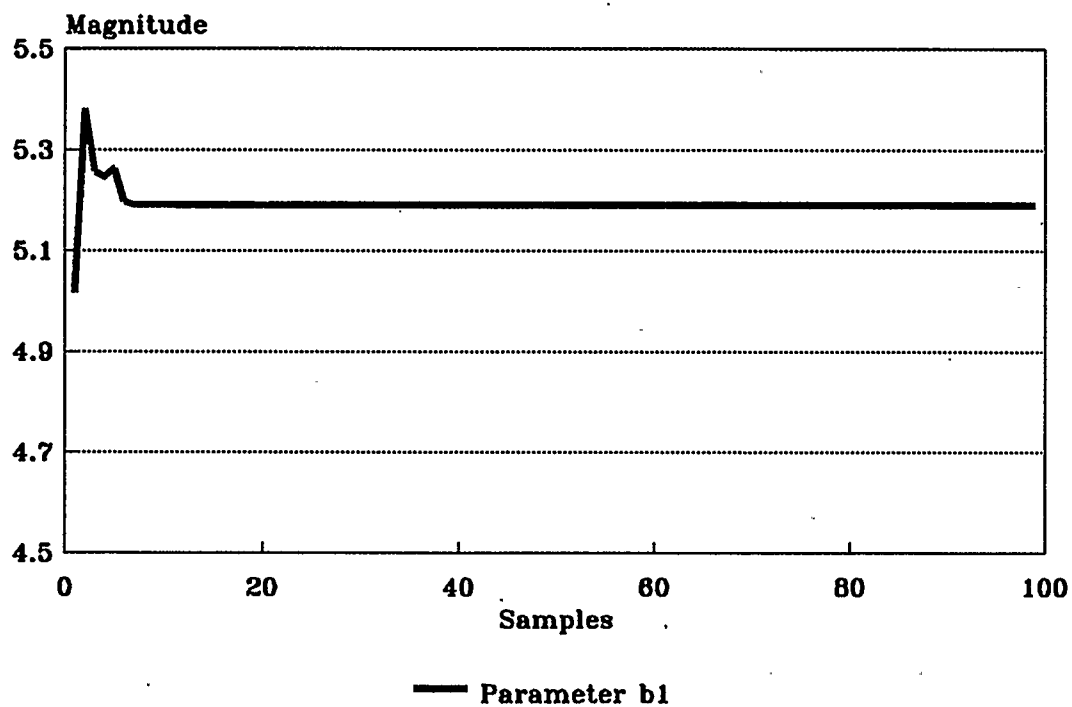

figure 4.10 PI adaptive controller
– Parameter b1

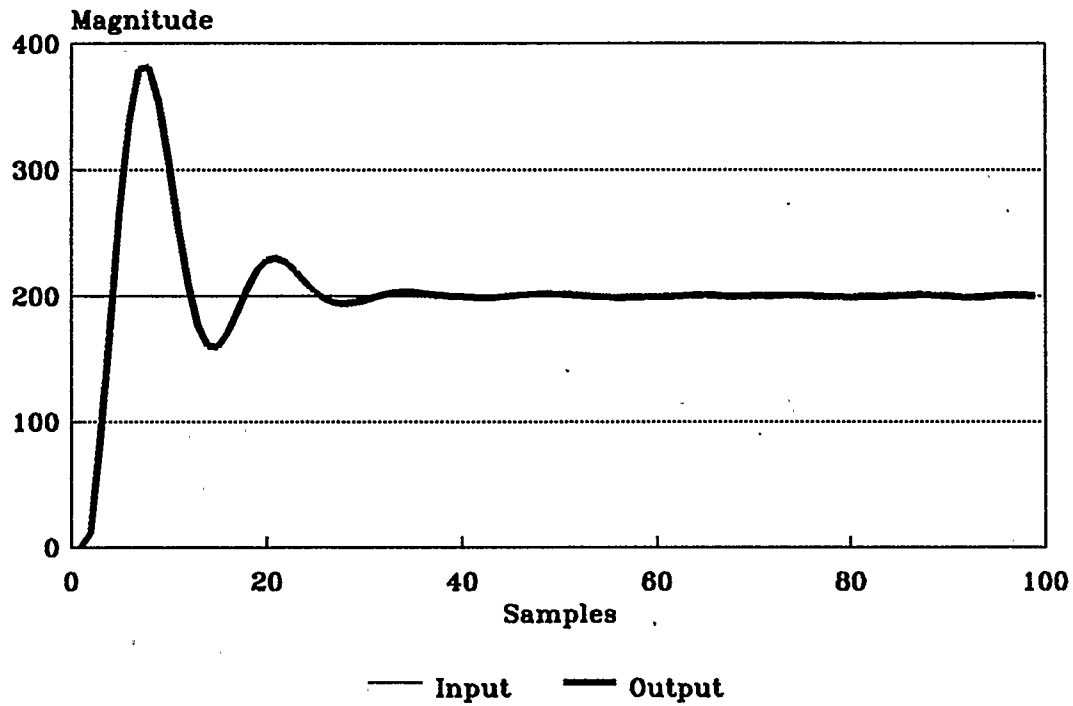

Figure 4.11 PI adaptive controller
– Input/Output

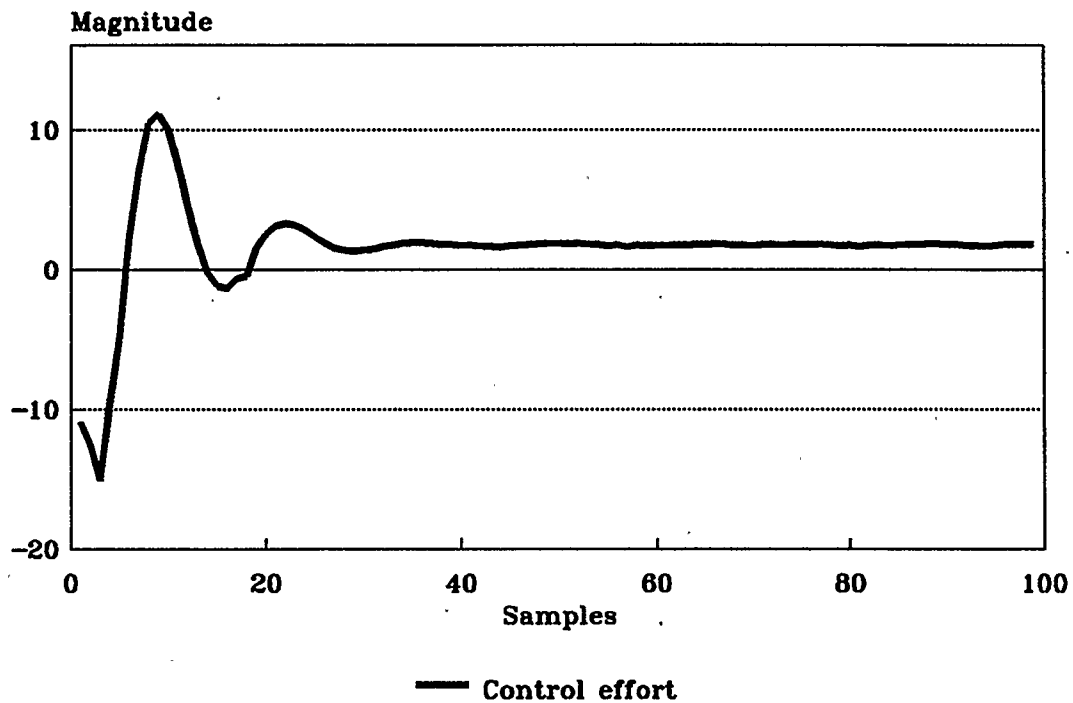

Figure 4.12 PI adaptive controller
– Control effort

4.4 POLE-SHIFTING DUAL LOOP ADAPTIVE CONTROLLER

4.4.1 INTRODUCTION TO ALGORITHM

PID adaptive controllers proposed in the last ten years can be divided into five types, i.e. i) pole assignment PID adaptive controller, ii) pole and zero cancellation principle PID adaptive controller, iii) rule based PID adaptive controller obtained from experience, iv) PID adaptive controller based on quadratic criterion and v) expert or intelligent PID adaptive controller. Generally speaking, PID adaptive controllers can not handle the open loop unstable system unless they are placed in the feedback path. Some PID adaptive controllers often cancel open loop system poles to get an ideal system response. In a practical application, pole and zero cancellation techniques can not really cancel poles or zeros. In an open loop stable system, the controller zeros and open loop poles, that are very close to each other, can be cancelled with negligible effect. But for an open loop unstable system, unstable poles can not really be cancelled. So the system response contains the exponential components which increase with time, and finally cause system instability.[34] A new algorithm is proposed to overcome this difficulty.

Figure 4.13 shows the main idea of this algorithm. The internal loop structure is the same as the pole assignment algorithm. The outside loop structure is a PID adaptive controller. Similar to the pole assignment design method, the internal loop pole and zero can be expressed by a group of equations. The pole and zero polynomials are respectively

$$A_{internal}(z^{-1}) = A(z^{-1})F(z^{-1}) + B(z^{-1})G(z^{-1}) \tag{4.7}$$

$$B_{internal}(z^{-1}) = B(z^{-1})H(z^{-1}) \tag{4.8}$$

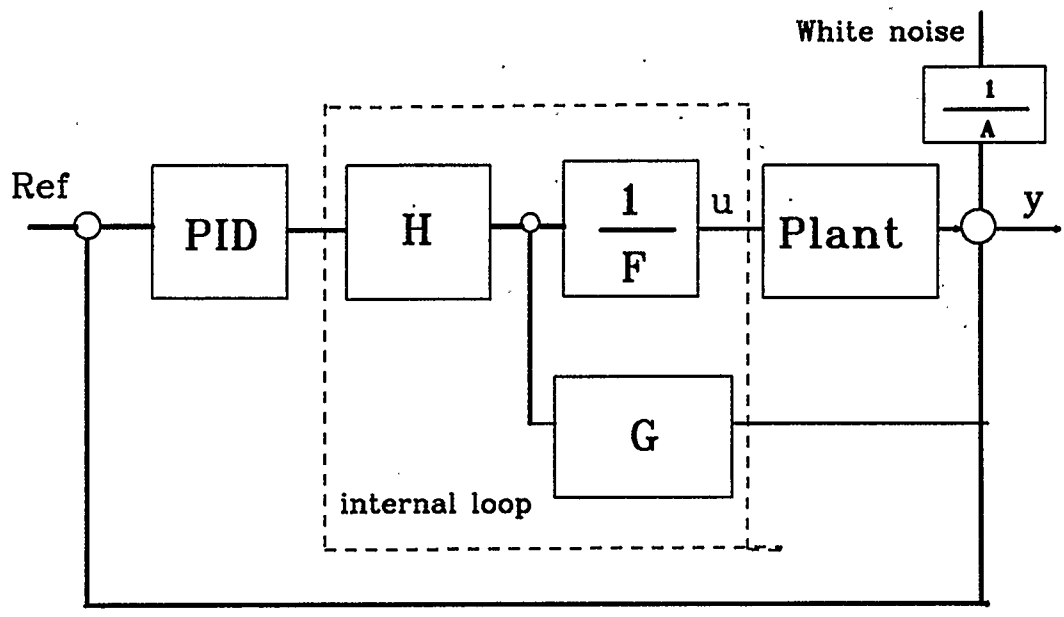

Figure 4.13 Dual loop adaptive controller

The outside loop is pole-shifting PID adaptive controller, $S(z^{-1})$ is polynomial, $I(z^{-1})$ equal to $1 - z^{-1}$. So the whole closed loop system pole and zero polynomials are

$$A_m(z^{-1}) = A_{internal}(z^{-1})I(z^{-1}) + B_{internal}(z^{-1})S(z^{-1}) \tag{4.9}$$

$$B_m(z^{-1}) = S(z^{-1})B_{internal}(z^{-1}) \tag{4.10}$$

if the closed loop poles can be chosen reasonably, this system can deal with open loop unstable system because the internal loop has polynomial $G(z^{-1})$ in the feedback path.

In some cases, for example, a first order system, the algorithm does not satisfy Diophantine equation. One of the parameters is adjusted on-line, which is similar to fixing b_0 in the identification of the self-tuning regulator. The following example gives an explanation of this idea. Considering a first order open loop unstable system

$$A(z^{-1}) = 1 + a_1 z^{-1} \tag{4.11a}$$

$$B(z^{-1}) = b_0 z^{-1} + b_1 z^{-2} \tag{4.11b}$$

where

$|a_1| > 1$, i.e. open loop unstable.

$|b_0| < |b_1|$, i.e. non-minimum phase system.

we have the following internal loop equation,

$$y(k) = \frac{BH}{AF + BG} u_{in}(k) + \frac{F}{AF + BG} \xi(k)$$

$$= \frac{B_{in}}{A_{in}} u_{in}(k) + \frac{F}{A_{in}} \xi(k) \tag{4.12}$$

where

$$A_{in}(z^{-1}) = A(z^{-1})F(z^{-1}) + B(z^{-1})G(z^{-1})$$

$$B_{in}(z^{-1}) = B(z^{-1})H(z^{-1})$$

$$F(z^{-1}) = 1 + f_1 z^{-1} \tag{4.13a}$$

$$G(z^{-1}) = g_0 \tag{4.13b}$$

$$H(z^{-1}) = 1 \tag{4.14}$$

Considering the internal loop as an extended system, a pole assignment or pole-shifting PI adaptive controller is used as an outside loop. Then we have the closed loop output equation

$$y(k) = \frac{B_{in}S}{(1-z^{-1})A_{in} + B_{in}S} Ref(k) + \frac{(1-z^{-1})F}{(1-z^{-1})A_{in} + B_{in}S} \xi(k)$$

or

$$y(k)=\frac{B_{in}S}{A_m}Ref(k)+\frac{(1-z^{-1})F}{A_m}\xi(k)$$

where

$$A_m(z^{-1})=(1-z^{-1})A_{in}(z^{-1})+B_{in}(z^{-1})S(z^{-1})$$

or

$$A_m(z^{-1})=(1-z^{-1})[A(z^{-1})F(z^{-1})+B(z^{-1})G(z^{-1})]+B(z^{-1})H(z^{-1})S(z^{-1})$$

Choosing

$$S(z^{-1}) = g_0 + g_1z^{-1} \tag{4.15a}$$

$$I(z^{-1}) = 1 - z^{-1} \tag{4.15b}$$

the closed loop equation can be written as

$$y(k)=\frac{(s_0+s_1z^{-1})(b_0z^{-1}+b_1z^{-1})}{(1-z^{-1})[(1+a_1z^{-1})(1+f_1z^{-1})+g_0(b_0z^{-1}+b_1z^{-2})]+(s_0+s_1z^{-1})(b_0z^{-1}+b_1z^{-1})}Ref(k)$$

$$+\frac{(1-z^{-1})(1+f_1z^{-1})}{(1-z^{-1})[(1+\alpha z^{-1})(1+f_1z^{-1})+g_0(b_0z^{-1}+b_1z^{-2})]+(s_0+s_1z^{-1})(b_0z^{-1}+z^{-2})]}\xi(k) \tag{4.16}$$

Let the closed loop poles be placed as a pole shifting PI controller

$$A_m(z^{-1}) = 1 + \alpha\hat{a}_1z^{-1} \tag{4.17}$$

where α is shifting factor, then the pole shifting polynomial equation is

$$(1-z^{-1})[(1+\alpha z^{-1})(1+f_1z^{-1})+g_0(b_0z^{-1}+b_1z^{-2})]+(s_0+s_1z^{-1})(b_0z^{-1}+z^{-2})=1+\alpha\hat{a}_1z^{-1}$$

When the system parameters are known, the controller parameters $F(z^{-1})$, $G(z^{-1})$ and $S(z^{-1})$ can be solved by using the following matrix equation:

$$\begin{vmatrix} 1 & b_0 & 0 \\ a_1-1 & b_1-b_0 & b_0 \\ -a_1 & -b_1 & b_1 \end{vmatrix} \begin{vmatrix} f_1 \\ g_0 \\ s_1 \end{vmatrix} = \begin{vmatrix} 1+\alpha a_1-a_1-s_0b_0 \\ a_1 - b_1s_0 \\ 0 \end{vmatrix}$$

The parameter s_0 is placed in the right side because there are only three equations with four unknown parameters f_1, g_0, s_0, s_1. So s_0 is fixed and its value depends on simulation or real time test.

The output error equation of the closed loop system is

$$e(k) = Ref(k) - y(k)$$

$$= \frac{(1-z^{-1})A_{in}}{(1-z^{-1})A_{in}+BS} Ref(k) - \frac{(1-z^{-1})F}{(1-z^{-1})A_{in}+BS} \xi(k)$$

From this equation, we can see that the steady state error of the closed loop system is

$$e(\infty) = 0$$

The above conclusion is evident because the outside controller is a PI controller which can eliminate any output error produced by the system.

Moreover, if the contaminated noise is a coloured one, $C(z^{-1})\xi(k)$, the closed loop equation should be modified as below:

$$y(k)=\frac{B_{in}S}{(1-z^{-1})A_{in}+B_{in}S} Ref(k) + \frac{(1-z^{-1})CF}{(1-z^{-1})A_{in}+B_{in}S}\xi(k)$$

Comparing eq (4.17e) with eq (4.17c), it is evidently seen that the closed loop output noise of eq (4.17e) is smaller than that of eq (4.17c).

4.4.2 SIMULATION RESULTS

The model equation is shown as

$$A(z^{-1}) = 1 - 1.056z^{-1}$$

$$B(z^{-1}) = 1.076z^{-1} + 5.226z^{-2}$$

$s_0 = 0.13$ (it is chosen by simulation)

The simulation results are shown in figures 4.14 to 4.18. Figure 4.14 shows parameter a1, the identified value is approximately -1.056. There is a deviations about the identified parameter value between -1.05 to -1.06, 1% of average of a_1. Figure 4.15 shows parameter b_0. The figure shows that parameter converges to 1.06 which is a little smaller than the model value 1.076. But this error is very small, (1.076 - 1.06)/1.076 < 2% of model value. Figure 4.16 shows the parameter b_1. The figure shows that parameter b_1 converges to 5.24 which is a little larger than the model value, error is (5.24 - 5.226)/5.226 < 1% of the model value b_1. Figure 4.17 shows the system output. The simulation results show that system is very stable which is the main concern, and the system has an overshoot although the closed loop pole is close to 0.7. This overshoot mainly comes from the extra zero from PI control part $s_0 + s_1z^{-1}$ which can be rewritten as $s_0(1 + s_1/s_0z^{-1})$. Figure 4.18 shows the system control effort, the control effort dynamic process finishes in 30 steps and is stable at 1.5 volts.

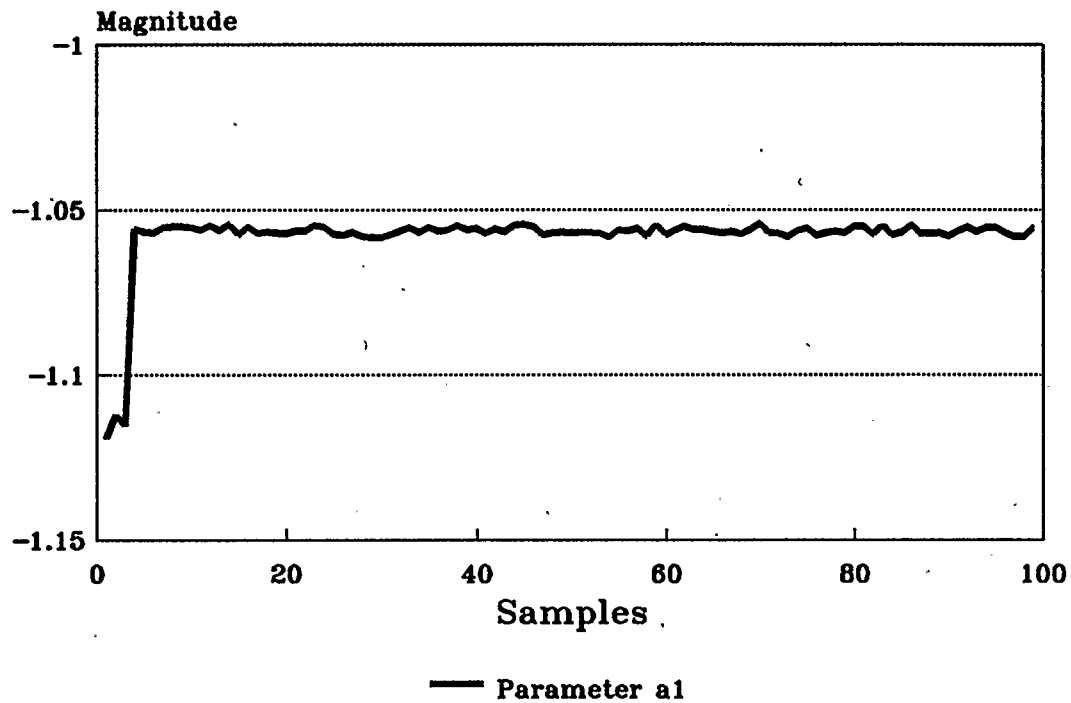

Figure 4.14 Pole-shifting dual loop adaptive controller – Parameter a1

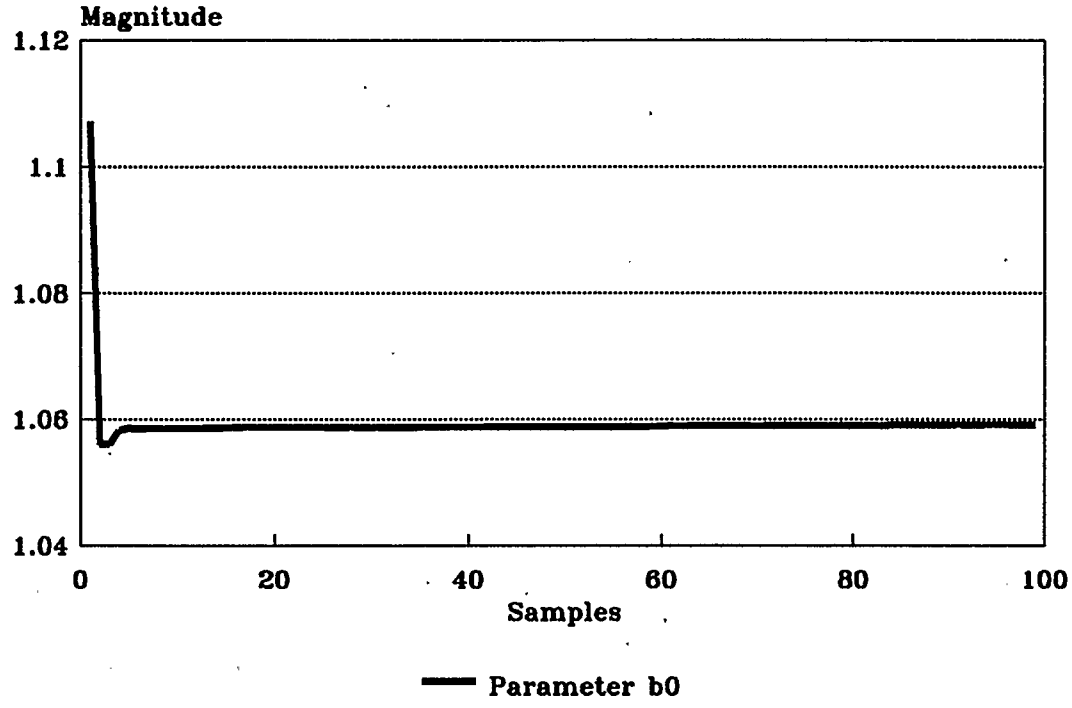

Figure 4.15 Pole–shifting dual loop adaptive controller – Parameter b0

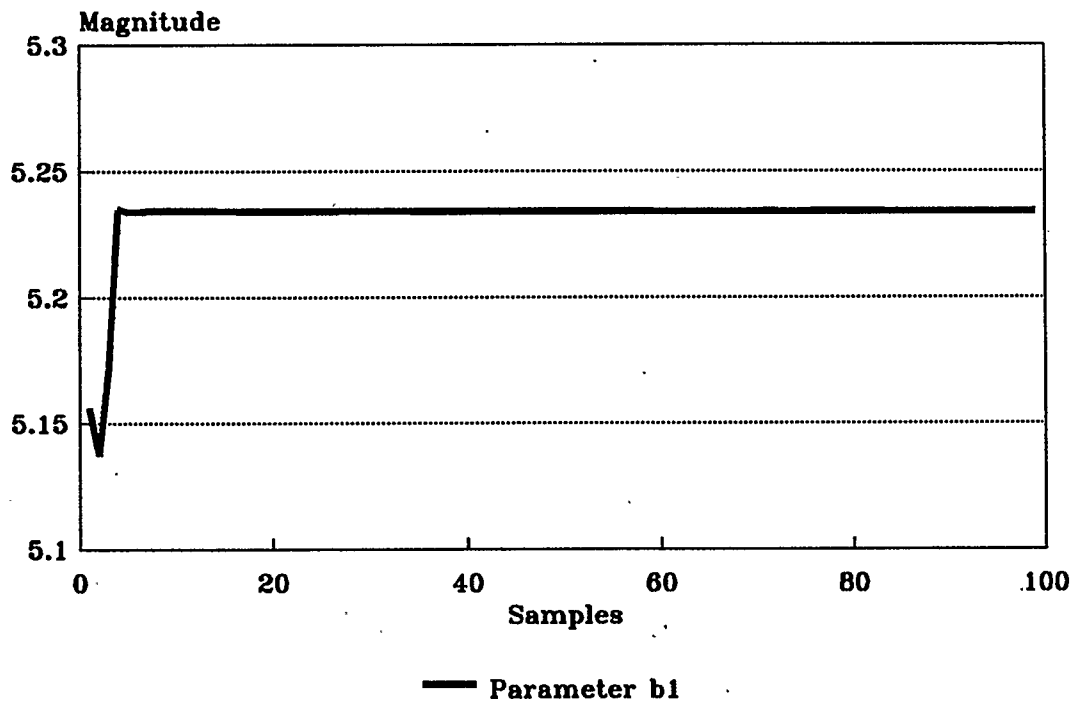

Figure 4.16 Pole–shifting dual loop adaptive controller – Parameter b1

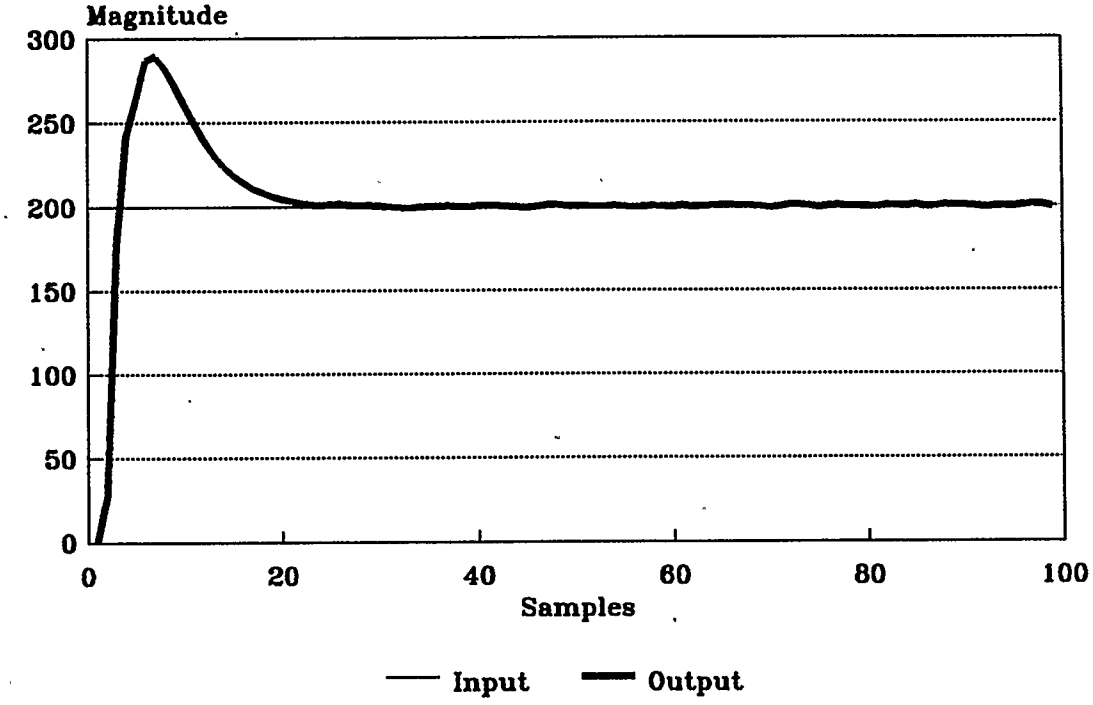

Figure 4.17 Pole-shifting dual loop adaptive controller - Input/Output

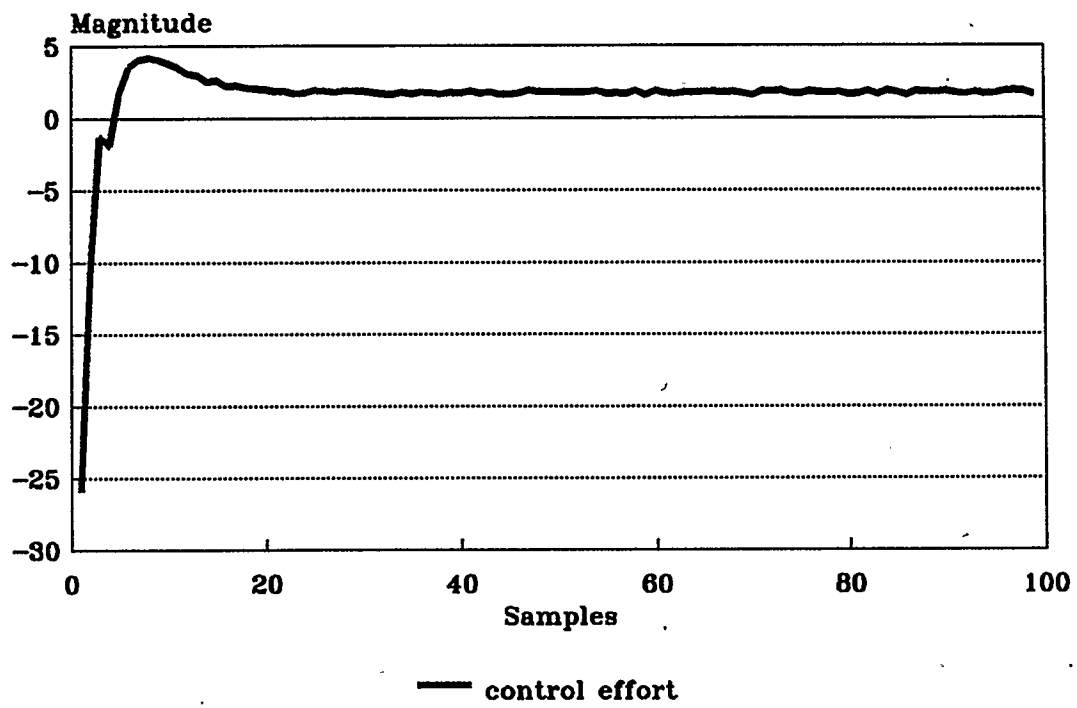

Figure 4.18 Pole-shifting dual loop adaptive controller – Control effort

4.5 APPROXIMATE SERIES COMPENSATION ADAPTIVE CONTROLLER

4.5.1 INTRODUCTION TO ALGORITHM

The series compensation method is a conventional design method which is based on frequency domain design. The new approximate series compensation method was proposed by Dr. Streets and K.H.H.Lau.[35] The proposed new adaptive algorithm is based on his work on s domain but is extended to the adaptive case here.

The desired system phase margin is PM.

$$PM \approx 70 - PO \tag{4.18a}$$

$$\beta = \tan((90 + PM)/2) \tag{4.18b}$$

$$td \approx \frac{1}{w_c} \tag{4.18c}$$

where

PO is the desired system overshoot, β is the width angle of the -1 slope at the crossover. td is half of the system response time, w_c is the crossover frequency.

From chapter 3, the model of cell-levitation apparatus system is expressed as:

$$G(s) = \frac{ke^{ts}}{s(s + a)} \tag{4.19}$$

According to the conventional series compensation method, the controller could have the following structure for a type II system:

$$F(s) = \frac{K_c(s + b)}{s(s + c)} \tag{4.20}$$

where

$$b = w_c/\beta, \quad c = w_c \times \beta, \qquad \text{if } a >> w_c \tag{4.21}$$

According to conventional series compensation method, the desired system is expressed in terms of criteria such as the system response time, the system overshoot, and the system steady state velocity or acceleration error. So from equation 4.18, for the known system response time, td and w_c can be obtained. The phase margin is known from the desired system overshoot, therefore, β can be obtained. Thus, controller parameters b and c are selected (if $a >> w_c$) and finally, using the identified plant model parameters, the plant gain K_c is determined.

For an adaptive control system, the system parameters are unknown and need to be identified on line. Thus Streets' equations are modified to z transfer function.

The controller equation is

$$F(z^{-1}) = \frac{cb_0 z^{-1} + cb_1 z^{-2}}{1 + ca_1 z^{-1} + ca_2 z^{-2}} \tag{4.22}$$

where

$$cb_0 = k(k_1 + k_2) \tag{4.23}$$

$$cb_1 = -k(k_1 e^{-cT} + k_2) \tag{4.24}$$

$$ca_1 = -(1 + e^{-cT}) \tag{4.25}$$

$$ca_2 = e^{-cT} \tag{4.26}$$

$$k_1 = \frac{b}{c} \tag{4.27}$$

$$k_2 = \frac{c - b}{c} \tag{4.28}$$

T is sampling interval, b and c are the parameters of controller in Laplace form. The plant model is expressed as follows:

$$\frac{b_0 z^{-1} + b_1 z^{-2}}{1 - a_1 z^{-1} + a_2 z^{-2}} \tag{4.29}$$

Since $|b_1| >> |b_0|$ and $|a_1| >> |a_2|$, the gain of the plant model G(s) can be approximated very closely as

$$k = \frac{\hat{b}_1}{\hat{a}_1 - 1} \ln\left(\frac{\hat{a}_1}{T}\right) \tag{4.30}$$

The following steps explain this new adaptive controller method.

Step 1: Calculate controller parameter b and c according to desired criterion.

Step 2: Use equation 4.22 to obtain the discrete controller equation parameters.

step 3: Use the identified plant parameters and equation 4.30 to calculate system gain k.

Step 4: Use k and desired closed loop system steady state velocity or acceleration gain to get controller gain k_c.

When plant model parameter changes, controller parameter k_c changes accordingly.

4.5.2 SIMULATION RESULTS

In simulation, only two parameters a_1 and b_0 (in terms a_1z^{-1} and b_0z^{-2}) are identified. The adaptive controller methods is used to obtain results. The simulation results are shown in figures 4.19 to 4.23. The figure 4.19 shows that parameter a_1 converges to -1 in 20 steps, the error is about (1.056-1)/1.056, 5% of 1.056. The parameter b_0 converges to 5.25 in 20 steps, the error is (5.25-5.226)/5.226, less than 1% of 5.226 . Figure 4.21 shows the system output. The system dynamics last 40 step, the overshoot is about (280-200)/200, 40% of 200. Figure 4.22 shows the control effort. The control effort dynamic process lasts 40 steps and converge to very small value.

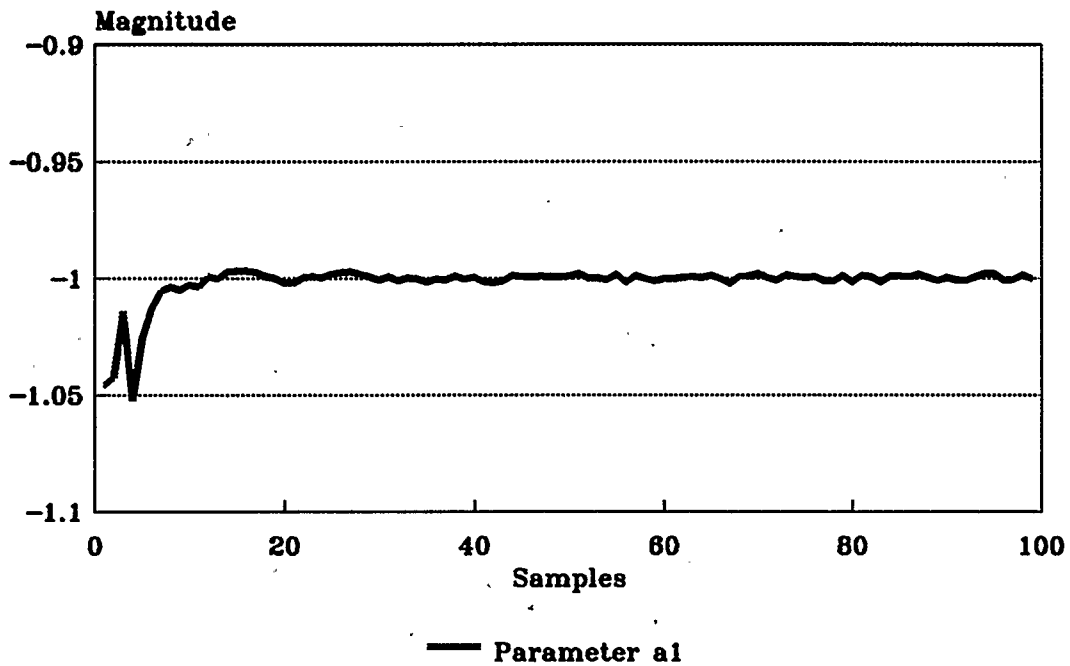

Figure 4.19 Approximate series compensation adaptive controller – Parameter a1

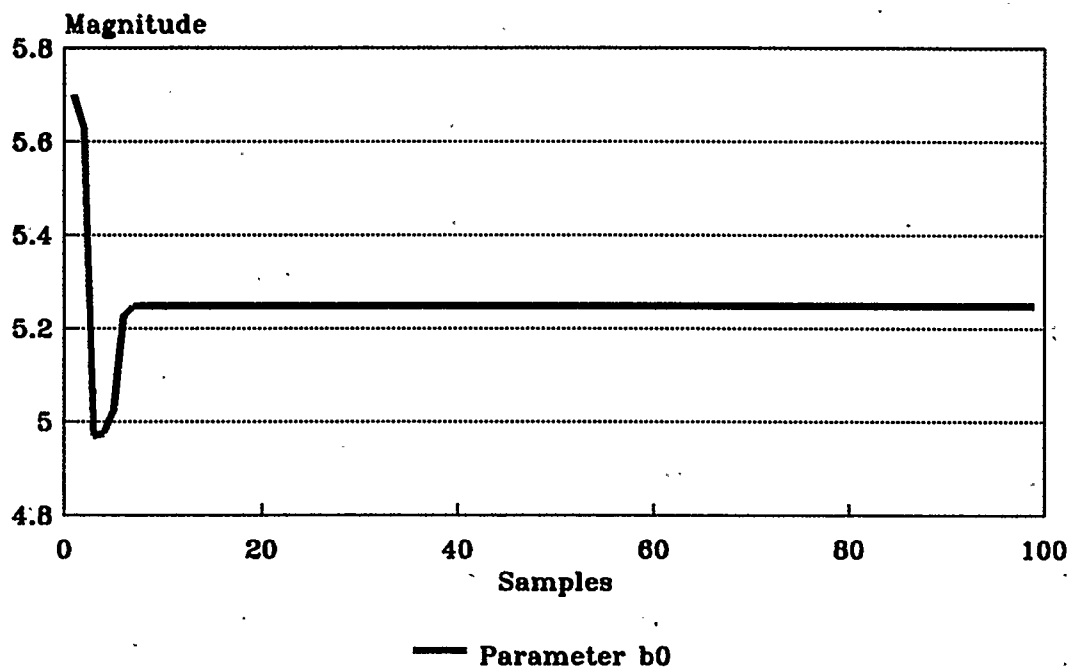

Figure 4.20 Approximate series compensation adaptive controller Parameter b0

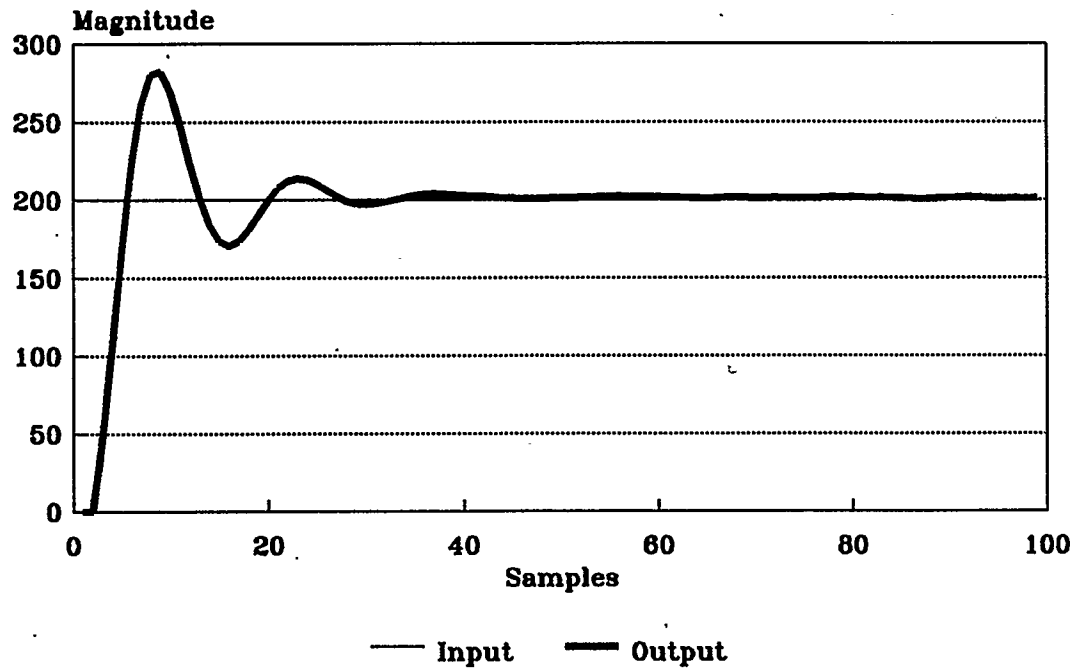

Figure 4.21 Approximate series compensation adaptive controller Input/Output

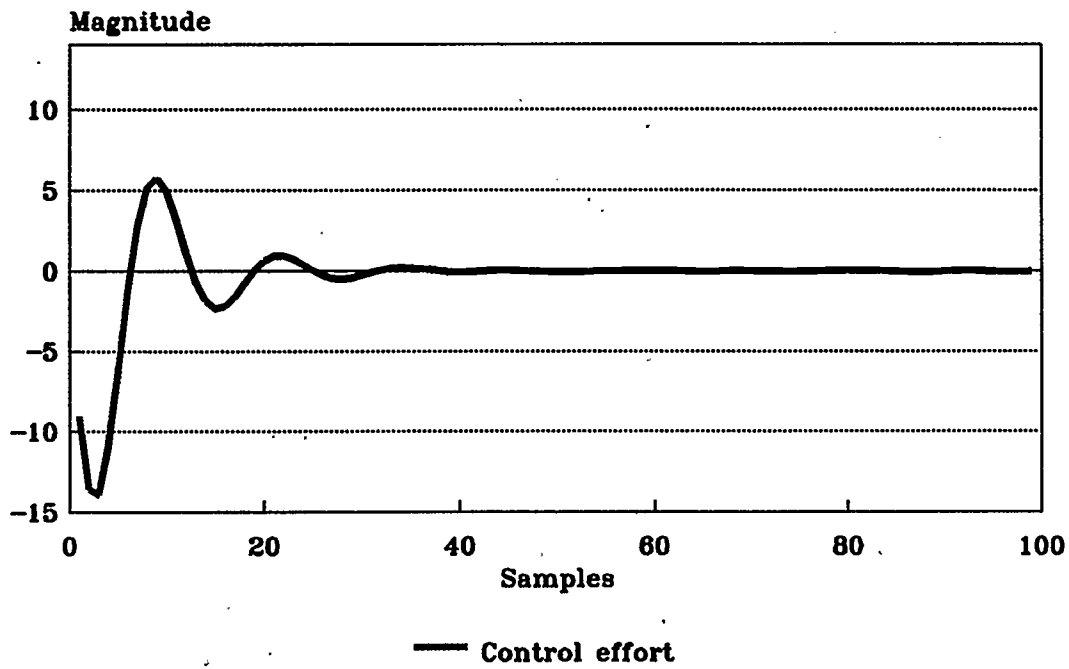

Figure 4.22 approximate series compensation adaptive controller Control effort

CHAPTER 5

EXPERIMENTAL RESULTS

5.1 INTRODUCTION

The basic experiment conditions are given in section 2.2 and the equipment arrangement is shown in figure 2.2. The following modifications are made to accommodate the adaptive case. The personal computer described in section 2.2 is used not only for the conventional digital PID controller, but also for the adaptive controller and the related identification. In the identification, the exponentially weighed least squares method given in section 3.3.3 by equations 3.9a and 3.9b is implemented. For the real time control, the pole assignment algorithm of section 4.2 covering equations 4.3 to 4.6b and PI adaptive controller of section 4.3 covering 4.7a to 4.7f are implemented.

Compared with the experiment procedures described in section 2.2, the following procedures and modifications are used for the adaptive control. The experiment starts at a high frequency of $5x10^6$ Hz using the conventional digital PID controller. Then the noise is added into the system, and identification is continued until the parameters converge. Then the system switches to the adaptive controller. When system output is stable into 200±1 pixel which is the control aim, identification is stopped to keep the cell in position. After sampling 25 data in this frequency as described in section 2.2, the system automatically scans to a lower frequency and samples data again. This procedure continues until system output exceeds the 200±1 band. The identification mechanism is restarted and continued until the parameters converge to new value. The new controller parameters are adopted. The system is stable in 200±1 and the procedure is used to scan

the complete frequency range.

In identification, the forgetting factor in exponentially weighed least squares method is varied from 0.95 to 1. The values of the last 20 steps are averaged to get a more accurate result. The PRBS noise is externally applied at the reference input, and its amplitude is ±4, 2% of set point reference signal. The identification process length is determined by comparing different step length such as 30 steps and 50 steps by the experiment.

Table 5.1 shows the relation between identification results and identification steps. The experiment conditions are given below.

The cell diameter is 30 μm, the distance between the cell and the electrode is 200

TABLE 5.1 RELATION BETWEEN IDENTIFICATION AND STEP LENGTH

test order	b_0 in group 1	b_0 in group 2
1	-6.236	-4.823
2	-5.208	-5.845
3	-5.456	-5.183
4	-5.248	-5.122
5	-5.187	-5.145
6	-5.291	-4.400
7	-4.808	-5.208
8	-5.240	-5.211
9	-5.670	-4.447
10	-5.215	-4.941
average	-5.36	-5.032
Max	+10.3%	+16.1%
Min	-10.3%	-12.6%

pixel (70 μm), the frequency is $5x10^6$ Hz. The test is divided into two groups, each group is repeated 10 times. The group 1 has a length of 50 steps, and group 2 has a length of 30 steps.

Table 5.1 shows that group 1 is more accurate than group 2. That is the maximin error and minimum error in group 1 are smaller than group 2. Longer step identification is very time consuming, and considered unnecessary. So 50 steps was selected.

The system output, control effort, parameters a1 and b0 at different frequencies are obtained in detail.

5.2 POLE ASSIGNMENT ADAPTIVE CONTROLLER

5.2.1 THE SYSTEM CHARACTERISTICS FOR THE STARTING PHASE

The pole assignment adaptive controller from section 4.2 is used as a starting point. Figures 5.1 to 5.4 show the results of the adaptive control. From these results, some observations are obtained.

a) in first 50 steps, parameters a1 and b0 (in figure 5.1 and 5.2) converge to -1.04 and -3.8 respectively.

b) after 50 steps, the system switches to the pole assignment adaptive control algorithm. Figure 5.3 shows that, when the system switches, the system has a dynamic overshoot, to the peak value of 230, 15% of reference value. After this process, this system settles to the 200±1 range, which is what is wished.

5.2.2 THE SYSTEM CHARACTERISTICS IN LOW FREQUENCY BAND

The figures 5.5 to 5.12 show typical sets of control results of pole assignment adaptive control system in low frequency for frequency of $8x10^4$ Hz and $5x10^4$ Hz.

Identification mechanism is started and parameters are updated. From these results, some observations are obtained.

a) The parameters a_1 and b_0 converge to -1.046 from -1.045 and -2.3 from -2.45 respectively at frequencies $8x10^4$ Hz. At frequency $5x10^4$ Hz, they converge to -1.044 from -1.043 and to -1.75 from -1.9 respectively. These results verify off-line identification, the parameter a_1 basically does not change, but the parameter b_0 reduces as the frequency changes to lower value. This is shown in figures 5.5, 5.6, 5.9 and 5.10).

b) When the noise is added into the system reference input, the system output has a relatively large perturbation. The peak value is about ±15, 7.5% of the reference. In 100 steps, the system output is stable into the 200±1 range as shown in figures 5.7 and 5.11.

c) The control value becomes larger when frequency becomes lower. At frequency $5x10^6$ Hz, control value is about 2.1 Volt, and at $8x10^4$ and $5x10^4$, it becomes 3.5 Volt and 5.1 Volt respectively.

The above-mentioned three points resemble the following analysis of the system. From the view of control engineering, the parameter b_0 reduction means that the system steady state gain becomes smaller, so in order to obtain the same output value 200, the control voltage value should be larger. Or from the system mechanical model, if the electric force equals the Fmg of the cell, the system output does not change. So the control aim is to make the electric force constant when frequency changes. The relation between controller voltage and electric force is $V^2 \propto F_{DEP}$, i.e $F_{DEP} = K(f)V^2$. If K(f) becomes smaller with frequency reduction, V should become larger.

5.3 PI ADAPTIVE CONTROLLER

Although the pole assignment adaptive control system can obtain good control result, a number of observations of control system quality showed that when the cells are light in colour, which may be from being out of focus, switching dynamics between conventional PID controller and the pole assignment adaptive controller make the image processing part unable to catch the cells correctly, the controller looses control and cells drop to bottom.

5.3.1 SYSTEM CHARACTERISTICS IN STARTING PHASE

Figures 5.13 and 5.14 show the convergence of parameters a_1 and b_0 at frequency $1x10^6$ Hz. Figure 5.15 shows that the system output does not have large dynamics. Peak value in whole identification process is ±2, 1% of the reference value, much better than using the pole assignment adaptive controller. Especially, there is no dynamic process between conventional PID controller and adaptive controller. This is the main advantage of this method.

5.3.2 SYSTEM CHARACTERISTICS IN LOW FREQUENCY BAND

Figures 5.17 and 5.18 show that the parameters a_1 and b_0 converge to -1.009 from -1.014 and -1 from -1.4 respectively at frequency 1600 Hz. Figures 5.19 and 5.20 show the system input/output and control effort respectively at frequency 1600 Hz.

The observations of control system quality over 80 tests indicate that this method gives good control for cells with widely varying parameters, and also gives good control for system startup. So it is adopted as the main control algorithm.

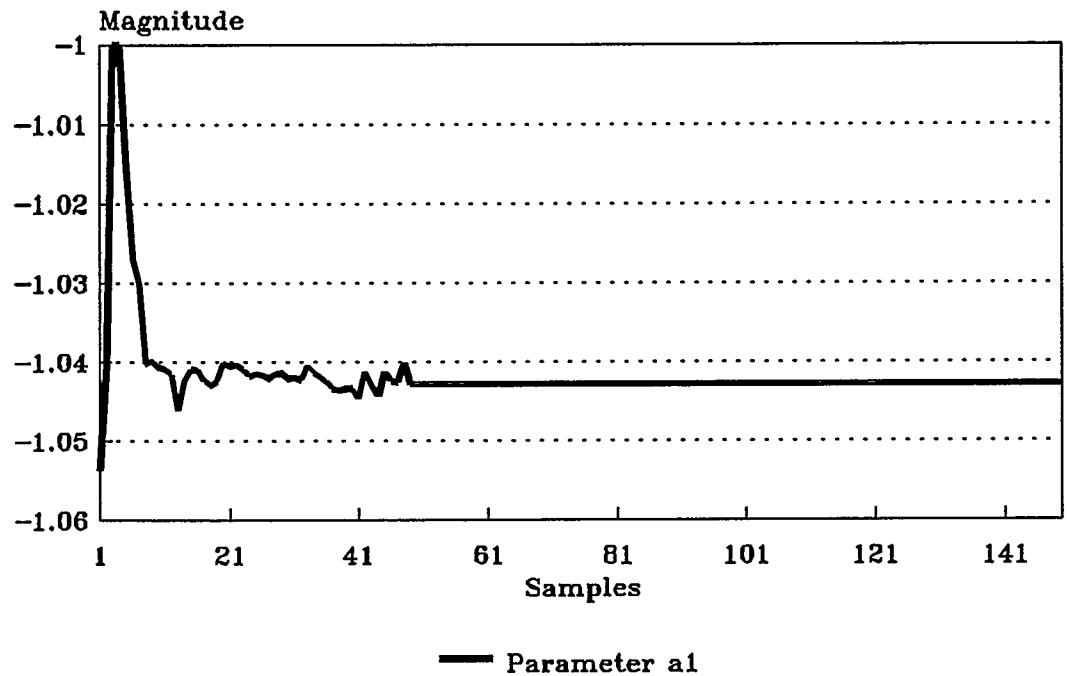

Figure 5.1 Pole assignment adaptive control system – Parameter a1
Frequency = 5000000 Hz

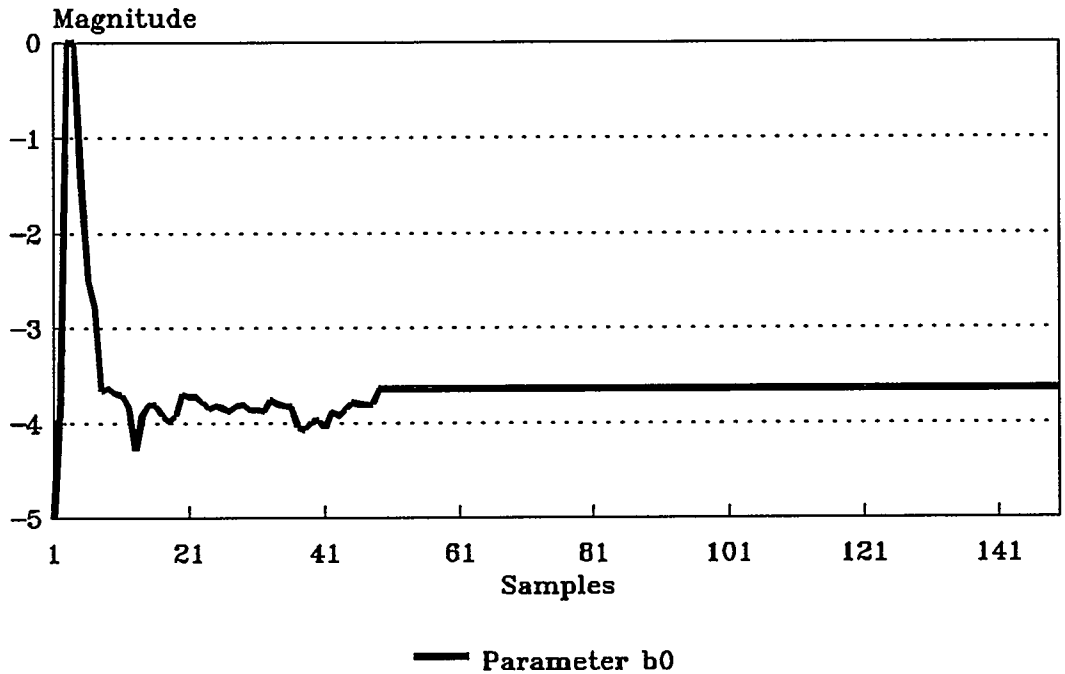

Figure 5.2 Pole assignment adaptive control system - Parameter b0
Frequency = 5000000 Hz

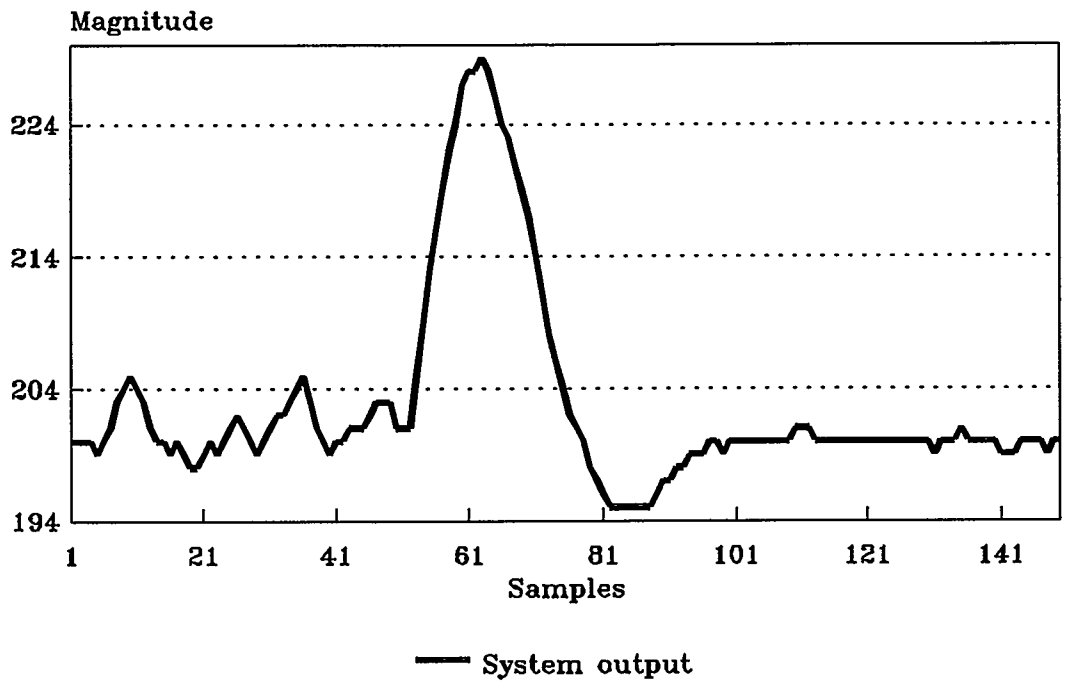

Figure 5.3 Pole assignment adaptive control system – system output
Frequency = 5000000 Hz

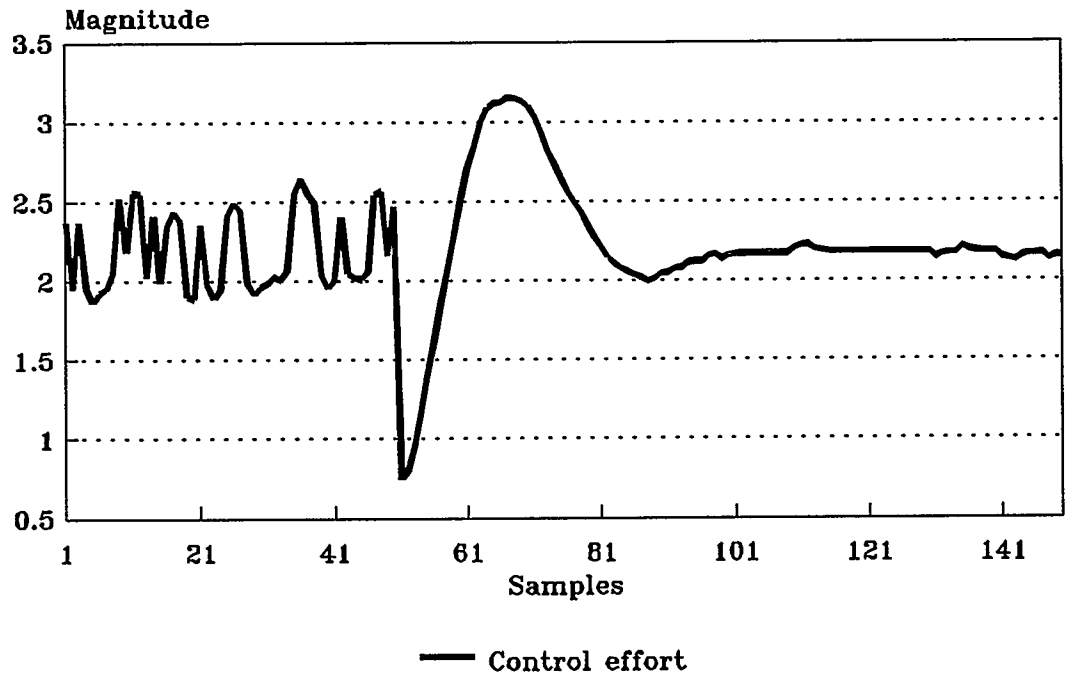

Figure 5.4 Pole assignment adaptive control system – Control effort Frequency = 5000000 Hz

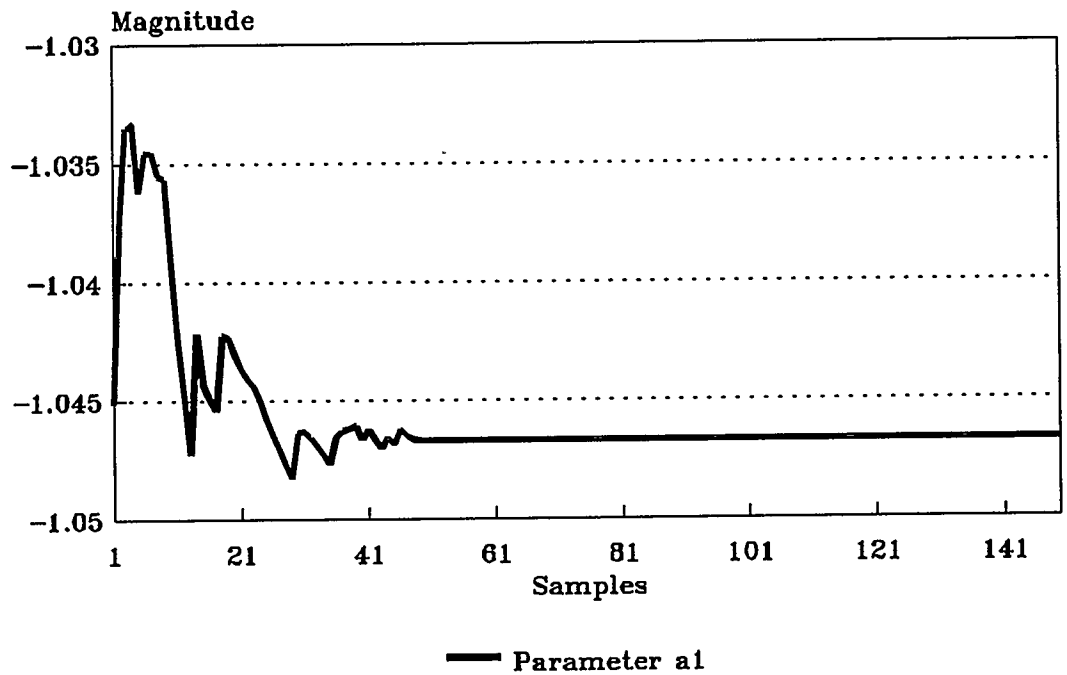

Figure 5.5 Pole assignment adaptive control system - Parameter a1 Frequency = 80000 Hz

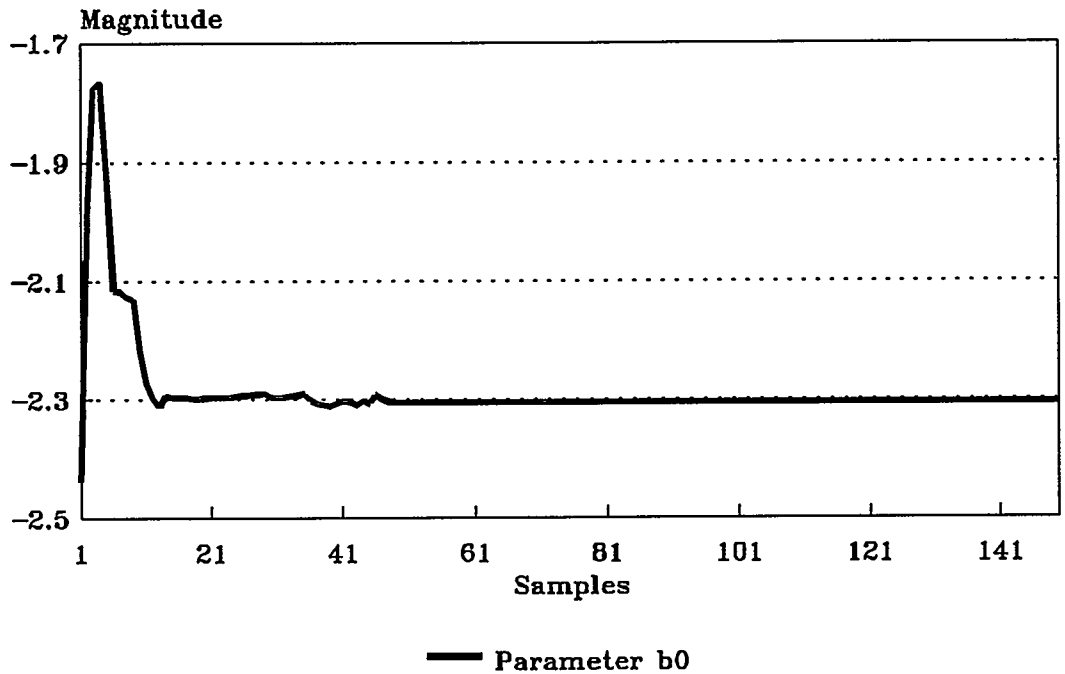

Figure 5.6 Pole assignment adaptive control system - Parameter b0 Frequency = 80000 Hz

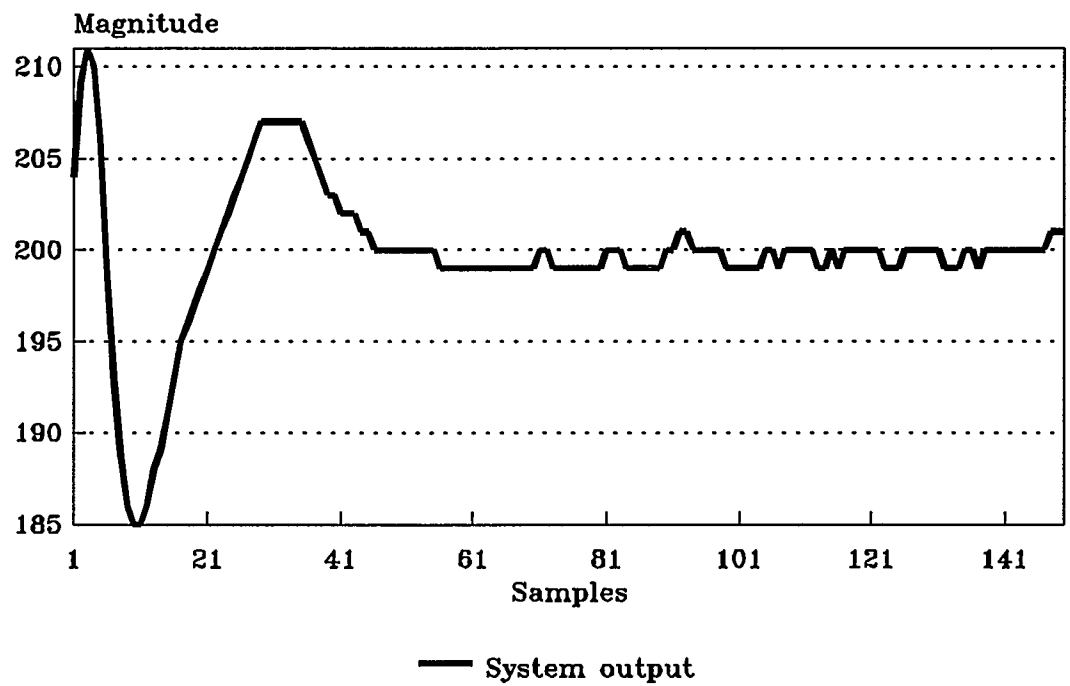

Figure 5.7 Pole assignment adaptive control system – System output Frequency = 80000 Hz

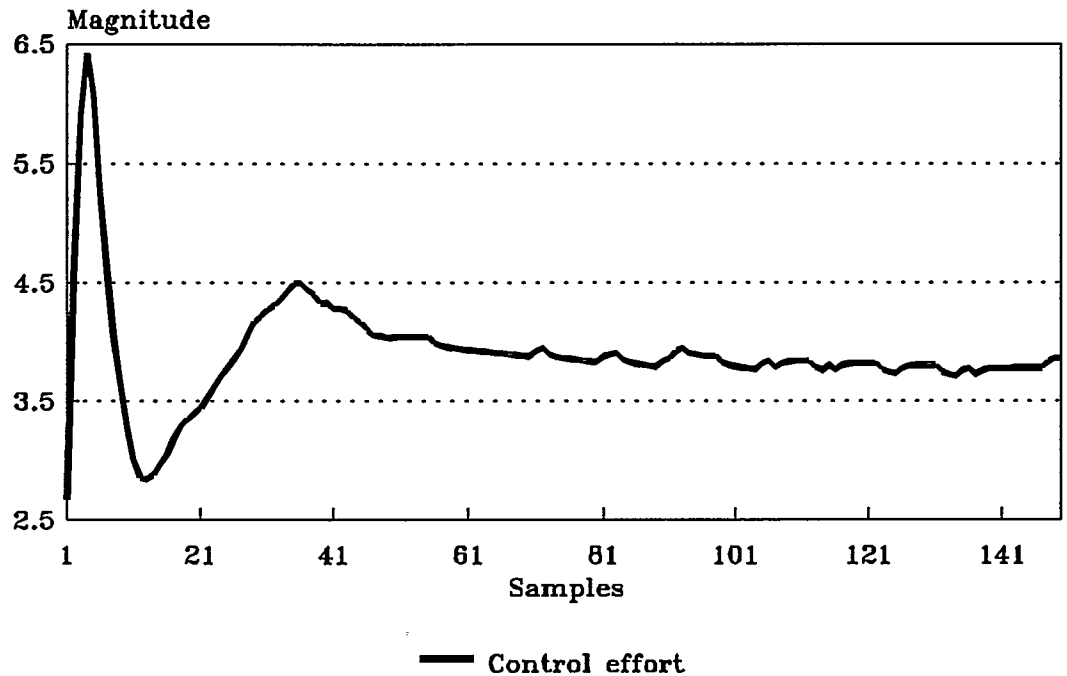

Figure 5.8 Pole assignment adaptive control system – control effort
Frequency = 80000 Hz

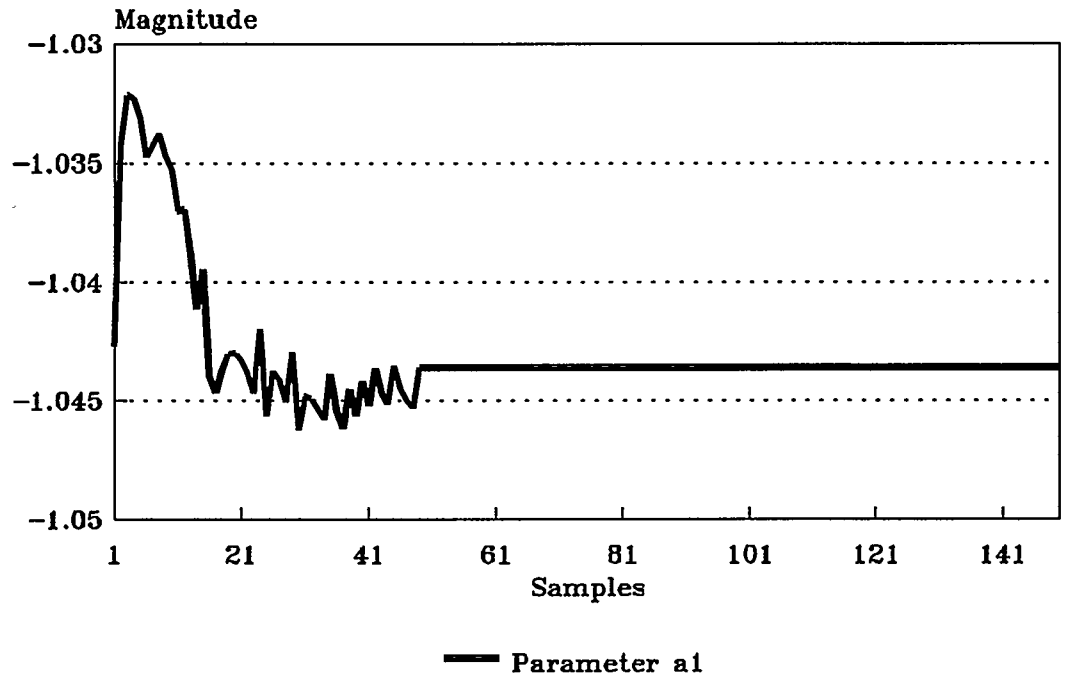

Figure 5.9 Pole assignment adaptive control system - Parameter a1 Frequency = 50000 Hz

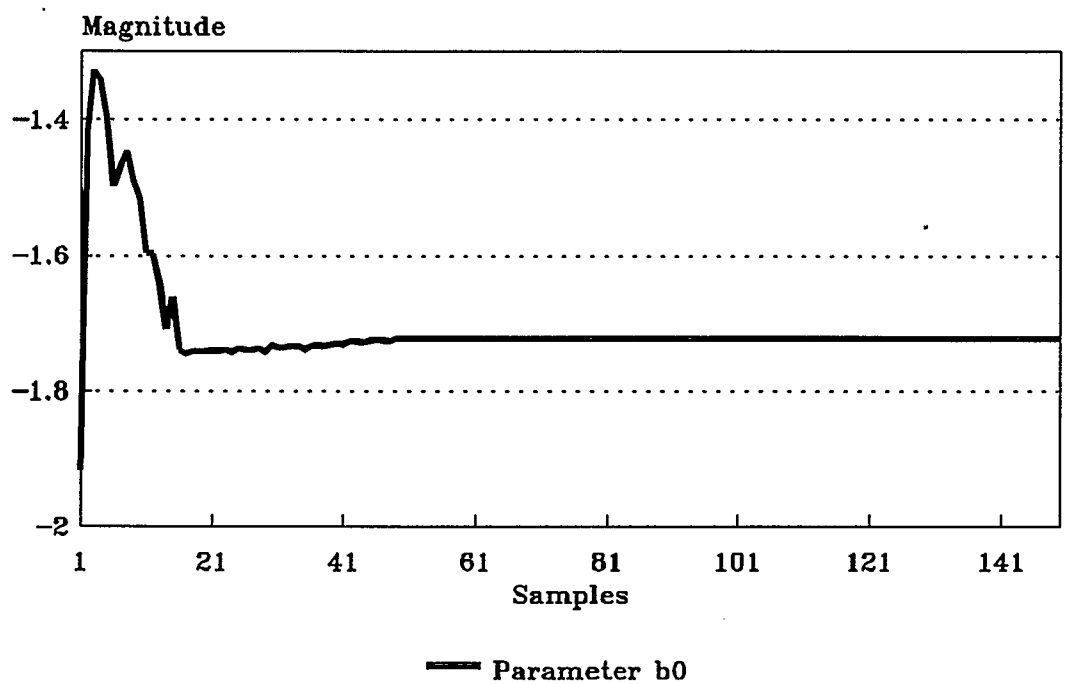

Figure 5.10 Pole assignment adaptive control system - Parameter b0
Frequency = 50000 Hz

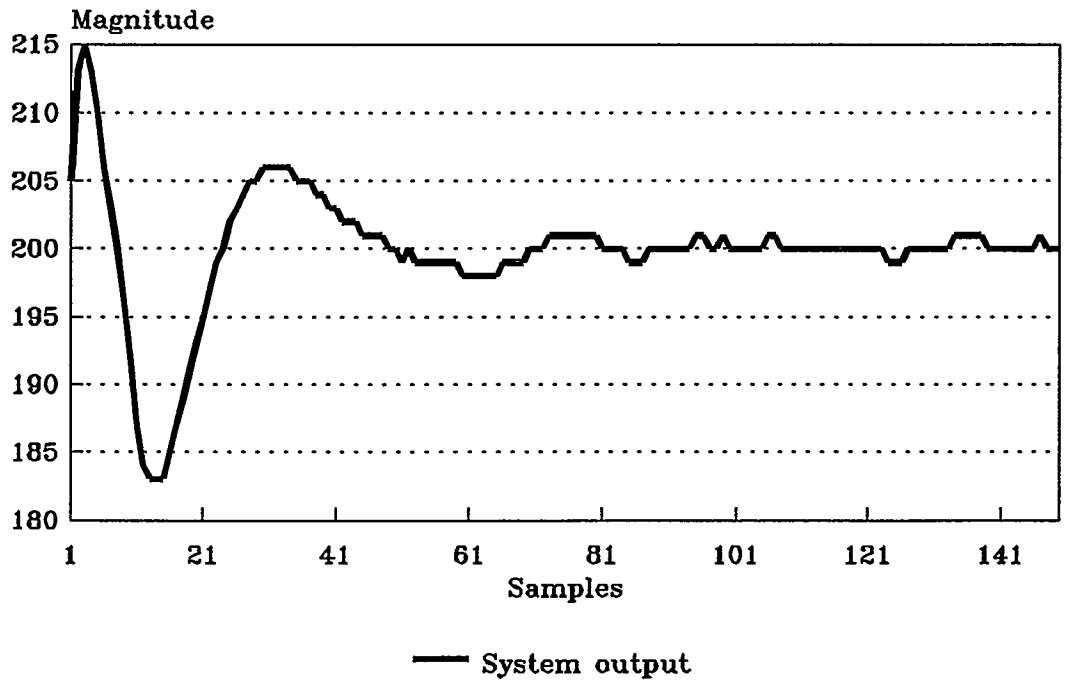

Figure 5.11 Pole assignment adaptive control system - system output
Frequency = 50000 Hz

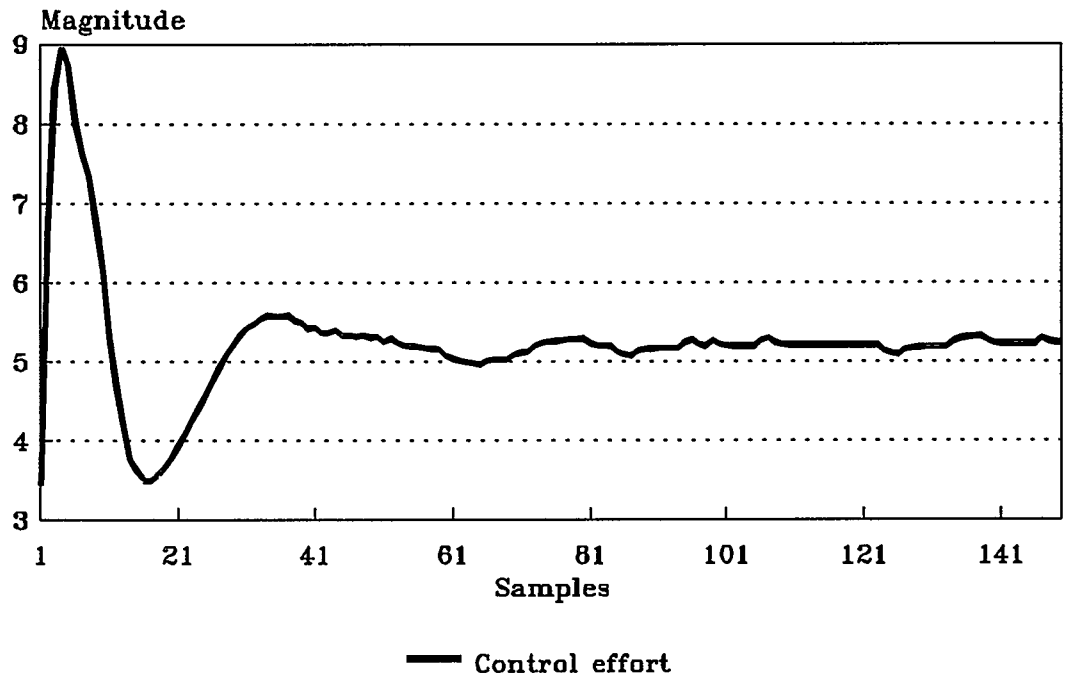

Figure 5.12 Pole assignment adaptive control system – control effort
Frequency = 50000 Hz

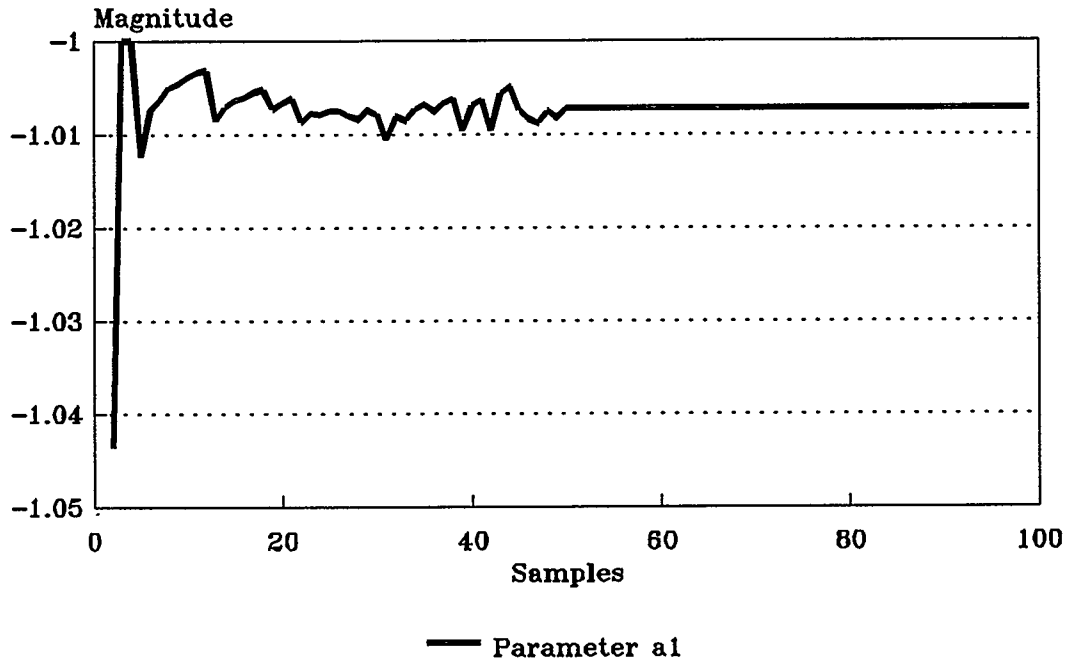

Figure 5.13 PI adaptive controller
Parameter a1
Frequency = 1000000 Hz

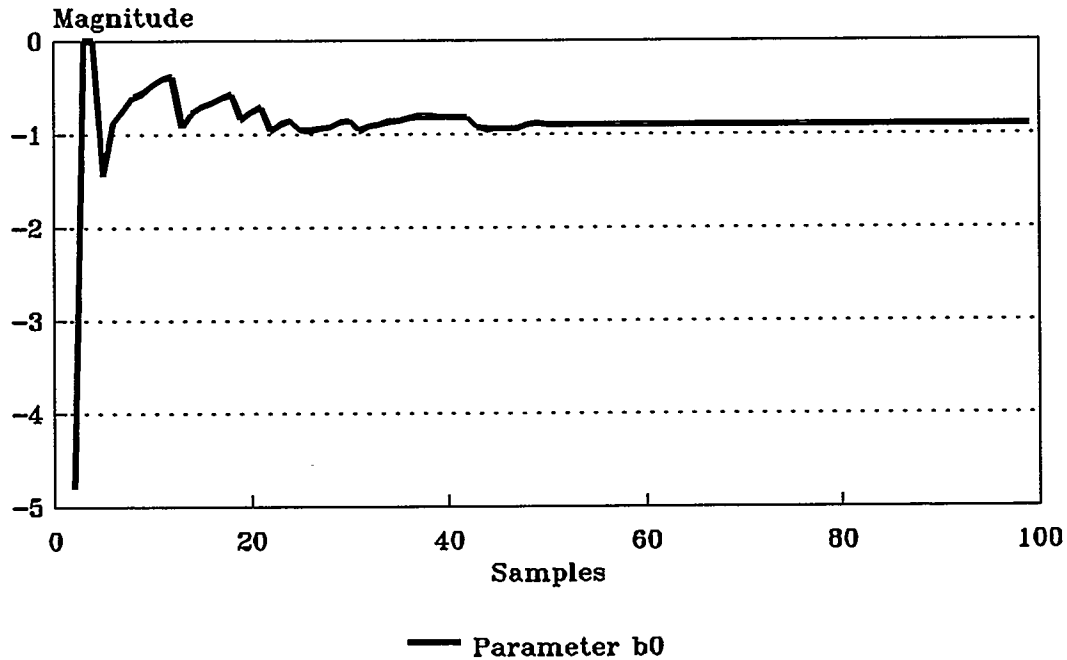

Figure 5.14 PI adaptive controller
Parameter b0
Frequency = 1000000 Hz

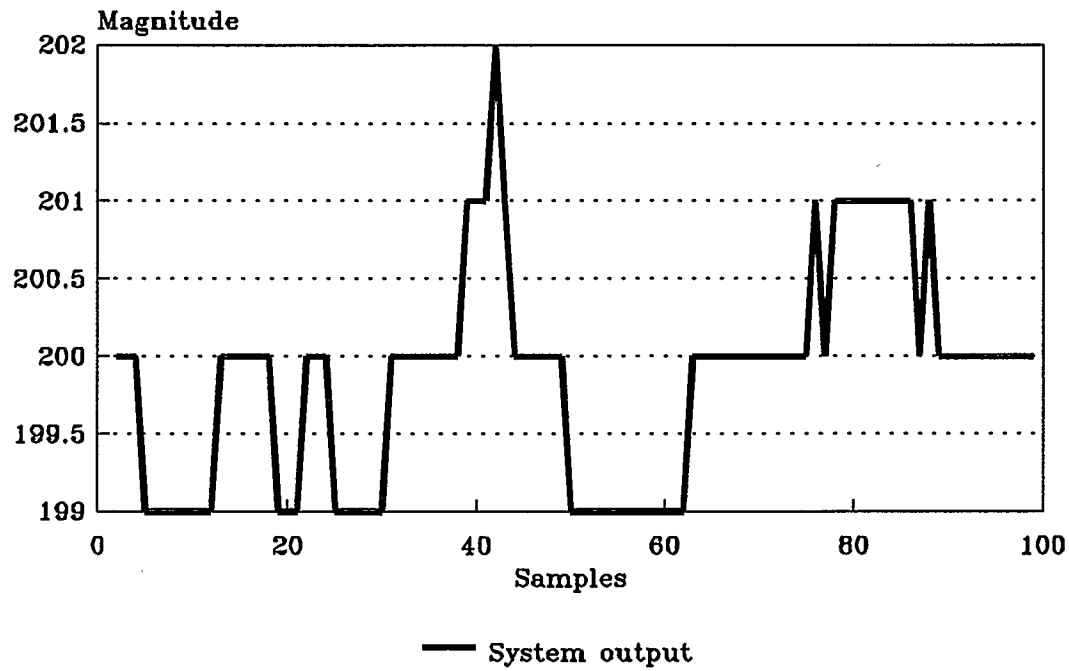

Figure 5.15 PI adaptive controller
system output
Frequency = 1000000 Hz

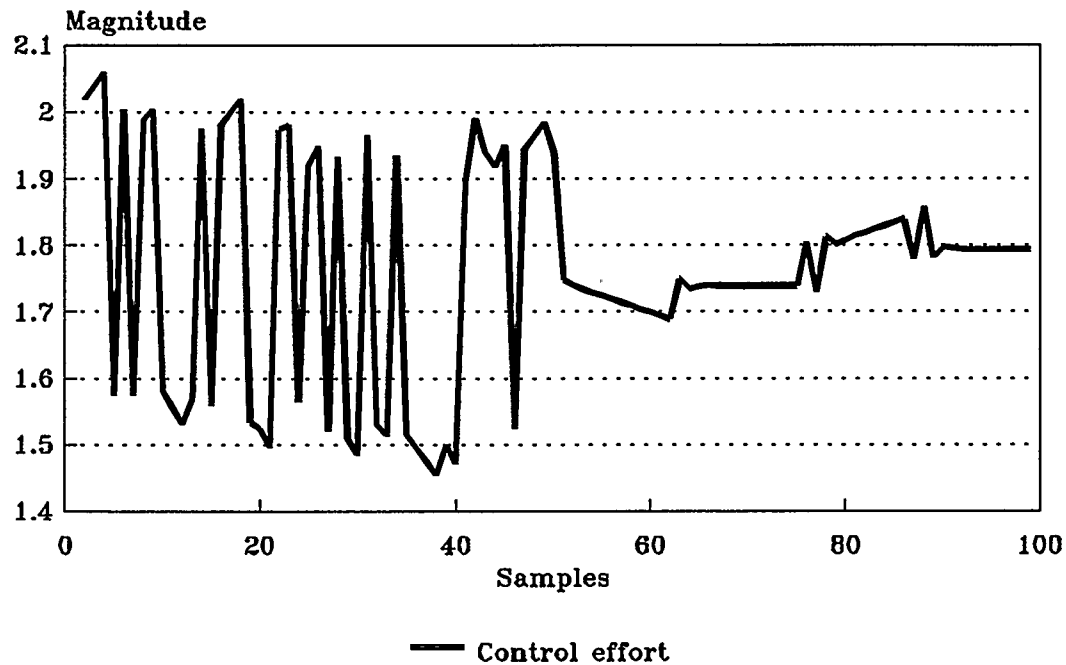

Figure 5.16 PI adaptive controller
Control effort
Frequency = 1000000 Hz

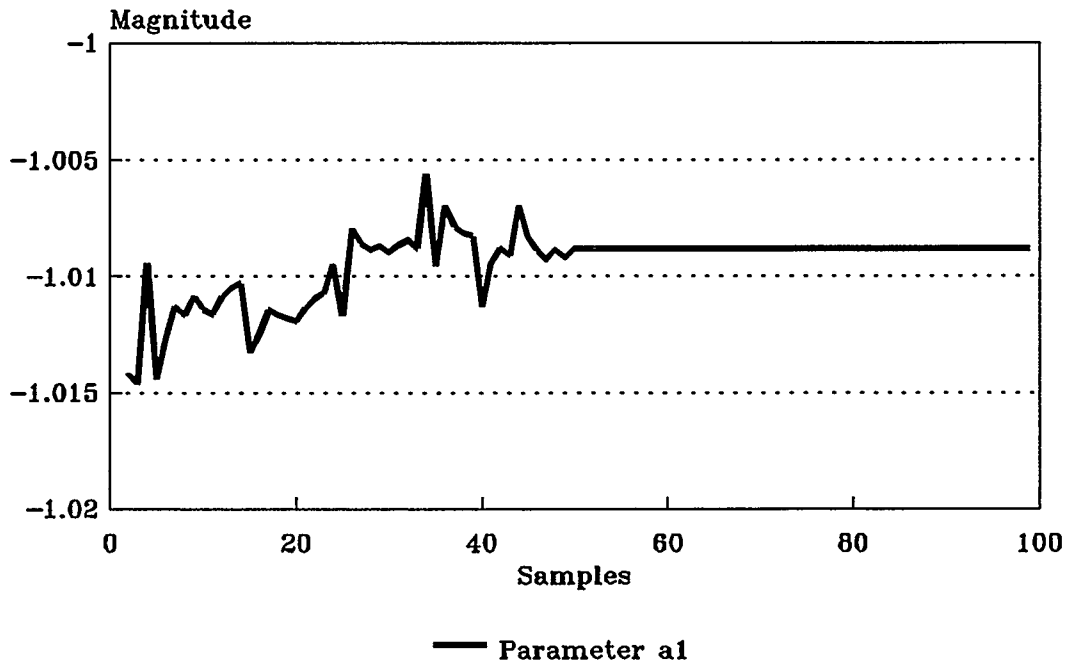

Figure 5.17 PI adaptive controller
Parameter a1
Frequency = 1600 Hz

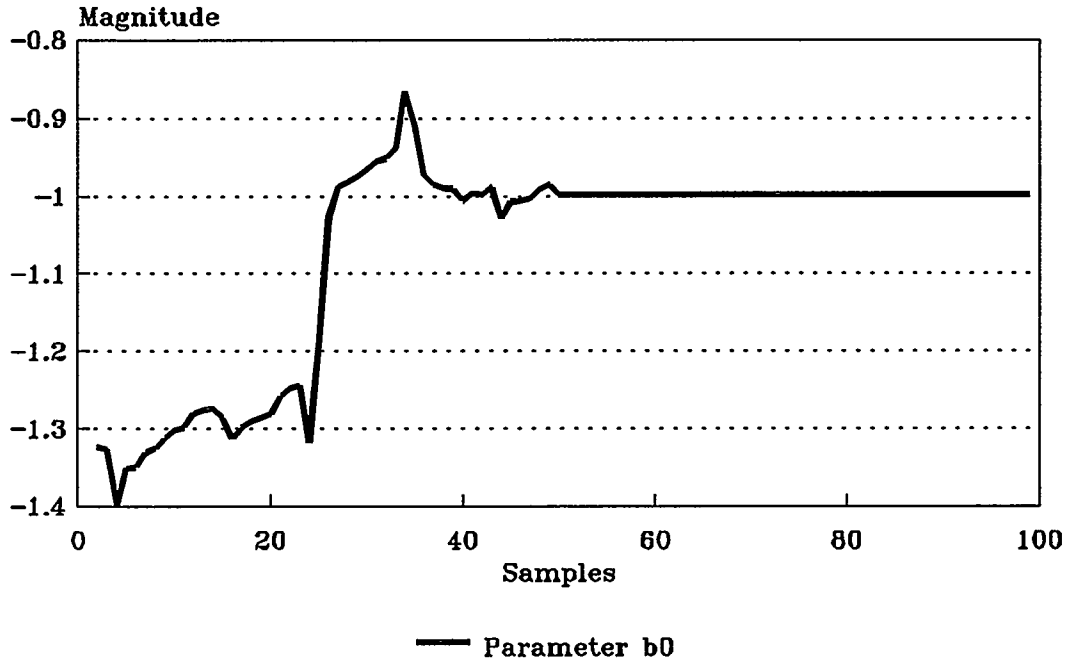

Figure 5.18 PI adaptive controller
Parameter b0
Frequency = 1600 Hz

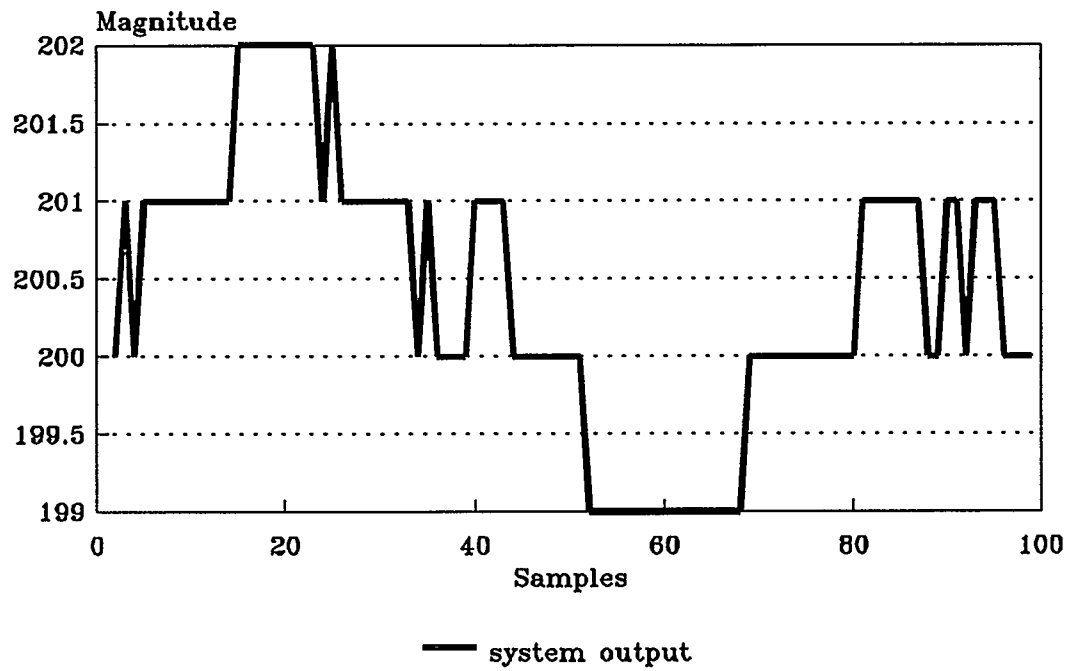

Figure 5.19 PI adaptive controller
system output
Frequency = 1600 Hz

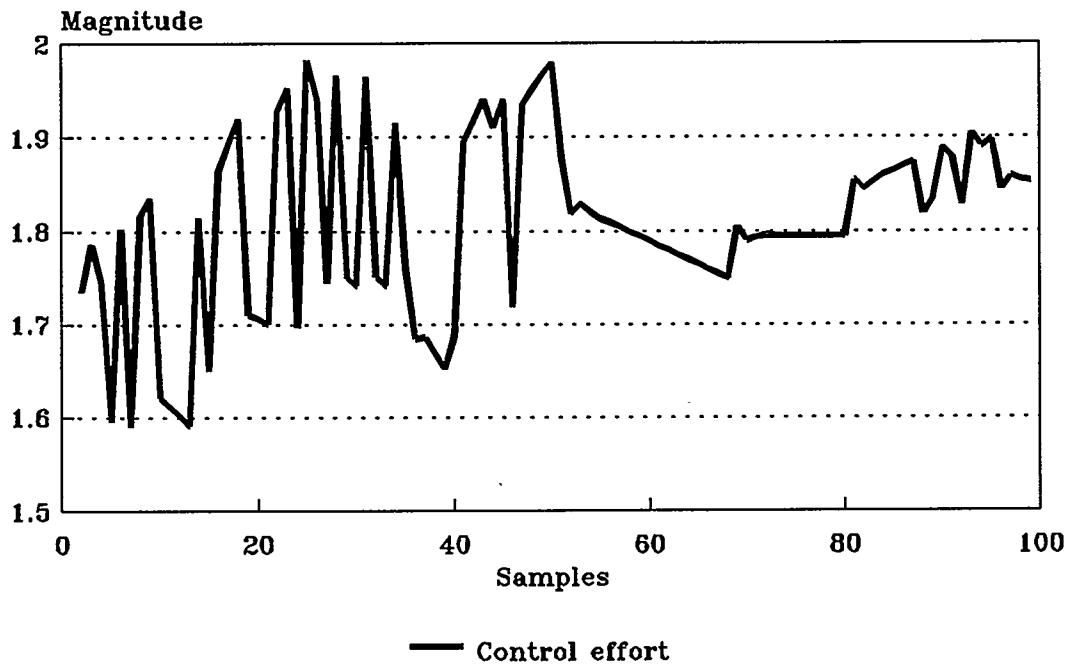

Figure 5.20 PI adaptive controller
Control effort
Frequency = 1600 Hz

CHAPTER 6

CONCLUSIONS

The objective of the thesis was to design and implement an adaptive controller for the cell-levitation apparatus. The work described in the thesis can be divided into:

(a) development of the model of cell-levitation apparatus which is based on mechanical analysis, and FFT, least squares, extended least squares, instrumental variable, maximum likelihood, generalized least squares, correlation least squares two step and nonlinear least squares method. The parameters of the cell-levitation apparatus system are obtained for the first time.

(b) development of the adaptive control system of cell-levitation apparatus based on four adaptive control algorithms, pole assignment adaptive controller, PI adaptive controller, pole-shifting dual loop adaptive controller and approximate series compensation adaptive controller.

(c) real-time implementation of the several adaptive control algorithms.

6.1 MODEL OF CELL-LEVITATION APPARATUS

The first contribution of this thesis is to give the model of cell-levitation apparatus. From the mechanical analysis of cell-levitation apparatus, a model of the second order structure considering disturbance is obtained. The advantage over the model in references is that it is considering a disturbance, so a more accurate model to describe the system is obtained, and then the model parameters are identified so that the parameterized model is obtained first time.

6.2 ADAPTIVE CONTROL SYSTEM

The second contribution of this thesis is to propose two adaptive controllers, one is pole shifting dual loop adaptive controller, the other is an approximate series compensation adaptive controller. The first method is mainly to overcome the weakness of a lot of PID adaptive controllers which can not handle an open loop unstable system. The second new algorithm is also a new adaptive control method which is especially suitable to the system with pure integral part. Other two adaptive controllers are also used in system design, they are pole assignment adaptive controller and PI adaptive controller. The simulation results show that these methods can obtain good results.

6.3 REAL-TIME IMPLEMENTATION

In realtime application, pole assignment adaptive controller and PI adaptive controller are used. Control results show that both methods can obtain good control results. They reduce the operator work and make the system easier to use and user friendly.

6.4 FURTHER RESEARCH

The work of this thesis makes the system easier to use. Because the purpose of this cell-levitation apparatus is to make the square of control variation minimum, some new adaptive algorithms should be proposed. These algorithms should be able to not only make system stable but also make the control effort minimum.

REFERENCES

1. K.R.Foster and H.P.Schwan (1989)
Dielectric Properties of Tissues and Biological Materials: A Critical Review, Critical Reviews in Biomedical Engineering, Vol. 17, pp. 25-101.

2. B.Sakmann and E.Neher (1983)
Single Channel Recording, Plenum Publishing Corp, New York.

3.R.E.Kalman (1958)
Design of a Self-optimizing Control System, Transaction of the ASME, Vol. 80, No. 2, pp. 468-478.

4. V.Peterka (1970)
Adaptive Digital Regulation of Noisy System, Proc. 2nd IFAC Symposium of Identification and Process Parameter Estimation, Prague, Paper 6.2.

5. K.J.Astrom and B.Wittenmark (1973)
On Self-tuning Regulators, Automatica, Vol. 9, No. 2, pp. 185-199.

6. D.W.Clarke and P.J.Gawthrop (1975)
Self-tuning Controller, Proc. IEE, Vol. 126, No.6 pp. 929-934.

7.J.M.Edmunds (1976)
Digital Adaptive Pole-shifting Regulators, PhD thesis, Control System Center, UMIST.

8.P.E.Wellstead, J.M.Edmunds, D.Prager and P.Zanker (1979)
Self-tuning Pole/Zero Assignment Regulator, Int. J. Control, Vol. 30, No.1, pp. 1-26.

9. Shi-jie Cheng, O.P.Malik and G.S.Hope (1986)
Self-tuning Stabiliser for a Multimachine Power System, IEE Proceeding, Vol. 133, Pt. C. No. 4, pp. 14-19.

10.G.C.Goodwin, P.J.Ranadge and P.E.Caines (1980)
Discrete Time Stochastic Adaptive Control, SIAM J. Control and Optimize, Vol. 19, No. 6, pp. 829-853.

11. A.Sano, H.Ohmori et al (1988)
Robust and Adaptive Control System for Regulation of Arterial Gas Pressures by Using Transcutaneous Sensors, 8th IFAC Symposium on Identification & System Parameter Estimation, pp. 1713-1718.

12. Sun Li, Huang Bingxian, Lee Ping (1988)
Adaptive Control of Blood Pressure. 8th IFAC Symposium on Identification & System Parameter Estimation, pp. 1759-1761.

13. Jingping Xie, (1991)
Measurement of Electrical Properties of Biological Cells Using a Dielectrophoretic Levitation system. Master's Thesis. University of Calgary.

14. T.B. Jones AND J.P.Kraybill (1986)
Active Feedback-controlled Dielectrophoretic Levitation, J. Appl. Phys. Vol. 60 pp.1247-1252.

15. F.W.Sears et al. (1982)
University Physics, Addison-Wesley Publishing Company.

16. T.B.Jones and J.P. Kraybill (1980)
Active Feedback-controlled Dielectrophoretic Levitation, IEEE Trans, Ind. Appl. IA-16 pp. 69-75.

17. W.R.Jones (1974)
Precision FFT Correlation Techniques for Nondeterministic Waveforms, IEEE EASCON Conv. Rec., pp. 375-380.

18. K.J.Astrom (1968)
Lectures on the Identification Problem- the Least Squares Method, Report 6086, Lund Institute of Technology, Division of Automatic Control.

19.P.Eykhoff (1974)
System Identification, Wiley, New York.

20. L.Ljung et al (1975)
Counter Examples to General Convergence of a Commonly Used Recursive Identification Method, IEEE Trans on Automatic Control, Vol. AC-20, pp. 643-652.

21.D.W.Clarke (1967)
Generalized-Least-Squares Estimation of the Parameters of a Dynamic Model, Proc. IFAC Symp. Identification in Automatic Control Systems, Prague, pp. 317.

22.R.Hasting-James and M.W.Sage (1969)
Recursive Generalized Least Squares Procedure for On-line Identification of Process Parameters, Proc. IEE, Vol. 116, pp. 2057-2062.

23. T.Soderstrom (1974)
Convergence of Identification Method Based on the Instrumental Variable Approach, Automatica, Vol. 10, pp. 685-688.

24. K.Y.Wong and E.Polak (1987)
Identification of Linear Discrete Time System Using the Instrumental Variable Approach, IEEE Trans on Automatic Control, Vol. AC-12, pp. 707-718.

25.R.Iserman et al (1974)
Comparison of Six On-Line Identification and Parameter Estimation Methods, Automatica, Vol. 10, pp. 81-103.

26. G.C.Goodwin and B.L.Payne (1977)
Dynamic System Identification - Experiment Design and Data Analysis, Academic Press, New York.

27. Cai Ji-Bing (1989)
System Identification, (In chinese), Beijing Technical University Publisher.

28. H.Akaike (1974)
A New Look at the Statistical Model Identification, IEEE Trans. Auto. Control, Vol. AC-19, pp. 716-723.

29. L.Ljung and T.Soderstrom (1983)
Theory and Practice of Recursive Identification, MIT Press.

30. I. Gustavsson (1975)
Survey of Application of Identification in Chemical and Physical Processes, Automatica, Vol. 11, pp. 3-24

31.Han, Guangwen (1980)
Identification and Parameter Estimation, (In Chinese), National Defence Publisher.

32.K.J.Astrom, B.Wittenmark (1987)
Computer Controlled System. Printice-Hall Inc.

33. Katsuhiko Ogata, (1970)
Modern Control Engineering, Prentice-Hall

34. Kin-hung Hillary Lau (1988)
Advances in Design of Filters and Controls, Master's Thesis, University of Calgary